Fracture Limit Prediction for Sheet Metal Forming by Damage Mechanics Approach

submitted by

Fung Lim Chung

for the degree of Master of Philosophy

DEPARTMENT OF MANUFACTURING ENGINEERING

THE HONG KONG POLYTECHNIC UNIVERSITY

2000

Abstract of thesis entitled

"Fracture Limit Prediction for Sheet Metal Forming by Damage Mechanics Approach"

submitted by Fung Lim Chung

for the degree of Master of Philosophy

at The Hong Kong Polytechnic University in February 2000.

Abstract

A number of investigations have been made for understanding the metal forming process and predicting the forming limit of sheet metal. The conventional method of analyzing the deformation is based on the plasticity theory and ignores the degradation of materials which is caused by the formation of micro-defects. In fact, the micro-defects play an important role in limit strains of materials. Therefore, there is a need to introduce damage modelling technique in metal forming prediction.

Previously, experimental results showed that the damage caused by uni-axial tensile loading was not isotropic, even though the material itself was originally isotropic. Therefore, it is necessary to develop an anisotropic elasto-plastic damage model for fracture limit prediction in metal forming. The objective of this research project is to develop a new method in analyzing and predicting the fracture limit of sheet metal with consideration of gradual deterioration of material. The approach used in this study takes into account the effects of initiation, coalescence and growth

of these micro-defects on a material element until its final rupture. The degradation and its effects on the material have been described by introducing the field variable ψ called 'continuity'. This tensorial variable characterized the progressive deterioration of mechanical properties.

For a representative volume element (RVE) of a damaged elasto-plastic material, the strain tensor could be decomposed into the elastic and plastic components under large deformation. A second order continuity tensor ψ was then proposed to characterize the anisotropic elasto-plastic damage state and its evolution process within a RVE of ductile metal material. The second order continuity tensor could be determined from the effective elastic stiffness matrix and satisfied the requirement of symmetry for derivation of the effective stress tensor, the effective elastic strain tensor and the effective elastic stiffness tensor. The corresponding anisotropic damage constitutive relations were formulated to model the damage-failure process for sheet metal.

Using the load-and-unload test, the effective stiffness matrix has been calculated under different loading conditions and hence the values of the continuity tensor were then determined. The current formulation does not require the assumption that the principal coordinate system of damage must coincide with that of the material, therefore it can be used to analyze more general problems. The proposed formulation has then been applied to aluminium alloy 2024T3 specimens which were damaged under uni-axial large strain. The experimental results showed that the effects of damage caused the effective stiffness of the aluminium alloy to decrease.

A damage-based criterion has been derived on the basis of the proposed formulation and was a non-linear function of the equivalent plastic strain. The criterion takes into the account of the triaxiality of stress, the elasto-plastic properties of orthotropic material, and the anisotropy of damage. Applying the damage criterion to sheet metal forming, the damage mechanics theory was extended to predict the fracture strains under different loading conditions.

Experimental verification has been done by Erichsen tests and uni-axial tensile tests. The fracture limit curve (FLC), i.e. the fracture strains of Al2024T3 sheet, were then determined by the damage-based fracture criterion. The microscopic examination has shown that coarse intermetallic particles exist in the aluminium alloy sheet. Breaking of these particles under high strain can open up micro-voids that initiate damage. The criterion has also been proven to be applicable for steel sheets such as HS-3 and A-K steel. The results showed that for the whole range of the strain ratio, the predicted fracture strains were in agreement with the experimental ones.

To conclude, a second order continuity tensor coupled with a damage-based criterion has been proposed in predicting the fracture limit strains. The proposed formulation has also been verified under various stretching conditions by different materials. The results showed that the predicted results were acceptable and reliable. In this research, it also showed that the damage mechanics theory could be extended to analyze and predict the fracture limit of sheet metals.

Acknowledgements

First of all, I would like to express my thanks to the Department of Manufacturing Engineering, The Hong Kong Polytechnic University for providing research funding to support this project.

I am deeply indebted to Dr. C.Y. Tang who supervised, encouraged and guided this study. He generously used his spare time to make the thesis possible. Without his patient encouragement I know that I would not have been able to achieve the goals. Sincere appreciation also goes to my co-supervisor Prof. T.C. Lee for his invaluable advice and suggestions in carrying out the research.

Special thanks are extended to Mr. W. Shen, Ms. L.H. Peng, all the technicians and my colleagues in the Department of Manufacturing Engineering for their advice, assistance and discussions in the experimental study.

Most of all, I wish to express my love to my parents and my wife who gave their endless support throughout my studies. Their love and sacrifice are the inspiration driving the work toward completion.

Nomenclature

α	Strain ratio
B	Material constant
b	Damage anisotropy factor
$\tilde{\mathbf{C}}(\psi)$	Effective elastic compliance tensor of damaged material
D	Scalar damage variable
E_1, E_2	Elastic moduli
$\mathbf{E}$	Intact elastic stiffness tensor
E_{ij}	Second order intact elastic stiffness tensor
$\tilde{E}_{ij}$	Second order effective elastic stiffness tensor
$\tilde{\mathbf{E}}(\psi)$	Effective elastic stiffness tensor
ε	Finite strain tensor
ε_{mn}	Nominal strain
ε_{ij}^{e}	Elastic strain tensor
ε_{ij}^{p}	Plastic strain tensor
$\dot{\varepsilon}$	Rate tensor
$\bar{\varepsilon}$	Equivalent strain
$\bar{\varepsilon}_c$	Critical value of the equivalent strain $\bar{\varepsilon}$
$\bar{\varepsilon}_{th}$	Threshold value of the equivalent strain $\bar{\varepsilon}$
$\dot{\bar{\varepsilon}}$	Rate of equivalent strain $\bar{\varepsilon}$
$\tilde{\varepsilon}$	Effective strain tensor
$\tilde{\varepsilon}_{ij}$	Symmetric second order effective strain tensor

f	Stress triaxiality factor
δ	Kronecker delta
$\mathbf{H}(\psi)$	Eighth order tenor operator
Φ	Helmholtz free energy density function
Φ_e	Elastic energy potential
G_{12}	Virgin shear modulus
$\tilde{G}_{12}$	Damaged shear modulus
J, K	Material parameter
σ	Stress tensor
$\tilde{\sigma}$	Effective stress tensor
$\mathbf{N}$	Strain damage influence tensor
N_{ijmn}	Fourth order damage influence tensor
$\mathbf{M}$	Stress damage influence tensor
$\boldsymbol{R}$	Thermodynamic force conjugates to the rate of the equivalent strain $\dot{\tilde{\varepsilon}}$
S_o	Material constant
ν	Isotropic Poisson's ratio
ν_{12}	Virgin Poisson's ratio for transverse strain in the x_2-direction when stressed in the x_1-direction
$\tilde{\nu}_{12}$	Damaged Poisson's ratio for transverse strain in the x_2-direction when stressed in the x_1-direction
$\boldsymbol{Y}$	Thermodynamic force conjugates to the continuity tensor ψ, often refers to as the damage growth force or the specific damage energy release rate
Ω	Dissipative potential
$\dot{\gamma}$	Non-negative Lagrange multiplier

ψ	Continuity tensor
ψ_c	Critical value of the continuity tensor
ψ_m	Mean value of the continuity tensor
ψ_i	Principle values of the continuity tensor, where $i = I, II$
Ψ_e	Elastic energy density function
Ψ^b	Elastic energy density corresponding to the bulk change of the damaged RVE
Ψ^d	Change in elastic energy density due to the distortion of the damaged RVE
ϕ	Angle between the principal coordinate system of the continuity tensor and that of the orthotropic material

Table of Contents

Chapter 1. Introduction

This chapter is divided into four sections. Section 1.1 describes the background of this research project. The research area is limited by a number of factors which are described in section 1.2, the scope of research. The objective of this research and a number of tasks to tackle the problems have been laid down in section 1.3. The layout of this thesis is described in section 1.4.

1.1 Background

For a successful operation in metal forming, knowledge of the formability of sheet metal is very useful. Metal forming is an important technology in manufacturing, especially in packaging and automotive industries. Sheet metal has its own limitation in the forming process and if the limitation is exceeded, material will rupture. Many studies have been performed to understand metal forming processes and predict forming limits of sheet metals (Swift 1952, Hill 1952, Marciniak and Kuczynsky 1967, Stören and Rice 1975, Bressan and Williams 1983). The conventional method in assessing the formability of metal is based on the classical plasticity theory.

Hill (1952) analyzed the formability of metal in a process of localized necking using classical plasticity theory. This analysis predicted the necking would not occur in a uniform sheet subject to biaxial stretching. In fact, loading condition in the sheet

metal forming process is non-proportional and is in biaxial loading status. Experimental studies (Ghosh and Hecker 1974, 1975, Painter and Pearce 1974) demonstrated that thin sheets subject to biaxial tension could fail by localized necking. Since the study of Keeler and Backofen (1963), forming limit analysis that characterizes the onset of plastic instability of sheet metal has stimulated continuous interest among engineers and researchers. The determination of the forming limit of metals has been studied (McClintock 1968, Azrin and Backofen 1970, Hecker 1975, Ghosh 1976, Onate et al 1988) experimentally and theoretically as well.

There are a number of factors governing the limit strains of metal forming, including strain hardening, plastic anisotropy and strain-rate sensitivity. These factors are affected by the presence of micro-defects that has been ignored by the plastic theory in a material element. The limit strains of metals depend on the formation and evolution of the micro-defects. Marciniak and Kuczynsky (1967) presented a method to predict the limit strain by considering the initial inhomogeneity of material. The progressive deterioration of mechanical properties of materials, such as the degradation of stiffness, strength and working life, is usually referred to as 'materials damage'. The instability and failure in metals involves considerable material damage, i.e. initiation and growth of micro-defects under deformation, therefore materials damage plays an important role in processing of metal.

The forming limit diagram (FLD) has been widely used in analyzing the sheet metal forming operation because the FLD is designed to define the localized necking of a material and is used to measure the maximum formability of sheet metal

products. The necking problem was widely studied by Swift (1952) and Mellor (1960). Keeler (1965) developed a convenient way of studying the limitation of the formability of sheet metal under biaxial stress. The diagram is now widely used and the plotting is based on the maximum principal surface strain as ordinate against the minimum principal surface strain as abscissa.

For fracture prediction under biaxial tension, Marciniak and Kuczynsky (1967) have demonstrated an initial approach. They proposed an analysis method by introducing a pre-existing material imperfection in the sheet. This method was later known as M-K theory and was supported by other researchers (Bassani et al 1979, Needleman and Rice 1978, Needleman and Triantafyllidis 1978). However, the predicted results of the forming limit diagram by either the Hill's theory or the M-K theory did not correlate well with the experimental data (Arzin and Backofen 1970, Marciniak et al 1973, Tadro and Mellor 1975).

Several theories have been proposed in the study of the forming limit diagram such as the J_2 flow theory and the J_2 deformation theory (Hutchinson et al 1978 and Hutchinson and Neale 1978). However, both theories showed some uncertainty in predicting the localized necking therefore they would not be reliable in analyzing the necking problem under non-proportional forming history.

The occurrence of macroscopic fracture of ductile metals is frequently induced by the gradual growth of internal damage. The internal damage refers to micro-voids, micro-cracks and other micro-defects of material. McClintock (1968) developed a fracture criterion based on the concept of growth and coalescence of pre-existing

cavities. Rice and Tracey (1969) theoretically presented a cavity growth model, which could be used to calculate the displacement field of an ideal plastic material with a spherical cavity under the action of remote stress. A void growth model was also introduced by Gurson (1975). Experimental evidence showed that most metallic materials contain different sizes and shapes of particles, including precipitates and inclusions, which cause micro-defects. The interaction between micro-defects is very complex during large deformation, and thus a number of related studies have been performed (Forsyth and Smale 1971, Ghosh and Hamilton 1982, Pilling and Ridley 1986).

Damage mechanics theory has emerged to take into account the effect of initiation, coalescence and growth of the micro-defects in material element up to its final rupture. This new theory has been successfully developed and applied to study a wide range of engineering problems such as ductile fracture (Chow and Wang 1987a-c, 1988a,b, Wang and Chow 1989), creep (Chaboche 1984) and fatigue (Chow and Wei 1991a,b).

In order to understand sheet metal forming processes thoroughly, classical theory of metal forming limit and fracture limit has been extended to incorporate the basic concept and methodology of damage mechanics. Early application of the damage mechanics theory to metal forming has been carried out by Schmitt and Jalinier (1982). They found that if the damage was done by decohesion of the particle-matrix interface, only a little damage was developed in uniaxial tension whilst a large damage was developed in equibiaxial stretching. Conversely, if the damage was done by fragmentation of the particle, an approximately the same

amount of damage was developed in uniaxial tension and equibiaxial stretching. Lee et al (1985) found that the plastic instability of sheet metal under biaxial tension suffered material degradation and confirmed the need for characterizing the forming limit diagram with the theory of damage mechanics. Some attempts have been made by Lemaitre (1983) and Li et al (1983) by using damage mechanics theory to predict the fracture limit diagram. The predicted results were yet to be justified and so have been verified in this study.

1.2 Scope of Research

There are a number of restrictions to confine the research area. The analysis of the metal is based on the two-dimensional case since the three-dimensional analysis required a certain number of parameters to be defined and so increased the difficulty in solving the problem. The material used is a thin sheet at 0.8 mm thickness therefore the changes in thickness has been ignored. The technique used in this study is the continuum mechanics theory. Some assumptions have been used in this theory such as using the fracture strain rather than the strain of plastic instability and the damage of a material was orthotropic although the damage was anisotropic. Fracture limit of anisotropic sheet metal has been studied in this research. The components of the continuity tensor of aluminium alloy 2024T3 under different magnitudes of pre-tensile strain have been determined experimentally. A second order continuity tensor ψ has then been proposed to characterize the state of anisotropic damage of a elasto-plastic representative volume element (RVE). The analysis carried out under room temperature.

The experimental tests included tension and dome test. The experimental procedure was carried out under quasi-static conditions and neglected the strain rate effect. A proportional loading condition was assumed. The effect of friction has not been taken into consideration. Metallographical examination was carried out and it was found that the coarse intermetallic particles were responsible for the nucleation of micro-voids. Overall, there was only theoretical and experimental method used in this research therefore there was no computational work done in this study.

1.3 Objective

The need in predicting the formability of material is an important aspect in manufacturing industries because material will rupture if the limit of formability is exceeded. The objective of this research project is to develop a new damage model in analyzing and predicting the formability of metal. After the objective was justified, literature survey was carried out by dividing into two main sections. Firstly, the damage mechanics was introduced and secondly, the sheet metal forming as background knowledge of this study was presented.

In order to fulfill the objective stated above, the development and construction of a damage model for sheet metal has been described by using second order continuity tensor coupled with the damage-based fracture criterion. Experimental verification has been carried out by using the Erichsen cupping test and the tension test, plus microscopic examination as well. The verification of the proposed model

was not only compared with the experimental works but also compared with the experimental data obtained from Ghosh (1976). The results showed a good correlation between the theoretical and the experimental data.

1.4 Layout of the Thesis

The layout of this thesis is as follows. Chapter 2 deals with literature survey providing a brief history of the damage mechanics before defining what is damage in section 2.1.1. The methods in measuring the damage and the recent applications in ductile fracture prediction are reviewed in sub-sections of Chapter 2, i.e. section 2.1.2 & 2.1.3 respectively. The second part of the literature survey is to review a background information in sheet metal forming industry (section 2.2.1) before applying the damage mechanics theory into sheet metal. Section 2.2.2 provides the conventional methods in formability prediction that acts as a comparison to the damage mechanics theory, and section 2.2.3 describes the applicability of damage mechanics in formability prediction. The methodology of this research is located in section 2.3 to show the methods and procedures in carrying out this project and the development of a damage model for fracture strain prediction.

Chapter 3 gives an overall development of a damage model for fracture strain prediction. Section 3.1 describes the derivation of the constitutive modelling. Sections 3.2 and 3.3 show the derivation of the continuity tensor and its procedure in determination of the continuity tensor respectively. The relation between continuity and damage parameters and the specific damage energy release rate are discussed in

sections 3.4 and 3.5 accordingly.

The results and discussions of the prediction of fracture strains for sheet metal forming are dealt in Chapter 4. In this chapter, section 4.1 introduces the development of damage-based fracture criterion in constructing the proposed damage model. In section 4.2 the theoretical prediction has been verified with the experimental values. A sound evidence in applying the damage-based fracture criterion to predict the fracture strains for sheet metal is also shown in it. Results and discussions have been located in section 4.3.

Conclusions are placed in Chapter 5 showing that the damage mechanics theory can be applied to the prediction of fracture strains for sheet metal forming by using second order continuity tensor coupled with the damage-based fracture criterion. Lack of computational work such as using the ABAQUS software and the finite element method in predicting the fracture strains of sheet metal has been mentioned in Chapter 6, therefore the use of computational methods is a suggested area for future works which is discussed briefly in the same chapter. The contribution of knowledge from this project has been described in Chapter 7. References, tables and figures are placed after Chapter 7.

Chapter 2. Literature Review

By carrying out literature survey, a thorough understanding of the background and the development between damage mechanics and sheet metal forming can be reviewed. The relationship and the importance of applying damage mechanics to the prediction of fracture strains in sheet metal can then be achieved.

Literature on damage mechanics has been divided into four sections. The first section 2.1 deals with the introduction of damage mechanics and states the reasons why fracture mechanics cannot be used in this project. Different types of damage failure and their applications have also been dealt with in the first section. Section 2.1.1 lays down the definitions of damage which included scalar, vector, second order tensor and fourth order tensor. A summary of the definitions has been presented in Table 1. Under the definitions of damage, a number of methods for measuring the damage are also reviewed in section 2.1.2. Since there are different kinds of fracture which occur in damage process and this research is limited to ductile fracture therefore the applications in ductile fracture prediction have been discussed in section 2.1.3.

A brief history and background knowledge of sheet metal forming has been reviewed in section 2.2. Failure in sheet metal forming process and conventional methods for predicting the formability of sheet metal have been dealt in section 2.2.1 and 2.2.2 respectively. The applicability of damage mechanics in formability prediction was discussed in section 2.2.3. The methodology and the procedures in carrying out this research project have been presented in section 2.3. The following

describes the findings of the literature review.

2.1 Damage Mechanics

Before the introduction of damage mechanics theory, engineers, scientists and researchers were using fracture mechanics to understand and to solve engineering problems in material failure. Fracture mechanics was used to calculate whether or not a defect of given size would propagate in a catastrophic manner under service loading and hence to determine the degree of safety of the material. In general, fracture mechanics uses global parameters such as the J-integral, crack opening displacement, and stress intensity factor to analyze the load carrying capacity of a structure containing cracks. Damage mechanics is the study, by using damage variables, of the deterioration of materials which are subjected to loading. The study of damage mechanics can be traced back to 1958. The modelling of metal damage from the mechanics approach was first proposed by Kachanov (1958).

All materials are composed of atoms and held together by bonds resulting from the interaction of electromagnetic fields. Damage is when some of the bonds of a solid connecting parts of its microstructure are missing. When damage process occurs, material starts debonding. Damage represents surface discontinuities in the form of microcracks or volume discontinuities in the form of cavities. It involves a rheological process which is different from deformation although the initial causes are identical, i.e. movement and accumulation of dislocations in metals, modification of intermolecular bonds in organic materials and micro-decohesion in minerals.

Damage mechanics deals with the effects of damage to the presence of microcracks on the mechanical properties of materials. This concept was adopted by Chaboche (1984, 1988s, 1992 and 1993), Chow (1987s, 1988s, 1991s and 1992s) and Lemaitre (1984 and 1985s). The theory of damage mechanics concerned with all materials at low and high temperatures under different kinds of loading and the theory described the evolution of the phenomena between the original state and the macroscopic crack initiation.

There are three stages in the progressive physical process of fracture. The first stage is the microscale which is the accumulation of microstresses in the neighbourhood of defects or interfaces and the breaking of bonds causing damage to the material. The second stage is the mesoscale which is the growth and the coalescence of microcracks or microvoids that together initiate the crack on the representative volume element (RVE). Damage mechanics deals with quantities defined at a mathematical point. From the physical point of view, these quantities represent averages on a certain volume. The RVE must be small enough to avoid smoothing of high gradients but large enough to represent an average of the microprocesses (see Figure 2-1). The final stage is the macroscale of which is the growth of crack. The microscale and the mesoscale stages have been studied by means of damage variables of the mechanics of continuous media defined at the mesoscale stage. Fracture mechanics studies the macroscale stage by means of variables defined at the microscale.

In mechanical point of view, the principle of the damage theory can be used to

analyze the resistance of structures used at the design level, to optimize the metal forming process, to avoid or reduce manufacturing defects, to modify the mechanical properties and to control the service conditions of the products. The mechanical variables cannot directly distinguish between a highly damaged volume element and an original one, therefore internal variables have been induced to represent the deteriorated state of the material. The states of materials damage are characterized by continuous distribution of internal state variables and called damage variables. It represents an average degeneration of the material due to the initiation and development of micro-defects (micro-cracks and voids).

Basically, there are four types of damage, namely brittle damage, creep damage, ductile damage and fatigue damage. The damage phenomena are different from the deformation phenomena which is due to several mechanisms. Brittle deformation process was defined as the change of crystalline lattice as a result of a net loss of bonds. The inelastic deformations are classified on the macroscale by the corresponding degradation of material parameters therefore leading to the damage which was measured by the partial loss (change of continuity) of stiffness. Macro-brittle damage produced by monotonic loads without appreciable irreversible deformations. Viscoplastic (or creep) damage occurs as a function of time for metals at average and high temperatures, corresponding to intergranular de-cohesions accompanying viscoplastic strains. Ductile plastic damage accompanies with large plastic deformation of metal at ambient temperature. Ductile deformation process has been defined as the flow of mass through the crystalline lattice while "the lattice itself, with material embedded on it, undergoes elastic deformations and rotations". During plastic deformation (glide of dislocations), the total number of bonds per

volume remains constant and the effective parameters of the material do not change except at very large plastic strains and the change of texture. Fatigue (or micro-plastic) damage is caused by stress repetitions and defined as a function of the number of cycles.

Various damage models have been derived from the theory of damage mechanics which is a branch of the solid mechanics. Damage mechanics was centered on micro-void / crack development, provides a better understanding of damage in structural failure by means of damage variables to represent the deterioration of a material element. Damage models have been applied in various engineering problems such as brittle failure, creep failure, ductile failure and fatigue failure in metal, polymer, concrete and metal matrix composite materials.

In brittle fracture, damage mechanics theories have been used to study the phenomenon of localized fracture in brittle materials. Among the phenomenological theories, the material compliance tensor itself was treated as an internal variable. The model presented a thermodynamically consistent formulation for mortar with anisotropic damage. The formulations of the model were material parameter sensitive (Yazdani 1993) and was used to bring in the effect of relative strengths in tension and compression. A new damage response tensor for cracking was also proposed by Yazadani in the same year and the difficulties of snap-back in deformation had been removed. The model was illustrated for different stress paths in mortar and concrete.

Progressive degradation of mechanical properties is an inherent feature of brittle material behaviour therefore the degradation of elastic properties reflects the damage

in brittle materials have been accumulated and the damage is then the consequence of the evolution of internal microcrack. The formulation of damage models is related to the appropriate choice of the mathematical form for the damage variable. The mode and stability of crack growth and the behaviour of brittle material depends on the sign and magnitude of applied stresses. An important issue of modelling different tensile and compressive responses of brittle materials was addressed by Lubarda et al (1994). A rate-type constitutive equation for elastic behaviour of brittle materials, whose elastic properties degrade during deformation process involving damage evolution, has been analyzed. Derived rate constitutive equations provided the explicit representation of the tangent compliance tensor. The proposed model (Lubarda et al 1994) was also applied to uniaxial tension and compression. The applicability of the proposed model could be extended when the plastic strains were incorporated in the proposed constitutive framework.

With the introduction of the turbines and the jet engines, materials used in these constructions are exposed to a hostile thermal environment and experienced a gradually increasing deformation known as creep. In contrast to the elastic deformation, creep is time dependent and associates with irreversible changes in the microstructure of the solid. These irreversible microstructural re-arrangements leads to creep rupture at stress levels well below those causing instantaneous failure.

A simple one-dimensional model could not be adequate in predicting the creep rupture stages therefore tensorial damage models evolved. Tensor function theory was a powerful tool for solving and describing the mechanical behaviour of materials under multiaxial states of stress such as creep damage and creep rupture. Betten

(1992) used the tensor function theory to formulate the constitutive and evolution equations for the anisotropic materials.

Creep rupture has been restricted to grain boundary cavities, therefore the interrelation between damage variable and metallographical parameters in creep damage could be introduced. The investigation was carried out by Murakami et al (1992) and the relation between damage variable and the metallographical parameters was used to apply in alloy steel. Creep damage in alloy steel has also been investigated by Hall et al (1996) using finite element based numerical procedure to predict creep crack growth in compact tension test, therefore the performance of materials in cracked structures could be assessed and on which materials selection could be based.

Ductile damage can be caused by different mechanisms such as nucleation, growth and coalescence of microvoids, internal and external necking. Any of these mechanisms can cause final fracture. Ductile fracture is due to the formation of microvoids during plastic deformation process. A number of damage models have been derived by Lemaitre (1985) based on the principle of total complementary energy. Chow and Lu (1992a,b) used to analyze growth and coalescence of microvoids for ductile damage. Tang and Lee (1995a,b) used to predict ductile fracture based on thermodynamics. In damage mechanics, the damage variable is used to describe the degradation processes in three phases (Mou and Han 1996) namely as the damage generation, damage growth and the damage instability. It is then desirable to develop a damage model for predicting the damage evolution in ductile materials.

An irreversible thermodynamics theory for constitutive equations has been proposed. This theory can be extended to the theory of damage mechanics by describing the internal state changes due to the material damage via the use of proper internal state variables. The model was based on the assumption of isotropic damage and constant stress triaxiality ratio during loading, therefore the model was only valid for proportional loading. Chow and Wang (1987a-c) have verified the model with their experimental results and were capable to predict damage evolution.

With the introduction of a new damage effect tensor (will be discussed in section 2.1.1), the constitutive equations of elasticity and plasticity coupled with damage have been derived for fatigue fracture (Chow and Wei 1991a,b). This fatigue damage model was constructed under multiaxial tension loading condition therefore this model has not yet been capable to cover tension-compression cycle of the material. The fatigue damage model has been extended and developed to assess fatigue damage in offshore structures (Li and Chow 1993). The model has been applied for the isotropic material in offshore structures which undergone low and high cycle fatigue and dynamic response. Due to the complex ocean environment, the analytical method was established by introducing the concept of duty strain range with spectral parameters and the history dependent damage model was also developed in analyzing the overload effects to the structures. In practice, the analytical procedure could be fully computerized for design purposes.

2.1.1 Definitions of damage

Damage has been defined by using damage variables and generally there are four different types of damage variables namely scalar, vector, second order tensor and fourth order tensor. The damage variable was firstly defined as scalar variable by Kachanov (1958) and was used in isotropic or one-dimensional studies of damage mechanics. Damage may be interpreted at the microscale as the creation of microsurfaces of discontinuities. For anisotropic damage, Kachanov introduced another three scalar variables ψ_1 , ψ_2 and ψ_3 to characterize the net area fractions of planes normal to the direction of the principal directions of stress. There is a limitation of this type of definition of damage as the principal directions of damage and the principal direction of stresses must coincide with each other.

The vector variables in defining the damage have also been attempted by Kachanov (1974) whereas a damage vector ψ_n in the direction n is used to characterize the damage state on the area element of a normal n and under a normal stress σ_n . In complementary description of a damage state of an element, an entire distribution of the vector ψ in all directions of the damage state is needed, and causing difficulty in describing a general state of damage to that element therefore vector variables cannot be used in defining the damage.

In order to extend the definition of damage to the general cases, a second order and a fourth order tensor have been introduced for three-dimensional anisotropic damage. A second order symmetric damage tensor variable has been defined as three orthogonal principal directions whereas the principal directions of the stress tensor

coincide with the principal directions of the damage tensor. The fourth order symmetric damage tensor variable is introduced through the stress-strain behaviour of the damaged material and the damage state can be characterized by the change of elastic constants.

Many researchers have used the above definitions of damage to derive different damage models and the descriptions of what they have done were discussed as follows.

In 1992, Chaboche (1992) used the scalar variable to describe the unilateral aspect of damage, to distinct damage regimes for tensile and compressive loadings. It was simple to understand and to use but it was unable to reproduce the anisotropy induced by damage. In the same year, Murakami et al (1992) stated that the scalar variable could provide physical background for continuum damage mechanics (CDM) and foundation for creep damage theory. Tang et al (1994, 1995a,b) stated that the scalar variable also could provide information about stiffness changes in x-direction but limited to one-dimensional analysis. They were then using plane stress analysis to predict the damage in x_2-direction and strengthening effect in transverse direction but this kind of analysis was over-estimate the transverse modulus.

A number of predictions have been made by using scalar variable (Tai and Yang 1986) to predict void growth and void coalescence with hypothesis of isotropy of damage, isotropy of plasticity, hypothesis of constant triaxiality ratio during loading, i.e. proportional loading of plasticity. Tai and Yang (1987a-c) used the scalar variable to predict fracture limit curves of sheet metals under the assumption of the

void growth governing microstructural processes and in the same year, they proposed a rupture criterion and applied to low-carbon steel specimen and plastic yielding, to predict the initiation and propagation of crack but it needed further investigation in ductile fracture. Recently, Lee et al (1997) used the scalar variable to predict forming limit curves by modifying the M-K model and removed the need for the assumption of an initial groove defect on the sheet metal surface.

Tai (1988) used an isotropic plastic damage model for orthotropic materials to combine with M-K model and showed that the effect of internal damage to the analysis of sheet metal forming limit. Other researchers (Groche and Doege in 1989) used the scalar variable in a micromechanical model to obtain a yield surface equation but it was difficult to quantitative description of the damage parameter. Li and Chow (1993) used the concept of duty strain range and history dependent to develop a fatigue damage model capable to assess fatigue damage in offshore structure. The analysis was carried out by computation without experimental verification. Later, Saanouni et al (1994) used the theory of representative of volume element (RVE) to represent the damaged area as RVE was free from any kind of stress. The RVE could be able to define energy release rate and be able to release store energy to formulate constitutive equation. The scalar damage variable also used the linear response to the effective strain and then resulted in kinematics formulation to numerical evaluations by Najar (1994).

For static analysis, the modulus of elasticity requires precise measurement of small strains. Damage is very localized and is measured in the order of 0.5-5.0 mm, therefore the best straight line in the stress-strain graph representing the elastic

loading or unloading is difficult to define because of the damaging history has already existed in the loading condition. The above stated problem can be rectified by using a weakened central section of a tested material and a small gauge or displacement transducer to evaluate in the range of $\sigma_{max} < \sigma < \sigma_{min}$ to obtain a $\pm$ 5 % relative precision. (where $\sigma_{max} = 0.85\sigma$ and $\sigma_{min} = 0.15\sigma$)

Apart from the scalar variable, tensorial variable has been used in describing the definition of damage. The tensor function theory is a powerful tool for solving complex problems such as creep damage. Constitutive theories and material laws are used to describe the mechanical behaviour of materials under multiaxial states of stress involving creep damage and creep rupture. The tensor functions properties with several argument tensors constitute a rational basis for a mathematical modelling of complex material behaviour such as the anisotropic solids. Anisotropic materials have oriented internal structures produced by forming processes and manufacturing procedures or induced by permanent deformation. The tensorial variable provided comprehensive theory of anisotropic continuum damage mechanics (CDM) to solve practical engineering problems with the assumption that the stress damage relationship of (σ-D) was in compression (Chow and Wang 1987a-c). In 1995, Chaboche and his co-investigators (1995) described elastic behaviour by using tensorial variable but could not verify the model by multiaxial experiments with non-proportional loading and future work needed.

Tai and Yang (1987b,c) constructed a ductile fracture parameter that could be determined by macroscopic method in predicting the initiation and propagation of crack. The damage rupture criterion was needed to derive for the problems of ductile

fracture. Murakami (1988) used the tensorial variable to represent the net reduction from Cauchy tetrahedron and did the distributed microcracks and cavities cause using effective stress from damaged material. Shen et al (1989) also used the asymmetric matrix to construct the 4^{th} order tensor. In the same year, Wang and Chow (1989) have predicted and measured the crack growth by using the tensorial variable. Other investigators, Chow and Wei (1991a,b), used the tensor variable to combine the elastic and plastic damage to predict the number of cycles to failure under tensile loading but it needed to extend the study to cover tension-compression cycles.

If a uniaxial load is applied to a representative volume of material and all the defects are opened so that no microforces are acting on the surfaces of microcracks or microcavities, it is convenient to introduce an effective stress to the surface that effectively resists the load. This definition of the effective stress has been applied on the material in tension. On contrary, if all the defects close, the effective stress is equal to the usual stress and if some defects close, such as in compression, the damage remains unchanged. In general, the effective stress tensor is non-symmetric. The effective stress concept has been used by Chaboche et al (1995) and Mou et al (1996). A damage mechanics model (Chaboche et al 1995) was proposed based on the relations between damage and elastic behaviour for brittle materials. The proposed model related to initial anisotropy and the unilateral character of damaged materials. The materials concerned were concrete and composites. The model has been simplified to the scalar character of the state variables describing the damage and the microcracks. The verification of the models and the damage criteria were needed such as multiaxial experiments with non-proportional loading.

In the study of brittle solids, low-order damage model could not describe the damage evolution of the brittle materials therefore it was necessary to use higher-order continuum framework (Lacy et al 1997) to predict the macroscopic response of solids containing high interactive defects. Further investigation of appropriate damage descriptors and numerical simulations involving irregularly distributed crack systems were needed to establish.

The hypothesis of energy equivalence stated that the elastic energy of the damaged material was obtained directly from that of the virgin undamaged material and the stress variable was replaced by effective stress. The work done by external forces during the same loading history was assumed to be unchanged between the damaged and the virgin material. In 1992, Chow and Lu (1992a,b) used the energy equivalence hypothesis to develop an anisotropic damage model under the condition of the stress history effect. A generalized damage model allowed non-linear relationship to be established among state variables between stress and strain but it needed to be extended to study flexure problems of composite laminates. The application of the hypothesis of energy equivalence was limited by not able to describe the phenomena other than elasticity and has been investigated by Chow and Lu (1992a). Their works correlated well with experiment and was able to characterize the fracture initiation of notched plates with ductile material. Chaboche (1993) used symmetry of the elasticity, eliminate the discontinuous stress-strain response but a simple case of elastic behaviour and rate independent damaging processes in brittle materials. In the same year, Yazdami (1993) used the 4^{th} order tensor which was capable to model non-linearity's in the lateral directions, to formulate in terms of material parameter sensitive and to remove snap-back in

deformation. The model has been illustrated for mortar and concrete and was suitable for computer implementation. Chaboche et al (1995) used the tensorial variable to describe elastic behaviour but could not verify the model by multiaxial experiments with non-proportional loading as they ignored the viscosity and hysteresis effects. With the hypothesis of elastic energy equivalence, Luo et al (1995) developed a large anisotropic damage theory and applied to the analysis of pure torsion and uniaxial tension with the assumption of a series of small incremental damage.

Hall et al (1996) used finite element based numerical procedure but more accurate result would be obtained if extremely fine mesh were used in the order of 6-7 grain diameters. Mou and Han (1996) stated that the tensorial variable was capable to derive damage evolution from the principles of incremental complementary energy, thermodynamics concepts and effective stress for ductile materials. Isotropic damage and the limitation were stress triaxiality ratio effect, therefore high ratio led to have a greater damage evolution, depended on strain hardening exponent and accumulated strain as well. Recently, Hayakawa and Murakani (1997) used Gibbs thermodynamic potential to determine the tensorial variable. Lacy et al (1997) using a high order to predict the macroscopic response of solids containing highly interactive defects because low order cannot determine the damage evolution equation accurately.

In order to have a better view of damage variables, all the different variables such as the scalar, vector and tensor variables plus their applications, advantages and limitations are listed in Table 1. In fact, there is no such individual variable to be used to describe any damage process effectively.

2.1.2 Measurement of damage

Definition of damage variables and some of their applications by other researchers have been discussed in section 2.1.1. Measurement of damage is also important to the precise definition of damage variables in order to obtain accuracy in predicting the degree of damage. There are three main areas in assessing experimental damage. They are the formulation of the constitutive laws and the damage evolution laws for the prediction of material failure. Secondly, the determination of the current damage state of a component for safety purposes and thirdly the evaluation of damage to determine the causes of failure.

The bonds between the molecules in a crystalline lattice may be ruptured, molecular chains in polymers broken and the cohesion at the fiber-matrix interface lost. This damage cannot be measured by non-destructive tests but instead can be measured indirectly by the effect it has on the effective material properties. The damage in a volume of material can be measured by the number of microcracks, the size and shape of the microcracks, the orientation and the position of the microcracks. This type of measurement is very cumbersome and intractable because the number of microcracks is large unless the observed volume is subjected to constant tractions and displacements.

Macro-damage is a continuum concept that is intuitively related to the microcracks. It is measured by the cumulative effect, which these microcracks and other micro defects have on the macroscopic response. The effect of many micro defects can be described analytically by a damage parameter only when the material

is statistically homogeneous in the neighbourhood of the observed material point of the configuration. At present, damage is defined as the micro defects which impair the ability to transmit the loads and resist the environmental influences. The damage may become a cause of, or lead to, the fracture.

In general, there are three different types of damage measurement (Lemaitre 1992) that can be carried out as follows:

I). Measurements at the scale of microstructure which leads to microscopic volume element with the help of mathematical homogenization techniques.

II). Global physical measurements which are used to convert to properties in characterizing mechanical resistance and link to the remaining life-time but this concept does not directly lead to a damage constitutive law.

III). Global mechanical measurements (modification of elastic, plastic or viscoplastic properties) which are easier to interpret in terms of damage variables using the concept of effective stress.

In microscopic measurement technique, it is a direct observation of micrographic pictures of RVE. The sample, which has undergone the microscopic observation, needs to have some preparation and so this is a destructive method otherwise the sample is observed on the surface by means of replica technique. This type of measurement can enable to obtain properties of damage volume element but it is difficult to define macroscopic damage variable and the law of evolution which in turn to use in continuum mechanics analysis.

Global physical measurements include measuring the variation of density, the variation of electrical resistance, the ultrasonic waves propagation and the measurement in acoustic emission. In pure ductile damage, the defects are cavities and may be assumed as roughly spherical. The volume of the cavities increases with damage therefore it is unable to use the measured value to derive a damage model. The variation of the electrical resistivity can be defined as the effective intensity of electrical current. The resistivity is affected by the damage by means of the change in volume only, therefore the measured damage variables will be in terms of a damage volume element and cannot be able to derive a damage model to represent the whole damaged element. The ultrasonic wave propagation technique is based on the variation of the elasticity modulus (will be discussed later) and measures the speed of ultrasonic waves. The measurement is limited to linear isotropic elastic material because the longitudinal and the transverse waves of ultrasound travels in a linear isotropic elastic cylinder, therefore this method cannot use in this research due to anisotropic material concerned. The acoustic emission technique is used to examine the sensitivity of materials by counting the acoustic emission that reflected from the progression of damage and is a useful tool in assessing the damage zone. This type of measurement technique is good for detecting the location of the damage zone and the results are qualitative as far as the damage variable concerned.

Mechanical measurements are the one used to derive damage variable in this research project and include the measurement of elasticity modulus, plasticity and viscoplastic properties. The state of elasticity coupled with damage allowing the damage variable can be evaluated in terms of Young's modulus. This method has been used extensively. However, the limitation to this method is that the damage

must be uniformly distributed in the material where strain is measured. The measurement of plasticity properties can be done under the low and high cycle fatigue damage. The viscoplastic (creep) damage can be measured by applying the hypothesis of equivalent strain to the power law of secondary creep. The fatigue and creep damages are beyond the scope of this research therefore the measurement of the elasticity modulus is the one applied in this project for ductile fracture prediction. The application of the mechanical measurements will be discussed in the next section.

2.1.3 Recent applications in ductile fracture prediction

In general, ductile damage can be caused by many different mechanisms including: nucleation, growth and coalescence of microvoids, internal and external necking. Any of these mechanisms can cause the final fracture. A damage evolution model for ductile material is derived. Damage evolution is an irreversible and evolving process governed by the second law of thermodynamics. An irreversible thermodynamics theory for constitutive equations has been proposed as the most general framework for unifying the modelling of inelastic deformation and internal damage of materials. This theory can be extended to the theory of damage mechanics by describing the internal state changes due to the material damage via the use of proper internal state variables. The damage variable D is treated as one of the internal state variables which influences the free energy of the system.

A damage evolution model for ductile materials has been derived based on the

concepts of incremental complementary energy and effective stress (Mou and Han 1996) but the model is only valid for proportional loading. According to this model, damage is dependent on the accumulated strain, the stress triaxiality ratio and the strain-hardening exponent of the material. The experimental results showed that the model is capable to predict damage evolution. Among the above stated factors influencing the damage evolution in ductile material, the stress triaxiality ratio has the greatest effects. This model was based on the assumption of isotropic damage and constant stress triaxiality ratio during loading. The verification of the model has also been compared with the experimental results done by Chow and Wang (1987a).

Ductile fracture relates to the density changes due to the inevitable formation of microvoids during the plastic deformation process, but this theory has not yet be readily to use for practical problems as it is difficult to measure the local changes in density. This project refers to sheet metal forming and the thickness of sheet metal is small, at 0.8 mm, therefore the density changes cannot be calculated in this case. A number of damage models have been derived such as the one created by Tang and Lee (1995a,b) which was used to predict ductile fracture. A void-damage model, by Chow and Lu (1992a,b), used to analyze growth and coalescence of microvoids for ductile damage. A model developed for anisotropic ductile damage (Lemaitre 1985) based on the principle of total complementary energy and applied to investigate ductile failure of notched plates (Sassnouni et al 1994). A microdamage evolution equation has been formulated (Tai and Yang 1986) based on the irreversible thermodynamics and orthogonal flow rule. A macrodamage equation was then obtained based on the principle of minimum strength. The damage model based on the incremental complementary energy and applied to determine the size of damage

zones and damage distributions in ductile materials.

Inhomogeneous materials have the existence of discontinuities such as micro-voids, micro-cracks and inclusions. When these materials undergo plastic or local plastic deformation, the stresses and strains within the deforming materials are not uniformly distributed therefore microcracks appear at the location of these defects. In damage mechanics, the damage variable is used to describe the degradation processes and interprets as three phases shown in Figure 2-2 (Mou and Han 1996). The first stage is the damage generation when the damage is very small and is mainly caused by void nucleation. The second stage is the damage growth when the damage increases as the voids grow. The final stage is the damage instability when ductile fracture occurs due to void coalescence. Therefore it is highly desirable to develop a damage model for predicting the damage evolution in ductile materials. From the above diagram, the damage growth period is very important as the load capacity and life expectancy of a structure are dependent principally on it.

As mentioned earlier, ductile damage leads to ductile (plastic) fracture when large plastic strain in metals is accompanied with nucleation and growth of microvoids and microcracks. By using the general equations of the continuum damage mechanics and applying the numerical methods, it is possible to predict the level of damage and the conditions of ductile fracture for different structures. In isotropic damage, the total strain component ε_{ij} consist of the elastic strain ε_{ij}^{e} and the plastic strain ε_{ij}^{p} .The damage criterion is based on the effective stress of the damaged material. When the internal variable ψ reaches its critical value, the damage growth becomes unstable and macrocrack (failure) occurs.

Chow and Wang (1987b) developed an anisotropic damage evolution equation and a constitutive equation of plasticity was formulated using a damage effect tensor $\underline{\underline{M}}(\underline{\underline{D}})$. Later, a generalized damage characteristic tensor $\underline{\underline{J}}$ has been developed to characterize anisotropic damage evolution. $\underline{\underline{J}}$ was compatible with $\underline{\underline{M}}(\underline{\underline{D}})$. and could be reduced to a scalar equation if the damage state was isotropic. $\underline{\underline{M}}(\underline{\underline{D}})$ was a symmetric 4^{th} order tensor. The proposed model involved the constitutive equations of elasticity, plasticity and damage to provide a comprehensive theory of anisotropic damage. Conducting simple tension test of Al2024-T3 has performed verification of the proposed model.

During plastic deformation process, a model (Zheng et al 1992) based on the irreversible thermodynamic and orthogonal flow rule taking the advantage of a specific free energy and plastic potential with internal variables has revealed the evolution of ductile damage. The model was suitable for proportional and non-proportional loading. By combining the proposed model with a constitutive equation for porous material and method of analysis of metal forming processes, it was possible to predict the ductile damage in the interior of a deforming body, to predict product quality and material workability as well.

Zhu and Cescotto (1995) constitutive model was also based on the irreversible thermodynamics to develop an energy-based anisotropic damage model at finite strains for ductile fracture. Three major anisotropies were considered including anisotropic elasticity, anisotropic plasticity and anisotropic damage. The model focused on the characteristic tensor and was based on the hypothesis of damage energy equivalence. The concept of energy played an important role in deriving the

damage effect tensor $\underline{M}(\underline{D})$, the damage characteristic tensor $\underline{I}$, the effective plastic characteristic tensor $\underline{H}$, and in establishing the plastic evolution law and the damage evolution law. The proposed anisotropic damage model was suitable for large-scale computation by implementing in the existing finite element programs to solve practical engineering problems.

Plastic deformation of metal is usually accompanied by internal damage which leads to the failure or fracture of metal components, therefore it is necessary to reveal the evolution characteristic of ductile damage metal in large plastic deformation processes. The fundamental principles of irreversible thermodynamics with internal variable were also used to establish a ductile damage model (Zheng et al 1996) which accounts for the dissipation of ductility of metal due to deformation as the internal damage variable. By taking the dissipation of ductility of metal induced by deformation as the internal variable could directly estimate the onset of macrocrack initiation and crack propagation of metal suffering complicated deformation processes.

Sheet metal forming is a localization procedure of deformation and damage. The investigation of the limits of sheet forming has been divided into two categories: flow theory and deformation theory of plasticity. The application of continuum damage mechanics (CDM) is to determine the limit strain of sheet forming. A CDM criterion for ductile fracture was carried out (Wang 1994) by tensile test under both proportional and non-proportional loading conditions. The mixed mode ductile fracture criterion was proposed which stated that the crack propagates in the direction of the maximum damage integral W_d and W_d reached its critical value.

Wang (1995) derived a new local fracture criterion to predict the forming limits of sheet then adopted the proposed fracture criterion. The criterion is also used for the selection of forming alloys and the forming technology. The application of CDM was to calculate the local stress and strain fields including the history effects and to determine the rupture of the volume element of materials.

2.2 Sheet Metal Forming

A wide variety of engineering and consumer products are made from sheet metal forming processes such as deep drawing, rolling, forging and stamping. The success of these processes depends upon various variables such as material properties, die geometry, lubrication and press speed. Knowledge of the above processes and the formability of metal could lead to improvements in the design of sheet metal components and the success of metal forming operation in the manufacturing industry.

In forming processes, sheet metal has its own stretchable limitation and if exceeded, the material will rupture. Sheet metal forming differs from bulk forming because tension predominates in sheet forming process and compression in bulk forming processes. Metal forming comprised of three phases, namely diffused necking, localized necking and final rupture. The failure in sheet forming can be caused by localized necking and or ductile fracture.

2.2.1 Formability of sheet metals

It is usual in engineering design against fracture that large plastic deformations need to be taken into account. There are three types of fracture namely cleavage, nucleation and growth of voids, and rupture. Cleavage is usually considered to be a form of brittle fracture and characterizes by no apparent deformation in the nearby region of the crack. Fracture by void is a typical feature in ductile fracture and the process in the growth of void consists of three sequential stages: void nucleation, void growth and void coalescence. Rupture, in general sense like necking and shearing, is a further type of ductile fracture which is associated with plastic instability.

There is an important issue in thorough understanding of the metal forming process because it eliminates costly machining and welding operations, and makes it possible to produce components at a very high rate. The ability of materials to undergo complex forming operations depends largely upon the degree of plastic stability conditions. Therefore, formability may be defined as the limiting response of a material to a particular forming process without the occurrence of instability.

Basically, there are two types of failure processes in sheet metal forming industry and they are the localized necking and the wrinkling. Both failure processes will occur in deformation process and affect the formability in sheet metals. The localized necking occurs when materials are subjected to stretching in the plane of the sheet and as shown in Figure 2-3. Once necking begins to develop in a critical small area on the sheet, plastic deformation will concentrate to that small necking

area. Wrinkling happens in relatively large areas when compressive in-plane stress is applied to that area.

The formability of metals has been conventionally analyzed by using the classical plasticity theory (Hill 1952). This theory predicts the localized necking will not occur in a uniform sheet but in fact the loading condition in the sheet metal forming process is non-proportional and is in biaxial loading status, therefore the flow theory and the deformation theory of plasticity are then developed. There is a common drawback to the above theories since they ignore the degradation of materials caused by the formation of micro-defects.

2.2.2 Conventional methods in formability prediction

For a successful sheet metal forming operation, knowledge of the formability of sheet metal is very important. Modelling the sheet metal forming conditions were made by using what is termed as formability test. The common method of presenting the results of such experimental measurements is in terms of the forming limit strains. The state of strain to be obtained is limited by two phenomena. They are the plastic instability giving rise to unexpected local changes of shape, and the damage which may produce unexpected cracks. The later phenomenon is focused at in this project.

Many researches have been performed to understand the metal forming process and predict the forming limit of sheet metal. The necking problem has been studied by Swift (1952) and Mellor (1960). The conventional method in predicting the formability of sheet metal was based on the classical plasticity theory (Hill 1952). The theory predicted the localized necking would not occur in a uniform sheet metal subjected to positive biaxial stretching. Later, Keeler (1965) developed an idea as a convenient way of studying the limitation of the formability of sheet metal under biaxial stress. The strain values were plotted based on the maximum principal surface strain as ordinate against the minimum principal surface strain as abscissa. The diagram is the well known forming limit diagram (FLD) and is widely used because the FLD is designed to define the localized necking of a material and is used to measure the maximum formability of sheet metal products. For example, sheet metal can fail in biaxial tension by tensile plastic instability (necking).

Accepted formability tests include the Erichsen and Olsen test for formability in Figure 2-4, the Swift test for deep drawing in Figure 2-5, and the Hecker and Ghosh test for assessing formability under various strain states (Williams 1993) in Figure 2-6. Each of these tests uses a simplified geometry, which generates a stress or strain state in the material, that is representative of a forming condition seen in a more complex part. The most common test in evaluating the formability of sheet metal is Erichsen test. It allows the effect of tool-workpiece interaction and lubrication on formability to be studied.

Hill's theory contradicted the practical experiences by Keeler (1968) and Hecker (1975a,b) whereas the sheet was marked with closed packed array of circles using

photoprinting techniques. After testing a series of widths of a specific sheet material, the deformation of the circles was measured in regions where unacceptable deformation of the sheets (necking or tearing) has occurred. The boundaries between failed and safe regions were plotted on the forming limit diagram in terms of major and minor strains (as shown in Figure 2-7).

The strain limit has been measured closely to the fracture point of a sheet metal. The strain values are plotted on a graph with major strains as ordinate and minor strains as abscissa, and so FLD be constructed. The FLD is a measure of the local limit of the surface strains that occur at the onset of a localized necking, and it is one of a number of limit strain loci which define the safe region for sheet forming in strain space and represents the limit strains for the most common failure mode such as tearing (Williams 1993). The understanding of the strain distribution is critical to the study of the formability of a material. A typical FLD is shown in Figure 2-8. Three general strain conditions are commonly observed in a forming operation:

a). Biaxial stretching (e.g. bulging), characterized by a tensile major and minor strain, is represented on the right hand side of the FLD.

b). The left side of the FLD represents drawing, where the material is allowed to draw-in, resulting in a positive major strain and a negative minor strain.

c). Plane strain deformation is characterized by a zero in-plane minor strain. This strain condition forms the tip of the FLD, the point of lowest formability, and is usually the limiting case in a complex forming problem.

As comparison to the above photoprinting technique, surface girding technique

coupled with some kind of photography was employed to analyze metal forming processes experimentally. Computerized procedures have also been developed to simplify data reduction process, but the girding technique along with ordinary photography was still laborious so that it led logically to the use of digital image process (DIP) by Joshi (1992). With the application of DIP for the measurement of strain, large deformation close to the fracture point and the plastic instability was then monitored. The accuracy of the DIP system could be improved by using equipment with higher pixel intensity and better resolution. The analysis of the strain distribution needed to have an addition of another camera to obtain at least two views of deforming samples.

There is a certain difficulty in correlating the experimental results from spherical punch stretch tests with the theoretical models due to the sensitivity of the analysis to the friction that is hard to evaluate. A method of stretch forming which eliminates this difficulty is the bulge test. The bulge test provide information on stretch forming for the limited condition of balanced biaxial straining therefore it can be used to determine a material's mechanical properties under biaxial loading conditions.

Since the FLD is experimentally determined, there is an uncertainty as to how the limiting strains should be defined since none of the test methods provide a clear distinction between necking and uniform deformation regions. The gauge size of the circles is generally used to measure strain because the strain gradients within the deformed sheet are always present. The magnitude of the strain gradients are different between test techniques that involve in or out of plane deformation which in

turn can change the FLD for a given test material (Zaverl 1982).

On the other hand, a number of experimental tests had been carried out by Azrin and Backofen (1970), Ghosh and Hecker (1974, 1975), Painter and Pearce (1974), and they demonstrated that thin sheets subjected to positive biaxial tension could be failed by localized necking, therefore an industrial problem was then be evolved and needed to be solved. For the prediction of localized necking under biaxial tension, Marciniak and Kuczynski (1967) have demonstrated an initial approach. They proposed an analytical method by introducing a pre-existing material imperfection in the sheet. This method was later known as M-K theory and was supported by other researchers (Needleman and Rice 1978, Needleman and Triantafyllidis 1978, Bassani et al 1979). Later, Shi (1989) developed a model based on the M-K method by introducing a strain gradient term in the constitutive equation to consider the bending effect on the localized necking in anisotropic sheets. The effects of strain gradient, punch curvature and sheet thickness on the forming limit diagram, beside the effects of strain and strain rate hardening, plastic anisotropy and deformation heating, were also considered.

However, the predicted results of the forming limit diagram by either the Hill's theory or the M-K theory (as shown in Figure 2-9) did not correlate well with the experimental data obtained by Azrin and Backofen (1970), Marciniak et al (1973), Tadros and Mellor (1975). In addition, a parameter was used in the M-K theory to describe the initial geometric non-uniformity of sheet metal. The predicted results were sensitive to the parameter and the selection of the parameter was arbitrary and non-physical, therefore the M-K theory could only be considered as a computational

tool rather than a scientifically based theory.

A bifurcation analysis of localized necking was proposed by Hutchinson et al (1978) and Hutchinson and Neale (1978a,b), using the J_2 flow theory and the J_2 deformation theory of plasticity. The results between these two theories showed some uncertainty whether a flow theory (based on a smooth yield surface) could be used to predict the localized necking. It was cleared that the deformation theory and the flow theory would not be reliable in analyzing the localized necking under non-proportional forming history.

A rather simple model of a material with a vertex on its yield surface was firstly recognized by Stören and Rice (1975). This model was then named as a finite strain version of the simplest deformation theory of plasticity. The shape of the yield surface could cause localization near the vertex. The necking of a sheet metal was found to lie perpendicular to the major principal direction under biaxial tension. The limit strains given by this analysis were more qualitatively in comparison with the M-K theory.

The effects of variations in material properties and the void growth model for porous plastic materials were introduced (Gurson 1975 and 1977, Needleman and Triantafyllidis 1978). Their analysis was based on the role played by void growth in triggering localized necking. The results showed that the predicted forming limit curves were very sensitive to the differences between the initial void concentrations inside and outside of an inhomogeneous area. Both theories were stated by Stören and Rice (1975) and Needleman and Triantafyllidis (1978), they showed that for high

hardening materials the limit strains would decrease or remain nearly constant with increasing biaxiality but for light hardening materials the limit strains would increase with increasing biaxiality.

Since the introduction of the void growth model by Gurson (1975), a number of investigators started showing their interest to the internal damage of material. Experimental evidence showed that most metallic materials contain different sizes of particles, including precipitates and inclusions, which cause micro-defects. Materials degradation has been studied in characterizing the de-cohesion of the particle-matrix interface and the fragmentation of the particles in metal forming (Parmar and Mellor 1980, Schmitt and Jalinier 1982).

2.2.3 Applicability of damage mechanics in formability prediction

Damage mechanics has been applied to metal forming by Schmitt and Jalinier (1982). They found that there were two cases of damage. One of them was the decohesion of the particle matrix interface. A small damage was developed in uniaxial tension while a large amount of damage was developed in equibiaxial stretching. The other case of damage was done by fragmentation of the particle. The degree in damage was about the same in uniaxial tension and equibiaxial stretching.

The damage models proposed by Lee et al (1985) and Lemaitre (1983) and Li et

al (1983) were related to fracture limit diagrams and performed the prediction of the fracture limit diagrams as well. It has already mentioned in section 2.2 that the metal forming comprised of three phases namely diffused necking, localized necking and final rupture. Theoretically, a forming limit diagram should contain the three phases as above. There were some shortcomings in Lemaitre and Li et al's works. In Lemaitre's work (1983), both material and damage were assumed to be isotropic. In Li et al's work (1983), the material was considered as an orthotropic but the damage was isotropic. In fact, both material and damage should be treated as orthotropic. The above drawbacks have been overcome and developed by Chow et al (1996a,b) and Lee et al (1997) without the assumption of initial groove on the sheet metal surface. The forming limit diagrams have been predicted by using VDIF steel, 2024T3 and 6111T4 aluminium alloys.

The formability of sheet metal can be improved by identifying an optimized strain paths and in turn a desired deformation can be achieved. A damage criterion based on a damage model for anisotropic material has been considered to be equivalent to the plastic strain criterion by taking into account of the stress state and can be used for orthotropic material, transversely isotropic material and isotropic material (Tai and Yang 1987a-c). They stated that the damage criterion for sheet metal forming can be applied to predict the fracture limit curve as comparison with the forming limit curve (see Figure 2-10). The proposed damage criterion involves shear joining of voids after considerable void growth is the governing microstructural process (Ghosh 1976).

An isotropic plastic damage model for an orthotropic material has also been

proposed based on the effective stress concept, on the hypothesis of strain equivalence and on thermodynamics. The derived model has been simplified for a transversely isotropic material in the plane stress state and can be applied to analyze the formability of sheet metal (Tai 1988). The proposed model showed that the internal damage of a sheet metal subject to biaxially stretching depended not only on the material properties but also on the effective plastic strain and stress state. The damage equation has been combined with the M-K model showing that the internal damage has a significant influence on the limit strains and the inhomogenities of material properties.

In general, the formability of sheet metal is a localization process of deformation and damage (Needleman et al 1978s). Keeler and Backofen (1963) work has investigated the limit of sheet forming in terms of flow theory (Marciniak and Kuczynski 1967, Hill 1952) and deformation theory (Stören and Rice 1975) of plasticity. Later, Krajcinovia and Lemaitre (1987) and the others (Wang and Chow 1989, Wang 1994, 1995) employed the damage mechanics to the formability of sheet metal. The application of the damage mechanics criterion is to be used to determine the limit strain of sheet forming. Wang (1995) applied the constitutive equations for elasticity-plasticity coupled with damage to derive a fracture criterion in predicting the forming limits of sheet. It has been assumed that the sheet was under plane stress state during the forming process. The derived model showed practical importance for the selection of forming alloys and the forming technology.

2.3 Research Methodology

The following flow diagram gives an overview of the research methodology.

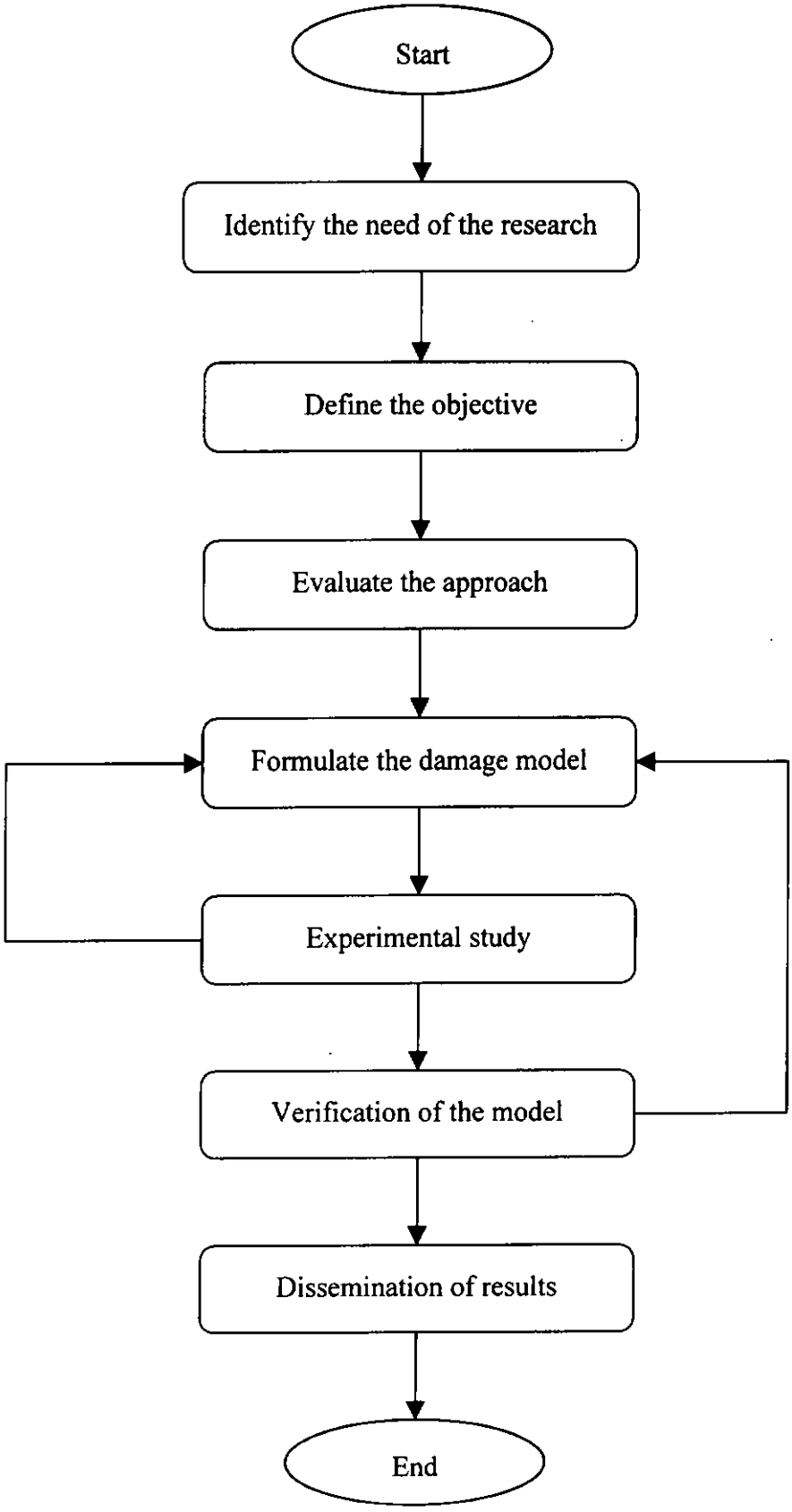

At the beginning of this study, search in background knowledge of damage mechanics and sheet metal forming has been carried out. The identification and the objective of the research have been laid down. Literature survey was described in this chapter. The evaluation of the approach to tackle the necking problem in sheet metal forming was the development of a damage model for fracture strain prediction. The approach was firstly to lay out the construction of the constitutive modelling, and then outlined the usage and determination of the continuity tensor. The proposed model was based on a fracture criterion and the model has been demonstrated by carrying out experimental tests such as the Erichsen test and tensile test. Further verification of the proposed model has been compared with the data obtained from Ghosh (1976). The results showed a good correlation between the theoretical prediction and the experimental works. At the end, a conclusion has been drawn out and stated that damage mechanics could be a reliable and accurate method to analyze and predict the fracture strain of sheet metal.

Chapter 3. Development of a Damage Model for Fracture Strain Prediction

In this research project, a second order continuity tensor (Tang et al 1998a-c, Tang et al 1999a,b), has been proposed to characterize anisotropic damage of an anisotropic material based on the hypothesis of elastic strain energy equivalence. The relationship between the continuity tensor and the effective elastic stiffness tensor of the anisotropic material has also been developed. The components and eigenvalues of the continuity tensor in terms of the apparent engineering elastic coefficients have been expressed explicitly for a 2-dimensional case. The present formulation does not require the assumption that the principal directions of damage must coincide with those of the material.

Before discussing the above proposed second order continuity tensor, constitutive modelling has been described in the following section since it shown a relationship between stress and strain. Section 3.2 describes the continuity tensor and its determination is illustrated in section 3.3. Also discussed is the relation between the continuity tensor and the damage parameters in section 3.4. The effect of the triaxiality of stress on the deformation-damage-fracture process has also been studied as well as presented in section 3.5.

3.1 Constitutive Modelling

As mentioned earlier in section 2.1, there were three progressive stages in the physical process of fracture. The second stage is the mesoscale level of a representative volume element (RVE), this is the growth and the coalescence of microcracks or microvoids which together initiate a crack. The constitutive equations for mechanics analysis are written at the mesoscale level and can be applied for most materials in general cases.

Under large deformation and for a RVE of an intact or damaged elasto-plastic material (Tang et al 1998b), the finite strain tensor ε can be decomposed into the elastic and plastic components as:

$$\varepsilon_{ij} = \varepsilon_{ij}^{e} + \varepsilon_{ij}^{p} \tag{3.1.1}$$

where ε_{ij}^{e} and ε_{ij}^{p} are the elastic strain tensor and the finite plastic strain tensor, respectively. Hence, the rate tensor $\dot{\varepsilon}$, with respect to time, can be expressed as

$$\dot{\varepsilon}_{ij} = \dot{\varepsilon}_{ij}^{e} + \dot{\varepsilon}_{ij}^{p} \tag{3.1.2}$$

The continuity tensor ψ, which is an internal state variable, describes the degradation of material integrity (Kachanov 1958, 1986, Tang 1995, Tang et al 1998a-c, Tang et al 1999a,b). Based on the law of thermodynamics, the Helmholtz free energy density function Φ is used to represent the thermodynamic state of a

RVE of a damaged elasto-plastic material (Figure 3-1). For an isothermal case, with consideration of coupling between elasticity and damage, the free energy density function expressed in the strain space is:

$$\Phi = \Phi_e(\varepsilon^e, \psi) + \Phi_p(\varepsilon^p, \bar{\varepsilon}) \tag{3.1.3}$$

where Φ_e and Φ_p are respectively the elastic and the plastic potentials.

Φ_p relates to the plastic strain tensor ε^p and the equivalent plastic strain $\bar{\varepsilon}$ where

$$\bar{\varepsilon} = (\frac{2}{3}\varepsilon_{ij}^p \varepsilon_{ij}^p)^{1/2} \tag{3.1.4}$$

With the assumption of small elastic deformation, the elastic potential Φ_e can be expressed in terms of the elastic strain energy density of damaged material as follows

$$\Phi_e = \frac{1}{2}\tilde{E}_{ijkl}\varepsilon_{ij}^e \varepsilon_{kl}^e \tag{3.1.5}$$

where $\tilde{\mathbf{E}}(\psi)$ is the effective elastic stiffness tensor and depends on the state of material damage. The stress tensor σ conjugating to ε^e can be obtained by the elastic stress-strain relation:

$$\sigma_{ij} = \frac{\partial \Phi_e}{\partial \varepsilon_{ij}^e} = \tilde{E}_{ijkl}\varepsilon_{kl}^e \tag{3.1.6}$$

From the anisotropy theory of damage mechanics, the effective stress tensor $\tilde{\sigma}$ and the effective elastic strain tensor $\tilde{\varepsilon}$ can be obtained from the following two transformations:

$$\tilde{\varepsilon}_{ij}^{e} = N_{ijkl}\varepsilon_{kl}^{e} \tag{3.1.7}$$

and

$$\tilde{\sigma}_{ij} = M_{ijkl}\sigma_{kl} \tag{3.1.8}$$

where **N** and **M** are the damage influence tensors. For a RVE of damaged material, the stress-strain relation can be established using eqs.(3.1.6), (3.1.7), and (3.1.8) together with the hypothesis of elastic strain energy equivalence. The nonlinear elastic stress-strain relation with damage can be derived as

$$\sigma_{ij} = N_{klij}N_{opmn}E_{klop}\varepsilon_{mn}^{e} \tag{3.1.9}$$

where **E** is the intact elastic stiffness tensor. Thus, the relation of the two elastic damage influence tensors can be expressed as:

$$M_{ijkl} = N_{klij}^{-1} \tag{3.1.10}$$

In a material damage process, the inequality of dissipation power can be derived on the basis of the second law of thermodynamics:

$$\sigma_{ij}\dot{\varepsilon}_{ij}^{p} - R\dot{\bar{\varepsilon}} - Y_{ij}\dot{\psi}_{ij} \geq 0 \tag{3.1.11}$$

The first term of the above expression is referred to as the dissipation power of plastic deformation. $\boldsymbol{R}$ is the thermodynamic force conjugating to the rate of the equivalent plastic strain $\dot{\bar{\varepsilon}}$ and expresses the increment in plastic yielding surface. Another thermodynamics force $\boldsymbol{Y}$ conjugates to the continuity tensor ψ, i.e.

$$Y_{ij} = \frac{\partial \Phi_e}{\partial \psi_{ij}} \tag{3.1.12}$$

$\boldsymbol{Y}$ is often referred to as the damage growth force or the specific damage energy release rate. Under the hypothesis of normal dissipativity, the evolution laws can be expressed as:

$$\dot{\varepsilon}_{ij}^{p} = \dot{\gamma} \frac{\partial \Omega}{\partial \sigma_{ij}} \tag{3.1.13}$$

$$\dot{\bar{\varepsilon}} = -\dot{\gamma} \frac{\partial \Omega}{\partial R} \tag{3.1.14}$$

$$\dot{\psi}_{ij} = -\dot{\gamma} \frac{\partial \Omega}{\partial Y_{ij}} \tag{3.1.15}$$

where Ω is the dissipative potential, which is constructed from the experimental results of plastic deformation and damage. $\dot{\gamma}$ is the non-negative Lagrange multiplier.

By Legendre transformation of the free energy density function with respect to strain, the complementary elastic energy density function Ψ_e can be obtained and

expressed as

$$\Psi_e(\sigma,\psi) = \frac{1}{2}\tilde{C}_{ijkl}\sigma_{ij}\sigma_{kl} \tag{3.1.16}$$

where $\tilde{\mathbf{C}}(\psi)$ is the effective elastic compliance tensor of damaged material. The relationship between $\tilde{\mathbf{C}}$ and $\tilde{\mathbf{E}}$ can be expressed as:

$$\tilde{C}_{ijmn}\tilde{E}_{mnkl} = \delta_{ik}\delta_{jl} \tag{3.1.17}$$

where δ is the Kronecker delta. Similar to the derivation of eqs.(3.1.6) and (3.1.12), the elastic stress-strain relation and the expression of specific damage energy release rate tensor in the stress space can be determined:

$$\varepsilon_{ij}^{e} = \frac{\partial \Psi_e}{\partial \sigma_{ij}} = \tilde{C}_{ijkl}\sigma_{kl} \tag{3.1.18}$$

and

$$Y_{ij} = -\frac{\partial \Psi_e}{\partial \psi_{ij}} \tag{3.1.19}$$

3.2 Continuity Tensor

For 2-dimensional analyses, the four damage parameters used for characterizing anisotropic damage of orthotropic materials are often defined directly from the

effective elastic properties as follows:

$$D_1 = 1 - \frac{\tilde{E}_1}{E_1} \tag{3.2.1}$$

$$D_2 = 1 - \frac{\tilde{E}_2}{E_2} \tag{3.2.2}$$

$$D_3 = 1 - \frac{\tilde{G}_{12}}{G_{12}} \tag{3.2.3}$$

$$D_4 = 1 - \frac{\tilde{\nu}_{12}}{\nu_{12}} \tag{3.2.4}$$

In general, a relation between the effective elastic stiffness tensor $\tilde{\mathbf{E}}$ and the intact elastic stiffness tensor **E** of anisotropic material element can be established on the basis of the equivalent elastic strain energy hypothesis (Shen and Wu 1992, Shen 1995), which is similar to the equivalent complementary elastic energy hypothesis (Cordebois and Sidoroff 1979), can be expressed as follows

$$\tilde{E}_{ijmn} = N_{klij} N_{opmn} E_{klop} \tag{3.2.5}$$

where **N** is a fourth order symmetric tensor, namely the damage influence tensor, that relates to the property of material damage.

For simplicity, the fourth order damage influence tensor **N** may be constructed by using a second order continuity tensor ψ (Shen and Wu 1992, Shen 1995) which is used to characterize directly anisotropic damage state of an anisotropic material element, i.e.

$$N_{ijmn} = \frac{1}{2}(\psi_{im}\delta_{nj} + \psi_{nj}\delta_{im}) \tag{3.2.6}$$

The continuity tensor is defined by eq.(3.2.6) which satisfies the symmetric requirement of the effective stress tensor, the effective elastic strain tensor and the effective elastic stiffness tensor. For example, if eq.(3.2.6) is tensorially multiplied by the nominal strain ε^e_{mn} , it can be obtained that

$$\tilde{\varepsilon}^e_{ij} = N_{ijmn}\varepsilon^e_{mn} = \frac{1}{2}\left(\psi_{im}\varepsilon^e_{mj} + \varepsilon^e_{in}\psi_{nj}\right) \tag{3.2.7}$$

which shows that the effective elastic strain $\tilde{\varepsilon}^e_{ij}$ is a symmetric second order tensor. By comparing eq.(3.1.6) with eq.(3.1.9) and considering eq.(3.2.6), we have

$$\tilde{E}_{ijmn} = \frac{1}{4}(\psi_{ki}\delta_{jl} + \psi_{jl}\delta_{ki})(\psi_{om}\delta_{np} + \psi_{np}\delta_{om})E_{klop} \qquad (i = 1,2,3) \tag{3.2.8}$$

which can be contracted in Voigt notation as

$$\tilde{E}_{ij} = H_{klij}E_{kl} \qquad (i,j,k,l = 1,2,....6) \tag{3.2.9}$$

$\mathbf{H}(\psi)$ is originally an 8^{th} order tensor operator. Due to symmetry, it generally has $21 \times 21 = 441$ independent components. For an initially intact orthotropic RVE, the values of H_{ijkl} are derived and the components of $\boldsymbol{H(\psi)}$ transforming $\boldsymbol{E}$ to $\tilde{\boldsymbol{E}}$ can be determined by eq.(3.2.9) as follows:

$$H_{1111} = \psi_1^2, H_{2222} = \psi_2^2, H_{3333} = \psi_3^2,$$

$$H_{1155} = H_{3355} = H_{1355} = \psi_5^2,$$

$$H_{1166} = H_{2266} = H_{1266} = \psi_6^2,$$

$$H_{2244} = H_{3344} = H_{2344} = \psi_4^2,$$

$$H_{4422} = H_{4433} = H_{5566} = H_{6655} = \psi_4^2/4,$$

$$H_{4455} = H_{5544} = H_{6611} = H_{6622} = \psi_6^2/4,$$

$$H_{4466} = H_{5511} = H_{5533} = H_{6644} = \psi_5^2/4,$$

$$H_{4444} = (\psi_2 + \psi_3)^2/4,$$

$$H_{5555} = (\psi_1 + \psi_3)^2/4,$$

$$H_{6666} = (\psi_1 + \psi_2)^2/4,$$

$$H_{4423} = \psi_4^2/2, H_{5513} = \psi_5^2/2, H_{6612} = \psi_6^2/2,$$

$$H_{1212} = \psi_1\psi_2, H_{1313} = \psi_1\psi_3, H_{2323} = \psi_3\psi_2,$$

$$H_{1412} = H_{1413} = \psi_1\psi_4/2, H_{1511} = H_{1513} = \psi_1\psi_5/2,$$

$$H_{1611} = H_{1612} = \psi_1\psi_6/2, H_{2422} = H_{2423} = \psi_2\psi_4/2,$$

$$H_{2512} = H_{2513} = \psi_2\psi_5/2, H_{2622} = H_{2612} = \psi_2\psi_6/2,$$

$$H_{3433} = H_{3423} = \psi_3\psi_4/2, H_{3533} = H_{3513} = \psi_3\psi_5/2,$$

$$H_{3623} = H_{3613} = \psi_3\psi_6/2,$$

$$H_{1555} = H_{3555} = \psi_5(\psi_1 + \psi_3)/2,$$

$$H_{1666} = H_{2666} = \psi_6(\psi_1 + \psi_2)/2,$$

$$H_{2444} = H_{3444} = \psi_4(\psi_2 + \psi_3)/2,$$

$$H_{1455} = H_{1466} = H_{2466} = H_{3455} = \psi_6\psi_5/2,$$

$$H_{1566} = H_{2544} = H_{2566} = H_{3544} = \psi_4\psi_6/2,$$

$$H_{2655} = H_{3644} = H_{1655} = H_{3655} = \psi_4\psi_5/2,$$

$$H_{4533} = H_{4566} = H_{4512} = H_{4513} = H_{4523} = \psi_4\psi_5/4,$$

$$H_{4622} = H_{4655} = H_{4612} = H_{4613} = H_{4623} = \psi_4\psi_6/4,$$

$$H_{5611} = H_{5644} = H_{5612} = H_{5613} = H_{5623} = \psi_6\psi_5/4,$$

$$H_{4544} = \psi_6(\psi_2 + \psi_3)/4, H_{4555} = \psi_6(\psi_1 + \psi_3)/4,$$

$$H_{4644} = \psi_5(\psi_2 + \psi_3)/4, H_{4666} = \psi_5(\psi_2 + \psi_1)/4,$$

$$H_{5655} = \psi_4(\psi_1 + \psi_3)/4, H_{5666} = \psi_4(\psi_2 + \psi_1)/4,$$

The reminding $H_{ijkl} = 0$.

Thus, in a 2-dimensional case, the corresponding values of E_{ij} and $\widetilde{E}_{ij}$ are

$$[E_{11}, E_{22}, E_{12}, E_{66}] \equiv [E_{1111}, E_{2222}, E_{1122} = E_{2211}, E_{1212}]$$

and

$$[\widetilde{E}_{11}, \widetilde{E}_{22}, \widetilde{E}_{12}, \widetilde{E}_{66}] \equiv [\widetilde{E}_{1111}, \widetilde{E}_{2222}, \widetilde{E}_{1122} = \widetilde{E}_{2211}, \widetilde{E}_{1212}]$$

Due to symmetry of the continuity tensor ψ, the eigenvalues ψ_i (i = I, II, III), which are also called the principal values of the continuity tensor, are the roots of the following eigen-equation:

$$\psi^3 - \psi^2 I_1 + \psi I_2 - I_3 = 0 \tag{3.2.10}$$

where I_i (i=1,2,3) are the i-th invariant of the continuity tensor ψ, and

$$\left.\begin{aligned} I_1 &= \psi_{ii} \\ I_2 &= \frac{1}{2}(\psi_{ii}^2 - \psi_{ij}^2) \\ I_3 &= \det(\psi) \end{aligned}\right\} \qquad (3.2.11)$$

The sheet metal to be investigated is 0.8 mm thick and the material is under plane stress condition because sheet forming is largely a plane stress operation , therefore the analysis has been generalized to 2-dimensional case rather than 3-dimensional one. It is assumed that the material orthotropy of an orthotropic material element does not change during the damage process under large strain. From equation (3.2.8), the relation between the effective and intact elastic stiffness tensor in matrix can be expressed, for 2-dimensional case, as:

$$\begin{bmatrix} \tilde{E}_{11} \\ \tilde{E}_{22} \\ \tilde{E}_{12} \\ \tilde{E}_{66} \end{bmatrix} = \begin{bmatrix} \psi_1^2 & 0 & 0 & \psi_6^2 \\ 0 & \psi_2^2 & 0 & \psi_6^2 \\ 0 & 0 & \psi_1\psi_2 & \psi_6^2 \\ \frac{1}{4}\psi_6^2 & \frac{1}{4}\psi_6^2 & \frac{1}{2}\psi_6^2 & \frac{1}{4}(\psi_1+\psi_2)^2 \end{bmatrix} \begin{bmatrix} E_{11} \\ E_{22} \\ E_{12} \\ E_{66} \end{bmatrix} \qquad (3.2.12)$$

where the effects of damage on the effective stiffness tensor are characterized by the continuity tensor ψ and ψ_i ($i = 1,2,6$) are the components of the continuity tensor in Voigt notation:

$$[\psi_1, \psi_2, \psi_6] \equiv [\psi_{11}, \psi_{22}, \psi_{12} = \psi_{21}]$$

The components of elastic stiffness tensor **E** and the engineering elastic coefficients of orthotropic material has the following relation:

$$\begin{bmatrix} E_{11} & E_{12} & 0 \\ E_{21} & E_{22} & 0 \\ 0 & 0 & E_{66} \end{bmatrix} = \frac{1}{1-\nu_{12}\nu_{21}} \begin{bmatrix} E_1 & \nu_{12}E_2 & 0 \\ \nu_{21}E_1 & E_2 & 0 \\ 0 & 0 & (1-\nu_{12}\nu_{21})G_{12} \end{bmatrix} \tag{3.2.13}$$

Similarly, for a 2-dimensional RVE of damaged material, eq.(3.2.13) becomes

$$\begin{bmatrix} \tilde{E}_{11} & \tilde{E}_{12} & 0 \\ \tilde{E}_{21} & \tilde{E}_{22} & 0 \\ 0 & 0 & \tilde{E}_{66} \end{bmatrix} = \frac{1}{1-\tilde{\nu}_{12}\tilde{\nu}_{21}} \begin{bmatrix} \tilde{E}_1 & \tilde{\nu}_{12}\tilde{E}_2 & 0 \\ \tilde{\nu}_{21}\tilde{E}_2 & \tilde{E}_2 & 0 \\ 0 & 0 & (1-\tilde{\nu}_{12}\tilde{\nu}_{21})\tilde{G}_{12} \end{bmatrix} \tag{3.2.14}$$

At the principal directions of damage, let

$$\psi_{12} = 0, \psi_{11} = \psi_I, \psi_{22} = \psi_{II}.$$

or

$$\psi_6 = 0, \psi_1 = \psi_I, \psi_2 = \psi_{II}$$

If the principal directions of damage coincide with those of the material, it can be derived in the major material coordination system that

$$\begin{bmatrix} \tilde{E}_{11} \\ \tilde{E}_{22} \\ \tilde{E}_{12} \\ \tilde{E}_{66} \end{bmatrix} = \begin{bmatrix} \psi_I^2 & 0 & 0 & 0 \\ 0 & \psi_{II}^2 & 0 & 0 \\ 0 & 0 & \psi_I\psi_{II} & 0 \\ 0 & 0 & 0 & \frac{1}{4}(\psi_I + \psi_{II})^2 \end{bmatrix} \begin{bmatrix} E_{11} \\ E_{22} \\ E_{12} \\ E_{66} \end{bmatrix} \tag{3.2.15}$$

In general, the principal coordinate system of damage is not coincide with that of the material, i.e. the component ψ_{12} or ψ_6 will be non-zero. Therefore, all the

three components of the continuity tensor in 2-dimensional space need to be determined in terms of both the effective elastic stiffness components $\widetilde{E}_{ij}$ and the intact elastic stiffness components E_{ij} .

3.3 Determination of Continuity Tensor

The determination of continuity tensor components ψ_i (i = 1,2,6) is performed in a major material frame. A set of equations can be re-written from eq.(3.2.12) as follows

$$\widetilde{E}_{11} = \psi_1^2 E_{11} + \psi_6^2 E_{66} \tag{3.3.1}$$

$$\widetilde{E}_{22} = \psi_2^2 E_{22} + \psi_6^2 E_{66} \tag{3.3.2}$$

$$\widetilde{E}_{12} = \psi_1 \psi_2 E_{12} + \psi_6^2 E_{66} \tag{3.3.3}$$

$$\widetilde{E}_{66} = \frac{1}{4}\psi_6^2 (E_{11} + E_{22} + 2E_{12}) + \frac{1}{4}(\psi_1 + \psi_2)^2 E_{66} \tag{3.3.4}$$

It can be obtained from eqs.(3.3.1) and (3.3.2) respectively that

$$\psi_1 = +\sqrt{\frac{\widetilde{E}_{11}}{E_{11}} - \psi_6^2 \frac{E_{66}}{E_{11}}} \tag{3.3.5}$$

and

$$\psi_2 = +\sqrt{\frac{\tilde{E}_{22}}{E_{22}} - \psi_6^2 \frac{E_{66}}{E_{22}}} \tag{3.3.6}$$

Besides, using eq.(3.3.3), it gives

$$\psi_1 \psi_2 = \frac{\tilde{E}_{12} - \psi_6^2 E_{66}}{E_{12}} \tag{3.3.7}$$

Substituting eqs.(3.3.5) and (3.3.6)into eq.(3.3.4), and using eq.(3.3.7), an expression about ψ_6^2 can be derived as follows:

$$\psi_6^2 = \frac{\dfrac{\tilde{E}_{11}}{E_{11}} + \dfrac{\tilde{E}_{22}}{E_{22}} + \dfrac{2\tilde{E}_{12}}{E_{12}} - \dfrac{4\tilde{E}_{66}}{E_{66}}}{\dfrac{E_{66}}{E_{11}} + \dfrac{E_{66}}{E_{22}} + \dfrac{2E_{66}}{E_{12}} - \dfrac{E_x}{E_{66}}} \tag{3.3.8}$$

and the coupling component ψ_6 of continuity tensor is thus:

$$\psi_6 = \pm\sqrt{\frac{\dfrac{\tilde{E}_{11}}{E_{11}} + \dfrac{\tilde{E}_{22}}{E_{22}} + \dfrac{2\tilde{E}_{12}}{E_{12}} - \dfrac{4\tilde{E}_{66}}{E_{66}}}{\dfrac{E_{66}}{E_{11}} + \dfrac{E_{66}}{E_{22}} + \dfrac{2E_{66}}{E_{12}} - \dfrac{E_x}{E_{66}}}} \tag{3.3.9}$$

where

$$E_x = E_{11} + E_{22} + 2E_{12} \tag{3.3.10}$$

The two normal components, ψ_1 and ψ_2, ($\psi_1 \geq 0, \psi_2 \geq 0$) of continuity tensor

can also determined by substituting eq.(3.3.8) into eqs.(3.3.5) and (3.3.6) respectively

$$\psi_1 = +\sqrt{\frac{\tilde{E}_{11}}{E_{11}} - \frac{\frac{\tilde{E}_{11}}{E_{11}} + \frac{\tilde{E}_{22}}{E_{22}} + \frac{2\tilde{E}_{12}}{E_{12}} - 4\frac{\tilde{E}_{66}}{E_{66}}}{\frac{E_{66}}{E_{11}} + \frac{E_{66}}{E_{22}} + \frac{2E_{66}}{E_{12}} - \frac{E_x}{E_{66}}} \frac{E_{66}}{E_{11}}} \tag{3.3.11}$$

and

$$\psi_2 = +\sqrt{\frac{\tilde{E}_{22}}{E_{22}} - \frac{\frac{\tilde{E}_{11}}{E_{11}} + \frac{\tilde{E}_{22}}{E_{22}} + \frac{2\tilde{E}_{12}}{E_{12}} - 4\frac{\tilde{E}_{66}}{E_{66}}}{\frac{E_{66}}{E_{11}} + \frac{E_{66}}{E_{22}} + \frac{2E_{66}}{E_{12}} - \frac{E_x}{E_{66}}} \frac{E_{66}}{E_{22}}} \tag{3.3.12}$$

It is noticed that the three components of the continuity tensor are obtained from the four eqs.(3.3.1)-(3.3.4), therefore one more expression can be derived from eqs.(3.3.3) and (3.2.4) as

$$\tilde{\nu}_{12} = \frac{-\tilde{E}_2 + \sqrt{\tilde{E}_2^2 + 4\left(\psi_1\psi_2 E_{12} + \psi_6^2 E_{66}\right)^2 \tilde{E}_2 / \tilde{E}_1}}{2\left(\psi_1\psi_2 E_{12} + \psi_6^2 E_{66}\right)\tilde{E}_2 / \tilde{E}_1} \tag{3.3.13}$$

The equality of eq.(3.3.13) may be used to assess the suitability of using the proposed formulation to characterize the behaviours of the damage.

Since the continuity tensor is a symmetric second order tensor, the principal values (ψ_I and ψ_{II}) and the corresponding principal direction ϕ can be calculated by using following formuli:

$$\left.\begin{aligned}\psi_I &= \frac{\psi_1+\psi_2}{2}+\sqrt{\left(\frac{\psi_1-\psi_2}{2}\right)^2+\psi_6^2}\\ \psi_{II} &= \frac{\psi_1+\psi_2}{2}-\sqrt{\left(\frac{\psi_1-\psi_2}{2}\right)^2+\psi_6^2}\end{aligned}\right\} \tag{3.3.14}$$

and

$$\phi=\frac{1}{2}\tan^{-1}\left(\frac{2\psi_6}{\psi_1-\psi_2}\right) \tag{3.3.15}$$

where ϕ is the angle between the principal coordinate system of the second order continuity tensor and that of the orthotropic material.

It is worth noting that in the principal damage system ($\psi_6 = 0$) the principal value of continuity tensor in eq. (3.2.12) may be obtained directly by the following formulae

$$\psi_I = (\widetilde{E}_{11}/E_{11})^{1/2} \tag{3.3.16}$$

and

$$\psi_{II} = (\widetilde{E}_{22}/E_{22})^{1/2} \tag{3.3.17}$$

Therefore, it is clear that the continuity tensor can be taken as a damage variable to reflect stiffness degradation of material.

In a 2-dimensional case, the mean value of continuity ψ_m can be estimated by

$$\psi_m = \frac{1}{2}(\psi_1 + \psi_2) = \frac{1}{2}(\psi_I + \psi_{II}) \qquad (3.3.18)$$

It shows that there is no damage while $\psi_m = 1$ and ψ_m decreases as the degree of damage increases.

The anisotropic damage state characterized by the second order continuity tensor can be presented by means of a Mohr's circle of continuity as shown in Figure 3-2 (*a*). The centre of the Mohr's circle is the mean value of the continuity ψ_m, which characterizes the degree of damage of the material element. A pair of points that are 180° apart on the Mohr's circle of continuity represent the component values of the continuity tensor ψ_1, ψ_2 *and* ψ_6 . The intact state of the material element is represented by point 'A' of the Mohr's circle where $\psi_1 = \psi_2 = 1, \psi_6 = 0$. When the damage evolves, as illustrated in Figure 3-2 (*b*), the center of circle will shift left and the radius of the circle will increase because of the irreversibility of the damage.

3.4 Relation between Continuity Tensor and Damage Parameters

The relation between the components of the elastic stiffness tensor and the engineering elastic properties for orthotropic material has been given by eqs.(3.2.13)

and (3.2.14) for 2-dimensional analysis. From eqs.(3.2.13) and (3.2.14), it can be obtained

$$\frac{\widetilde{E}_{11}}{E_{11}} = \frac{1-\nu_{12}\nu_{21}}{1-\widetilde{\nu}_{12}\widetilde{\nu}_{21}}\frac{\widetilde{E}_1}{E_1} \tag{3.4.1}$$

By substituting eqs. (3.2.1), (3.2.2), (3.2.4) and (3.2.14) into the above equation, the below expression is resulted:

$$\frac{\widetilde{E}_{11}}{E_{11}} = H(1-D_1) \tag{3.4.2}$$

where

$$H = \frac{1-\nu_{12}\nu_{21}}{1-\nu_{12}\nu_{21}(1-D_4)^2\dfrac{1-D_2}{1-D_1}} \tag{3.4.3}$$

Similarly,

$$\frac{\widetilde{E}_{22}}{E_{22}} = H(1-D_2) \tag{3.4.4}$$

Besides, it can be obtained from eqs.(3.2.3) and (3.2.14) that

$$\frac{\widetilde{E}_{66}}{E_{66}} = \frac{\widetilde{G}_{12}}{G_{12}} = 1-D_3 \tag{3.4.5}$$

and from eqs.(3.2.1)-(3.2.3),

$$\frac{\tilde{E}_{12}}{E_{12}} = \frac{(E_1 - \nu_{12}^2 E_2)(1-D_1)(1-D_2)(1-D_4)}{E_1(1-D_1) - \nu_{12}^2 E_2(1-D_2)(1-D_4)^2} \tag{3.4.6}$$

By substituting eqs.(3.4.2)-(3.4.6) into eqs.(3.3.11), (3.3.12) and (3.3.9), the components of the continuity tensor ψ_i (i = 1, 2, 6) which are functions of the damage parameters D_i (i = 1, 2, 3, 4) can be derived respectively as follows:

$$\psi_1 = +\sqrt{1 - D_1 - \frac{\Delta}{\Omega}\frac{E_{66}}{E_{11}}} \tag{3.4.7}$$

$$\psi_2 = +\sqrt{1 - D_2 - \frac{\Delta}{\Omega}\frac{E_{66}}{E_{22}}} \tag{3.4.8}$$

and

$$\psi_6 = \pm\sqrt{\frac{\Delta}{\Omega}} \tag{3.4.9}$$

where

$$\Delta = H(1-D_1) + H(1-D_2) - (1-D_3) + \frac{(E_1 - \nu_{12}^2 E_2)(1-D_1)(1-D_2)(1-D_4)}{E_1(1-D_1) - \nu_{12}^2 E_2(1-D_2)(1-D_4)^2} \tag{3.4.10}$$

and

$$\Omega = \frac{E_{66}}{E_{11}} + \frac{E_{66}}{E_{22}} + \frac{2E_{66}}{E_{12}} - \frac{E_{11} + E_{22} + 2E_{12}}{E_{66}} \tag{3.4.11}$$

3.5 Specific Damage Energy Release Rate

By substituting eq.(3.2.12) into eq.(3.1.17) and then into eq.(3.1.16), the complementary elastic energy density function expressed in the principal coordinate system of damage (i.e. $\psi_6 = 0$) for the plane stress problem can be written in Voigt notation as

$$\begin{aligned}\Psi_e &= \frac{1}{2}\tilde{C}_{ij}\sigma_i\sigma_j \\ &= \frac{1}{2}(\tilde{C}_{11}\sigma_1^2 + \tilde{C}_{22}\sigma_2^2 + 2\tilde{C}_{12}\sigma_1\sigma_2 + \tilde{C}_{66}\sigma_6^2) \quad (i,j = 1,2,6)\end{aligned} \tag{3.5.1}$$

in which

$$\tilde{C}_{11} = \frac{C_{11}}{\psi_I^2},\ \tilde{C}_{22} = \frac{C_{22}}{\psi_{II}^2}$$

$$\tilde{C}_{12} = \frac{C_{12}}{\psi_I\psi_{II}},\ \tilde{C}_{66} = \frac{C_{66}}{(\psi_I + \psi_{II})^2} \tag{3.5.2}$$

and σ_i (i=1,2,6) are the components of stress tensor in Voigt notation,

$$[\sigma_1, \sigma_2, \sigma_6] \equiv [\sigma_{11}, \sigma_{22}, \sigma_{12}]$$

C_{ij} and $\tilde{C}_{ij}$ are the components of the intact elastic compliance tensor and the effective elastic compliance tensor in Voigt notation respectively, i.e.

$$[C_{11}, C_{22}, C_{12}, C_{66}] \equiv [C_{1111}, C_{2222}, C_{1122} = C_{2211}, C_{1212} + C_{2121} + C_{1221} + C_{2112}]$$

and

$$[\tilde{C}_{11}, \tilde{C}_{22}, \tilde{C}_{12}, \tilde{C}_{66}] \equiv [\tilde{C}_{1111}, \tilde{C}_{2222}, \tilde{C}_{1122} = \tilde{C}_{2211}, \tilde{C}_{1212} + \tilde{C}_{2121} + \tilde{C}_{1221} + \tilde{C}_{2112}]$$

In order to study the effect of the triaxiality of stress on the deformation-damage-fracture process, the specific elastic energy Ψ_e is divided into two parts (Lemaitre 1992), i.e.

$$\Psi_e = \Psi^b + \Psi^d \tag{3.5.3}$$

The Ψ^b reflects the elastic energy density corresponding to the bulk change of the damaged RVE while the Ψ^d represents the change in elastic energy due to the distortion of the damaged RVE. Moreover,

$$\begin{aligned} \Psi^b &= \frac{1}{2}\sigma_m^2 \tilde{C}_{ijkl}\delta_{ij}\delta_{kl} \\ &= \frac{1}{2}\sigma_m^2\left(\frac{C_{11}}{\psi_I^2} + \frac{C_{22}}{\psi_{II}^2} + \frac{2C_{12}}{\psi_I \psi_{II}}\right) \end{aligned} \tag{3.5.4}$$

and

$$\begin{aligned} \Psi^d &= \frac{1}{2}\tilde{C}_{ijkl}\sigma'_{ij}\sigma'_{kl} \\ &= \frac{1}{2}\left(\frac{C_{11}}{\psi_I^2}\sigma'_1\sigma'_1 + \frac{C_{22}}{\psi_{II}^2}\sigma'_2\sigma'_2 + \frac{2C_{12}}{\psi_I\psi_{II}}\sigma'_1\sigma'_2 + \frac{4C_{66}}{(\psi_I + \psi_{II})^2}\sigma_6^2\right) \end{aligned} \tag{3.5.5}$$

where the hydrostatic stress

$$\sigma_m = \frac{1}{3}\sigma_{kk} \tag{3.5.6}$$

and the deviatoric components of the stress tensor is

$$\sigma'_{ij} = \sigma_{ij} - \frac{1}{3}\,\sigma_{bb}\delta_{ij} \tag{3.5.7}$$

Therefore, the specific damage energy release rate corresponding to the bulk change and to the distortion of the RVE are derived separately by making use of eqs.(3.1.19) and (3.5.4)-(3.5.6) as follows:

$$Y^b = \sigma_m^2[\frac{C_{11}}{\psi_I^3} + \frac{C_{22}}{\psi_{II}^3} + (\frac{1}{\psi_I} + \frac{1}{\psi_{II}})\frac{1}{\psi_I\psi_{II}}C_{12}] \tag{3.5.8}$$

and

$$\begin{aligned} Y^d = {} & \frac{C_{11}}{\psi_I^3}\sigma'_1\sigma'_1 + \frac{C_{22}}{\psi_{II}^3}\sigma'_2\sigma'_2 + (\frac{1}{\psi_I} + \frac{1}{\psi_{II}})\frac{1}{\psi_I\psi_{II}}C_{12}\sigma'_1\sigma'_2 \\ & + \frac{8C_{66}}{(\psi_I + \psi_{II})^3}\sigma_6^2 \end{aligned} \tag{3.5.9}$$

It should be noted that the trace of tensor $\boldsymbol{Y}$ is a measure of energy density. In the principal damage coordinate system,

$$Y = tr(Y_{ij}) = Y_I + Y_{II} \tag{3.5.10}$$

If $\psi_I > \psi_{II}$, the ψ_{II} is the minimum of $\psi_i (i = I, II)$. Let the damage anisotropic ratio

$$b = \psi_{II} / \psi_{I} \leq 1 \tag{3.5.11}$$

The damage anisotropy factor b depends on the strain ratio and the loading history. The equivalent stress $\bar{\sigma}$, which is similar to Simo and Ju's (1987) definition, is now introduced as

$$\bar{\sigma} = [b^3 C_{11}\sigma_1'\sigma_1' + C_{22}\sigma_2'\sigma_2' + (1+b)bC_{12}\sigma_1'\sigma_2' + \frac{8b}{(1+b)^3}C_{66}\sigma_6^2]^{1/2} \tag{3.5.12}$$

Hence, the bulk and distortion components of the release rate of specific damage energy can be obtained as

$$Y^d = \frac{\bar{\sigma}^2}{\psi_{II}^3} \tag{3.5.13}$$

and

$$Y^b = \frac{\sigma_m^2 A}{\psi_{II}^3} \tag{3.5.14}$$

where

$$A = b^3 C_{11} + C_{22} + (1+b)bC_{12} \tag{3.5.15}$$

Finally, the total release rate of specific damage energy is

$$Y = \frac{\bar{\sigma}^2}{\psi_{II}^3} f = Y^d f \tag{3.5.16}$$

where the function $f = f(\sigma_m / \bar{\sigma})$ can be interpreted as the triaxiality of stress given

by

$$f = 1 + \left[b^3 C_{11} + C_{22} + (1+b) b C_{12} \right] \left(\frac{\sigma_m}{\bar{\sigma}} \right)^2 \qquad (3.5.17)$$

f is called the stress triaxiality factor. The stress triaxiality factor defined by eq.(3.5.17) does not only depend on the stress state but also relates to the anisotropy of both material and damage.

Chapter 4. Prediction of Fracture Strains for Sheet Metal Forming

In this chapter, the damage model discussed in the last chapter will be used to predict the fracture strains for sheet metal forming. The prediction is based on a fracture criterion which will be discussed in the following section. Experimental works have been carried out by the Erichsen cupping test and the tensile test of aluminium alloys 2024T3. The verification and the experimental procedure have been discussed briefly in section 4.2. The results show good correlation with the theoretical ones and also compared with Ghosh (1976) data by using other materials such as HS-3 steel, A-K steel and Al2036T4. The discussions and the results are presented in section 4.3.

4.1 Development of Damage-Based Fracture Criterion

For a RVE of damaged material as shown in the last chapter (see Figure 3-1), a second order continuity tensor ψ is used to describe the anisotropic damage of material. The relationship between the continuity tensor ψ and the effective elastic stiffness coefficients of the damaged material has been given in the principal damage co-ordinate system for a 2-dimensonal case as follows:

$$\psi_i = (\widetilde{E}_{ii} / E_{ii})^{1/2} \qquad (i = I, II \text{ and no sum for } i) \tag{4.1.1}$$

where ψ_i $(i = I, II)$ is the principal values of continuity tensor, E_{ij} and $\widetilde{E}_{ij}$ are the components of the intact elastic stiffness tensors and the effective elastic stiffness tensor of the damaged orthotropic material, respectively. With no loss of generality, $\psi_I > \psi_{II}$, ψ_{II} is the minimum of ψ_i $(i = I, II)$ and the damage anisotropy ratio b has been defined in eq.(3.5.11).

Due to minimum integrity or maximum damage in this principal direction of material, ψ_{II} is selected as a governing parameter to establish the damage evolution equation. Therefore, the damage evolution equation of elasto-plastic material is derived for 2-dimensional case (Lemaitre 1984) as

$$\dot{\psi}_{II} = -\frac{Y}{S_0}\dot{\bar{\varepsilon}} \tag{4.1.2}$$

where the equivalent plastic strain $\bar{\varepsilon} = (\frac{2}{3}\varepsilon_{ij}^p \varepsilon_{ij}^p)^{1/2}$ (see eq.(3.1.4)) . Let $\varepsilon_{ij} = \varepsilon_{ij}^p$ for large deformation case, S_0 is a material dependent parameter. It is assumed that the stress-strain relation of the damaged material under multi-axial loading is of the power law type:

$$\frac{\bar{\sigma}}{\psi_{II}} = K\bar{\varepsilon}^n \tag{4.1.3}$$

in which the equivalent stress (Tang et al 1999a) is expressed as

$$\bar{\sigma} = \left[b^3 C_{11}\sigma_1'\sigma_1' + C_{22}\sigma_2'\sigma_2' + (1+b)bC_{12}\sigma_1'\sigma_2'\right]^{1/2} \tag{4.1.4}$$

Assuming that

$$\alpha = \frac{\sigma_2'}{\sigma_1'} = \frac{\varepsilon_2}{\varepsilon_1} \tag{4.1.5}$$

be the strain ratio, the relationship between the minimum principal continuity ψ_{II} and the equivalent strain $\bar{\varepsilon}$ can be expressed (Tang et al 1999a) as

$$\psi_{II} = \left[1 - \frac{1}{2n+1} Bf < \bar{\varepsilon}^{2n+1} - \bar{\varepsilon}_{th}^{2n+1} >\right]^{1/2} \tag{4.1.6}$$

where

$$f = 1 + \frac{\left[b^3 C_{11} + C_{22} + (1+b)bC_{12}\right](1+\alpha)^2}{b^3 C_{11} + \alpha^2 C_{22} + \alpha(1+b)bC_{12}} \tag{4.1.7}$$

which is constant in proportional loading case, and

$$B = 2K / S_0 \tag{4.1.8}$$

In eq.(4.1.6), f is the stress triaxiality factor and $\bar{\varepsilon}_{th}$ is the threshold value expressed by the equivalent plastic strain for the initiation of damage. When the equivalent strain $\bar{\varepsilon}$ exceeds this threshold value $\bar{\varepsilon}_{th}$, the continuity of material

decreases $d\psi_{II} < 0$ with the increase in plastic deformation, i.e. $\psi_{II} < 1$ if $\bar{\varepsilon} > \bar{\varepsilon}_{th}$ otherwise if $\bar{\varepsilon} \le \bar{\varepsilon}_{th}$, $\psi_{II} = 1$.

In the critical case when microdefects, i.e. damage, coalescence to form a macrocrack, the minimum principal continuity ψ_{II} will reach the critical value ψ_c and the fracture of RVE takes place. Therefore, the damage-based fracture criterion characterized by the minimum principal value of continuity can be taken as

$$\psi_{II} = \psi_c \tag{4.1.9}$$

For ductile fracture to occur, the minimum continuity component ψ_{II} reaches a critical value ψ_c, i.e. $\bar{\varepsilon} = \bar{\varepsilon}_c$, the fracture criterion (Tang et al 1998a) can be expressed as

$$\psi_{II} = \psi_c = \left[1 - \frac{1}{2n+1} Bf < \bar{\varepsilon}_c^{2n+1} - \bar{\varepsilon}_{th}^{2n+1} > \right]^{1/2} \tag{4.1.10}$$

It should be noted that for fracture to occur, $\psi_{II} = \psi_c$ = constant. Thus, the two principal components of fracture limit strain of the sheet metal can be expressed as

$$\hat{\varepsilon}_1 = \frac{\sqrt{3}}{2(1+\alpha+\alpha^2)^{1/2}} \left\{ \frac{f_{uni}\left(\bar{\varepsilon}_c^{2n+1} - \bar{\varepsilon}_{th}^{2n+1}\right)_{uni}}{1 + \dfrac{\left[b^3 C_{11} + C_{22} + (1+b) b C_{12}\right](1+\alpha)^2}{b^3 C_{11} + \alpha^2 C_{22} + \alpha(1+b) b C_{12}}} + \bar{\varepsilon}_{th}^{2n+1} \right\}^{\frac{1}{2n+1}} \tag{4.1.11}$$

and

$$\hat{\varepsilon}_2 = \alpha \hat{\varepsilon}_1 \tag{4.1.12}$$

where $\hat{\varepsilon}_1$ and $\hat{\varepsilon}_2$ are the major strain and the minor strain of fracture limit, respectively. The variables with the subscript "*uni*" in eq.(4.1.11) are to be determined by a uni-axial tensile test.

In order to determine the continuity tensor ψ, it is required to find $\bar{\varepsilon}_c$ and $\bar{\varepsilon}_{th}$. The critical strains $\bar{\varepsilon}_c$ and $\bar{\varepsilon}_{th}$ may be determined from uniaxial tensile test, i.e.

$$\bar{\varepsilon}_c = (\frac{f_{uni}}{f})^{n/(n+2)} \bar{\varepsilon}_c^{uni} \tag{4.1.13}$$

and

$$\bar{\varepsilon}_{th} = \bar{\varepsilon}_{th}^{uni}$$

where f_{uni} and $\bar{\varepsilon}_{th}^{uni}$ are the values of f and $\bar{\varepsilon}_{th}$ determined from the uniaxial tensile test.

4.2 Theoretical Prediction and Experimental Verification

Aluminium alloys Al2024T3 have been chosen for this study because they are an important class of material in the aviation industries which can be processed at room temperature under hydraulic or mechanical press. The tensile strength and yield strength of the alloy measured at room temperature are 435MPa and 290MPa,

respectively. The chemical composition of Al2024T3 is Si:0.50, Fe:0.50, Cu:3.80~4.90, Mn:0.30~0.90, Mg:1.20~1.80, Cr:0.10, Zi:0.25, and Ti:0.15.

In naturally aged condition, the wrought metal contains coarse intermetallic compounds. The grain morphology of the undamaged aluminium alloy sheet is shown in Figure 4-1 (a). The average grain size is roughly 40μm. Under 400× magnification, as shown in Figure 4-1 (b), the presence of the coarse intermetallic compounds, such as $CuMgAl_2$, Cu_2MnAl_{20}, and Cu_2FeAl_7, can be observed easily. At $\bar{\varepsilon} = \bar{\varepsilon}_{th}$, these coarse particles will break and micro-voids will be formed. Under further action of plastic strain, the micro-voids will grow and coalesce to form a macro-crack that leads to final rupture of the material.

To determine the fracture limit curve (FLC) of the aluminium alloy sheet, two groups of specimens were prepared for tests: one group for uni-axial tensile tests while the other group for Erichsen cupping tests. The alloy sheet of 0.8mm thickness was cut into blanks of various widths 10mm~100mm. One test sample of each test consisted of four specimens. The method used to determine the limit strains of the sheet metal required printing the grid onto the specimen surface. A negative photo-resist technique of applying a surface grid was adopted in this experimental study. Its major advantage over other techniques is that polishing or etching does not alter the as received surface. An array of 1.975mm diameter circles was printed onto the surface of each specimen. The fracture strains were obtained by measuring the deformation of the circle at which fracture firstly occurred.

The uni-axial tensile tests were used to determine the fracture strains for $\alpha < 0$.

The specimens were stretched uni-axially by a 100kN MTS universal tensile tester. For $\alpha > 0$, the cupping tests were performed by a Hille 20/40 tons universal sheet metal testing machine to determine the fracture strains. As shown in Figure 4-2, the alloy sheet was clamped with a circular die at a constant holding force of 8kN. A tool consisted of a 20mm diameter steel ball was then pushed into the sheet until fracture occurred in the stretched specimen.

4.3 Results and Discussions

From the experimental results (Lee et al 1995, Tang and Lee 1995), the equivalent strain threshold of damage $(\bar{\varepsilon}_{th})_{uni}$ and the equivalent fracture strain $(\bar{\varepsilon}_c)_{uni}$ can be taken as 0.5% and 25.0%, respectively. Moreover, the following material parameters have been computed: $n = 0.21$, $B = 1.08$, $C_{11} = 0.013\text{GPa}^{-1}$, $C_{22} = 0.014\text{GPa}^{-1}$, $C_{12} = -0.005\text{GPa}^{-1}$ and $C_{66} = 0.035\text{GPa}^{-1}$. The principal components of the continuity tensor and the damage anisotropy ratio have been determined and listed in Table 2.

In Table 2, b decreases as the equivalent pre-strain $\bar{\varepsilon}$ increases. Therefore, it may be implied that the anisotropy of damage is more prominent at high strain. From Table 2, the damage anisotropic ratio b at ductile fracture may be set to 0.937. The value of f_{uni} can be calculated by letting α = -0.5 in eq.(4.1.7). Substituting these values into eq.(4.1.11) and assuming $\bar{\varepsilon}_{th} = (\bar{\varepsilon}_{th})_{uni}$, the major fracture strain $\hat{\varepsilon}_1$ can be determined for a given value of α. Hence, the corresponding value of the minor

fracture strain $\hat{\varepsilon}_2$ can also be determined from eq.(4.1.12). In order to verify the damage-based ductile fracture criterion, the critical value of ψ_{II}, at which ductile fracture of each specimen occurs, has been calculated by eq.(4.1.6). As shown in Figure 4-3, the critical values of ψ_{II} remain almost constant. Thus, the fracture criterion, $\psi_{II} = \psi_c$, is valid.

For $-1<\alpha<+1$, the predicted fracture strains have been computed using eqs.(4.1.11) and (4.1.12). Thus, the predicted FLC and the experimental fracture strains are plotted in Figure 4-4. Although scatter of the experimental results are observed, the predicted and the experimental fracture strains follow a similar trend. Figure 4-4 also shows the FLCs correspond to $(\bar{\varepsilon}_c)_{uni}$ = 20% and 30%. $(\bar{\varepsilon}_c)_{uni}$ is usually treated as a measure of material ductility. Therefore, it is reasonable to expect the fracture curve shifts upward while $(\bar{\varepsilon}_c)_{uni}$ increases and downward while $(\bar{\varepsilon}_c)_{uni}$ decreases.

The intact elastic property of 11 samples made of aluminum alloy 2024T3 was firstly measured. Each sample contained three uni-axial tensile specimens. The grain morphology of the alloy is shown in Figure 4-5 and the average grain size is approximately 40μm. For aluminium alloy 2024T3, the coarse intermetallic particles (see Figure 4-5) are cracked and micro-voids are opened up under excessive tensile strain (Forsyth and Smale 1971). Further increase in strain will cause the micro-voids to grow. Final rupture will occur while the micro-voids are coalesced by shear bands to form a macro-crack. Initially, the micro-voids are isolated and small. Under large deformation, micro-voids may change their shape and become elongated. It

may be expected that the elongation of micro-voids causes the macroscopic damage slightly anisotropic.

The tensile specimens were cut to the geometry, as shown in Figure 4-6, from a 3.8mm thick Al2024T3 plate by milling. They were then pre-strained to produce different degree of damage by uni-axial tension (Tang 1995). For example, the specimen S_4 was loaded to strain ε_4' and then unloaded to obtain a certain degree of damage, as shown in Figure 4-7. Afterwards, the specimens were set to measure their apparent engineering elastic coefficients, including the effective Young's modulus, the effective shear modulus and the effective Poisson's ratio. The shear tests for the measurements of the effective shear modulus were carried out using the modified Iosipescu technique (Tang and Lee 1995). Figure 4-8 shows the shape of the Iosipescu specimens whose V-notches were prepared by electro-discharge machining.

It has been found that the intact state elastic property does not satisfy isotropic condition

$$G = \frac{E}{2(1+\nu)}$$

and the elastic moduli E_1 and E_2 were of different values. Therefore it is reasonable to assume that the intact state of this material is orthotropic with four independent elastic parameters (E_1, E_2, G_{12} and ν_{12}) and their experimental values are shown in the second row of Table 3. The experimental values of effective engineering elastic properties $\tilde{E}_1$, $\tilde{E}_2$, $\tilde{G}_{12}$ and $\tilde{\nu}_{12}$ of the specimen with specific degree of damage are

given in Table 3.

The experimental result reveals that the effective elastic properties $\tilde{E}_1$, $\tilde{E}_2$, $\tilde{G}_{12}$ degrade as the values of pre-strain increases, but the effective Poisson's ratio $\tilde{\nu}_{12}$ remains almost unchanged. The degradation of apparent elastic properties of the material may be considered to be the effects of material damage. The damage parameters D_i (i = 1, 2...4) can be calculated from eqs.(3.2.1)-(3.2.4) and their values are listed in Table 4.

The results listed in Table 4 are illustrated graphically in Figure 4-9. These damage parameters reflect the reduction of the elastic properties corresponding to the measurement coordinate system. Although they cannot collectively characterize the state of damage and the degree of material degradation, each parameter can illustrate that the degree of damage increases as the value of pre-strain increases. Since the value of $\tilde{E}_1$ was measured at the same direction of the pre-strain, the value of D_1 was higher than the others. The degradation of the elastic tensile property at the transverse direction and the shear property had a similar trend and were of similar magnitude.

On the other hand, the components ψ_1, ψ_2 *and* ψ_6 of continuity tensor have been determined from eqs.(3.3.5), (3.3.6) and (3.3.7), respectively, and their values are plotted in Figure 4-10. The principal values (ψ_I and ψ_{II}) and the mean value ψ_m of the continuity tensor calculated from eqs.(3.3.11)-(3.3.14) are shown in Figure 4-11.

It can be observed that the principal values of continuity tensor characterize the

anisotropy of damage and the value of ψ_m represents the degree of damage. The principal direction of the continuity tensor ϕ versus the pre-strain ε_1 is plotted in Figure 4-12. It is thus clear that the principal coordinates of damage do not coincide with those of the major material coordinates. For aluminium alloy 2024T3, the values of the angle $\phi(\approx 45° - 49°)$ change only slightly under tensile strain damage. It may be implied that the principal directions of damage remain almost unchanged as the damage develops. The effective stiffness components $\widetilde{E}_{ij}$ expressed in the major material coordinate system and in the principal coordinate system of damage are shown in Figures 4-13 and 4-14, respectively.

In Figure 4-13, the degradation of the elastic properties of aluminum alloy 2024T3 due to large strain is evident. The values of effective stiffness components $\widetilde{E}_{11}$ and $\widetilde{E}_{22}$ decrease as the pre-strain ε_1 increases. The decreases in the values of $\widetilde{E}_{12}$ and $\widetilde{E}_{66}$ are less remarkable. The elastic property of the material is initially weak orthotropy. The increase in the degree of the damage, however, does not enlarge the orthotropy of the elastic properties of the material.

As shown in Figure 4-14, the orthotropy of the elastic properties of the material is very weak, even though the effective elastic properties are presented in the principal coordinates system of damage. The values of $\widetilde{E}_{16}$ and $\widetilde{E}_{26}$ are consistently close to zero irrespective of increasing in degree of the damage. The degradation of effective stiffness components $\widetilde{E}_{ij}$ relating to the mean value of continuity tensor is plotted in Figure 4-15. It can be observed that the effective stiffness $\widetilde{E}$ reduces linearly with decreasing of the mean value ψ_m of the continuity tensor. Therefore,

the mean value ψ_m of the continuity tensor can be used to describe the degree of materials damage.

Examining the equality of eq.(3.3.13) one can assess the applicability of the current formulation. By substituting the experimental raw data and the component values of the continuity tensor into eq.(3.3.13), the expected values of the apparent Poisson's ratio $\tilde{\nu}_{12}$ are determined and listed in Table 5. The percentage difference of the two values is within the range of (–4.9%, +2.5%), therefore the proposed method is applicable in characterizing the damage of aluminum alloy 2024T3 under large strain. At the highest pre-strain $\varepsilon_1 = 21.34$ %, the effective stiffness components $\tilde{E}_{ij}$ of a plate element of different material orientations can be computed (Lekheniskii 1983) and are shown in Figure 4-16. It can be seen that there are slight changes in the effective stiffness components under different material orientations. The result indicates that the overall anisotropy of the damage and the material exists but is not very significant.

For further verification of the proposed model and the criterion, the fracture limits of aluminium alloy Al2036T4, HS-3 steel and A-K steel sheets are predicted. The results are compared with those reported by Ghosh (1976). By taking the fracture strains under uniaxial stretching $\hat{\varepsilon}_1^{uni} = 0.76$ and $\hat{\varepsilon}_2^{uni} = -0.32$ for Al2036T4 sheet, the fracture strains $\hat{\varepsilon}_1$ and $\hat{\varepsilon}_2$ can be computed within the whole range of $-1 \le \alpha \le 1$. Hence, the fracture limit curves of Al2036T4 have been determined and plotted in Figure 4-17 for b = 0.6, 0.8, and 1.0. The predicted results shown in Figure 4-17 illustrate the influence of damage anisotropy on the predicted fracture

strains. Comparing with the experimental data (Ghosh 1976), it is found that the current method of ductile fracture prediction can produce an accuracy result for Al2036T4 sheet.

Biaxial stretching of a sheet metal is taken as an example to demonstrate how to apply the proposed method to predict the fracture limit. For illustrative purpose, it is assumed that the material and the damage are both isotropic for plane stresses during the entire forming process. Therefore,

$$C_{11} = C_{22} = \frac{1-\nu^2}{E},\ C_{12} = -\frac{\nu(1+\nu)}{E},\ C_{66} = \frac{1+\nu}{E},\ \text{and } b = 1$$

where E and ν are Young's modulus and Poisson's ratio, respectively. Consider a 2-dimensional RVE of the metal sheet. From eq.(3.1.4) the equivalent strain can be expressed in terms of the principal strains as

$$\bar{\varepsilon} = \frac{2}{\sqrt{3}}(\varepsilon_1^2 + \varepsilon_1\varepsilon_2 + \varepsilon_2^2)^{1/2} = \frac{2}{\sqrt{3}}\varepsilon_1(1+\alpha+\alpha^2)^{1/2} \qquad (4.3.1)$$

where α is the strain ratio of biaxial loading, and $\varepsilon_i (i = 1,2)$ are the principal values of the strain tensor ε_{ij}. In the principal coordinate system of stress, the hydrostatic stress and the equivalent stress defined by eqs.(3.5.6) and (3.5.12), respectively, can be expressed as

$$\sigma_m = \frac{1}{3}(\sigma_1 + \sigma_2) = \sigma_1' + \sigma_2' \qquad (4.3.2)$$

and

$$\bar{\sigma} = \left(C_{11}\sigma_1'\sigma_1' + C_{22}\sigma_2'\sigma_2' + 2C_{12}\sigma_1'\sigma_2'\right)^{1/2} \tag{4.3.3}$$

where σ_i' (i=1,2) is the deviatoric component of stress.

The stress triaxiality factor is a function of the strain ratio α. Eq. (4.1.7) can be simplified under uniaxial tension for which $\alpha = -1/2$ and $b = 1$. Hence,

$$f_{uni} = 1 + \frac{C_{11} + C_{22} + 2C_{12}}{4C_{11} + C_{22} - 4C_{12}} \tag{4.3.4}$$

The fracture strain components, $\hat{\varepsilon}_1$ and $\hat{\varepsilon}_2$, of RVE in the total region of the strain ratio ($-1 \le \alpha \le 1$) can be obtained by substituting eq.(4.3.1) into eq.(4.1.13), i.e.

$$\hat{\varepsilon}_1 = \frac{\sqrt{3}}{2}\bar{\varepsilon}_c^{uni}\left(\frac{f_{uni}}{f}\right)^{\frac{n}{n+2}}\left(1+\alpha+\alpha^2\right)^{-1/2} \tag{4.3.5}$$

For pure shearing case, the value of f is minimal as the hydrostatic stress is equal to zero. For the cases b = 1.00, 0.55, and 0.40, the values of f have been plotted against the strain ratio α in Figure 4-18. It can be observed that the damage anisotropy ratio has significant effect on the stress triaxiality factor. When the strain ratio $\alpha \approx 0.16$, the influence of the damage anisotropy ratio on the stress triaxiality factor is maximal. On the other hand, the values of f at α = −1.0 and 1.0 are not affected from the influence of damage anisotropy.

The fracture strain curves of HS-3 steel and A-K steel have been computed by using eqs.(4.3.5) and (4.1.12). The mechanical properties of these materials used in computation are listed in Table 6. In Figure 4-19 and 4-20, the predicted and the experimental fracture strains are plotted where the experimental data are extracted from reference (Ghosh 1976).

For HS-3 steel, the experimental data fall close to the predicted fracture limit curve, as shown in Figure 4-19. As for A-K steel, it can be observed from Figure 4-20 that the current formulation can provide a good prediction of fracture strain. However, the fracture limit is found to be under-estimated slightly within $\alpha > 0$ for the two materials. In this example, the damage and the materials are assumed to behave isotropically throughout the forming process. The overall accuracy of the predictions is considered acceptable, even though the following factors are assumed negligible such as the anisotropy of the material, the damage anisotropy, the initial imperfection and the inhomogeneity of the material.

The conventional method of analyzing metal forming is based on the classical elasticity and plasticity theories and ignores the degradation of material that is caused by the formation and growth of micro-defects. Failure to take into account of the micro-defects in real-life materials and their geometrical effects are the major deficiencies in the conventional method for the limit strains prediction. By applying the technique proposed in this study, engineers can use the continuity tensor to describe the characteristics of internal damage and use the damage evolution law to predict the growth of damage under different loading path. The criterion provides information to characterize the anisotropic damage in ductile damaged material. Together with the

damage evolution equation, the damage-based fracture criterion has been developed to predict the fracture limit strains in sheet metal forming and satisfactory predictions have been achieved.

Chapter 5. Conclusions

In this study, the techniques of applying damage mechanics to predict the fracture limit of aluminium alloys have been presented. In order to capture the anisotropic nature of damage, a second order continuity tensor was used to characterize the effect of strain damage on the mechanical properties of material. The relationship between the apparent elastic properties and the continuity tensor has been derived. The derivation showed that the components of the continuity tensor could be determined from four scalar damage parameters. For two-dimensional analysis, the continuity tensor could also be represented by a Mohr's circle of continuity, where the state of damage was represented graphically.

The continuity tensor was determined from the effective elastic stiffness matrix and it satisfied the requirement of symmetry for derivation of the effective stress tensor, the effective elastic strain tensor and the effective elastic stiffness tensor. The corresponding anisotropic damage constitutive relations were formulated to model the damage-failure process for sheet metal. The specific damage energy release rate tensor $\mathbf{Y}$, which takes the stress triaxiality and damage anisotropy into account, has also been derived by means of decomposing $\boldsymbol{Y}$ into the hydrostatic and the deviatoric parts in the stress space. The stress triaxiality factor f not only depended on the stress state but also related to the anisotropy of both material and damage, a treatment that was neglected in a similar investigation by Lemaitre (1992). The damage evolution equation was established in terms of plastic damage dissipation potential and plastic stress-strain relation. The minimum principal component of

continuity ψ_{II} , that was a function of the equivalent plastic strain, the triaxiality factor and the strain hardening parameter, was taken as the predominant factor governing the damage-failure process. Together with the damage evolution equation, the damage-based criterion has been developed to predict the fracture strains for the whole range of strain ratio α for aluminium alloy sheet.

The proposed formulation has been successfully applied to aluminium alloy 2024T3 which was damaged under uni-axial tension test. The experimental results showed that the effects of damage caused the effective stiffness of the aluminium alloy to decrease. The proposed continuity tensor has been found to be capable of describing this phenomenon. Using the experimental results, the components of the continuity tensor have been determined. Microscopic examination has shown that the damage of the aluminium alloy was due to nucleation and coalescence of micro-voids under high strain. The microscopic examination also reviewed that coarse intermetallic particles existed in the aluminium alloy sheet. Breaking of these particles under high strain could open up micro-voids that initiate damage. The experimental results showed that ductile fracture of the aluminium alloy sheet occurred while the minimum principal continuity ψ_{II} reached a critical value. The current formulation did not require the assumption that the principal coordinate system of damage should be coincide with that of the material. Therefore, it could be used to analyze more general damage problems where the principal directions of damage did not coincide with those of the material.

With the application of damage mechanics theory, the prediction of fracture limit of materials has been approved by demonstrating a certain number of

experimental works such as the Erichsen cupping test and the tension test. The deformed circular grid, which was photoprinted onto the surface of material, has been measured by using a conventional light travelling microscope. The predicted fracture limit of Al2024T3 has been computed for $-1<\alpha<+1$ (see Figure 4-4) and showed that the measured fracture strains were placed within the range of $(\bar{\varepsilon}_c)_{uni}$ = 20% and 30% . Since $(\bar{\varepsilon}_c)_{uni}$ is usually treated as a measure of material ductility, therefore as $(\bar{\varepsilon}_c)_{uni}$ increases the fracture limit curve shifts upwards otherwise as $(\bar{\varepsilon}_c)_{uni}$ decreases the fracture limit curve moves downwards.

Capability of the proposed method in fracture strain prediction has been extended and compared with the results of other materials. It has been applied to biaxial stretching of steel sheets of which the fracture strains of HS-3 and A-K steels have been predicted. Under the assumptions of constant strain path and proportional loading, the anisotropic theory of damage mechanics has been applied to develop a fracture criterion in sheet metal forming. Hence, the fracture limit curve of Al2036T4 sheets has been computed using the fracture criterion with an assumption that f is independent of $\bar{\varepsilon}$. The predicted result has then been compared with the experimental findings, as well as the data extracted from Ghosh (1976), and showed that the predicted values are in agreement with the experimental ones.

As compared with other previous models, which are mostly empirical ones, the current development starts from the basic principle and provides a more scientific and realistic approach for the prediction of fracture limit strains in sheet metal forming such that the effects of stress triaxiality, damage anisotropy and ductility are taken into account.

Chapter 6. Future Works

Throughout the investigation of the sheet metal forming, it was proved that the damage mechanics theory could be suitable for describing and for analyzing the fracture strains in sheet metal forming. At present, the second order continuity tensor coupled with the damage-based criterion has been used to predict the fracture strains of sheet metal. The proposed anisotropic elasto-plastic damage model is capable of predicting the fracture limit in sheet metal forming but the analysis is limited to two-dimensional case. In fact, the sheet metal forming is three-dimensional problem therefore it is recommended to extend the analysis by applying the finite element method. In ductile damage, the damage is often distributed over a certain volume of the structural component with complicated shape. Analytical calculation becomes more complex and time consuming or even impossible. Finite element software, such as ABAQUS can be applied accordingly, so that a complete simulation of ductile fracture can be performed.

In comparison to the conventional measurement of strain, the damage measurement may be done by using digital camera to record a whole forming process of sheet metal. Moreover, we have assumed the proportional type of loading but in fact, sheet metal can be formed under non-proportional loading path. Therefore the verification and the prediction of fracture strains may be further elaborated under non-proportional loading.

Chapter 7. Contribution to Knowledge

It is amongst the first attempt to study fracture limit using damage mechanics approach. A second order continuity tensor has been used to characterize the state of damage. Hence, a damage model has been developed to predict the evolution of damage for sheet metal forming. A criterion has been proposed for the prediction of fracture strain such that damage and triaxiality of stress are taken into account. The formulation and prediction, verified by the experimental findings, are useful for solving sheet metal forming problems.

In the conventional plasticity approach, the degradation of material due to large deformation is usually ignored. The proposed method is more realistic and has been used to produce one refereed international journal paper and two refereed international conference papers.

References

Abdul-Latit, A. and Saanouni, K., *Int. J. Damage Mech.*, Vol. 3, July (1994), 237.

Arrieux, R., Bedrin, C. and Boiven, M., *Proc. 12th IDDRG Congress*, Italy, (1982), 61.

Azrin, M. and Backofen, W.A., *Metal Trans.*, Vol. 1, October, (1970), 2857.

Bassani, J.L., Hutchinson, J.W. and Neal, K.W., *Metal Forming Plasticity Symposium*, H. Lippman, ed. Springer-Verlag, Berlin, Vol. 1, (1979), 1.

Betten, J., *Engng. Fracture Mech.*, Vol. 25, Nos.5/6, (1986), 573.

Betten, J., *Int. J. Damage Mech.*, Vol. 1, January (1992), 47.

Bressan, J. D. and Williams, J. A., *J. Mech. Sci.*, Vol. 25, (1983), 155.

Brownrigg, A., Spitzig, W.A., Richmond, O., Teirlinck D. and Embury, J.D., *Acta Metallurgica*, Vol. 31, (1983), 1141.

Chaboche, J. L., *Nuclear Engineering and Design*, Vol. 79, (1984), 309.

Chaboche, J.L., *Int. J. Damage Mech.*, Vol. 1, April (1992), 148.

Chaboche, J.L., *Int. J. Damage Mech.*, Vol. 2, October (1993), 311.

Chaboche, J.L., *J. Applied Mech.*, Vol. 55, March (1988a), 59.

Chaboche, J.L., *J. Applied Mech.*, Vol. 55, March (1988b), 65.

Chaboche, J.L., Lesne, P.M. and Maire, J.F., *Int. J. Damage Mech.*, Vol. 4, January (1995), 5.

Chow, C.L. and Lu, T.J., *ASME Summer Mechanics and Material Conferences*, Tempe AZ., (1992a), 21.

Chow, C.L. and Lu, T.J., *Int. J. Damage Mech.*, Vol. 1, (1992b), 191.

Chow, C.L. and Wang, J., *Damage Mechanics in Composites*, ASME AD, Vol. 12, (1987a), 1.

Chow, C.L. and Wang, J., *Engng. Fracture Mech.*, Vol. 27, (1987b), 547.

Chow, C.L. and Wang, J., *Engng. Fracture Mech.*, Vol. 30, No. 5, (1988a), 547.

Chow, C.L. and Wang, J., *International Journal of Fracture*, Vol. 38, (1988b), 83.

Chow, C.L. and Wang, J., *International Journal of Fracture*, Vol. 33, No. 3, (1987c), 3.

Chow, C.L. and Wei, Y., *International Journal of Fracture*, Vol. 50, (1991a), 301.

Chow, C.L. and Wei, Y., *Theoretical and Applied Fracture Mechanics*, Vol. 16, (1991b), 123.

Chow, C.L., Yang, F. and Asundi, A., *Int. J. Damage Mech.*, Vol. 1, July, (1992), 347.

Chow, C.L., Yu, L.G. and Demeri, M. Y., *Journal of Engineering Materials and Technology*, Vol. 119, (1997), 346.

Chow, C.L., Yu, L.G. and Demeri, M.Y., *SAE Technical paper 960598*, SP-1134, (1996a), 83.

Chow, C.L., Yu, L.G. and Demeri, M.Y., *Sheet Metal Stamping for Automotive Applications*, (1996b), 70.

Cordebois, J.P. and Sidoroff, F., *Mechanical Behavior of Anisotropic Solid*, Collogue Enromech 115, Martinus Nijhoff, The Hague, (1979), 761.

Demeri, M., Chow, C. L. and Tai, W. H., *Development in Sheet Metal Stamping*, SAE SP-1322, (1988), 53.

Drucker, D.C., *Trans ASME J. Eng. Mat. and Tech.*, Vol. 106, October (1984), 286.

Forsyth, P.J.E. and Smale, A.C., *Engng Frac. Mech*, Vol. 3, (1971), 127.

Ghosh, A. K., *Metallurgical Transactions A*, Vol. 7A, No. 4, (1976), 523.

Ghosh, A.K. and Hamilton, C.H., *Metallurgical Transactions A*, Vol.13A, (1982), 733.

Ghosh, A.K. and Hecker, S.S., *Metal. Trans.*, Vol. 5, (1974), 2161.

Ghosh, A.K. and Hecker, S.S., *Metal. Trans.*, Vol. 6A, (1975), 1065.

Ghosh, S.K. and Predeleanu, M., *Materials Processing Defects*, Published by Elsevier, (1995).

Gouveia, B.P.P.A., Rodrigues, J.M.C. and Martins, P.A.F., *Int. J. of Mechanical Sciences*, Vol. 38, No. 4, (1996), 361.

Graf, A. and Hosford, W., *Int. J. Mech. Sci.*, Vol. 36, No. 10, (1994), 897.

Groche, P. and Doege, E., *Numiform 89*, Thompson et al. (eds), Balkema, Rotterdam, (1989), 445.

Gronosstajski, J., Dolny, A. and Sobis, T., *Proc. 12th IDDRG Congress*, Italy, (1982), 39.

Gurson, A.L., *ASME J. Eng. Mater. Technol.*, Vol. 99, (1977), 2.

Gurson, A.L., *Plastic flow and fracture behavior of ductile materials incorporating nucleation, growth and interaction*, PhD thesis, Brown University, (1975).

Hall, F.R., Hayhurst, D.R. and Brown, P.R., *Int. J. Damage Mech.*, Vol. 5, October, (1996), 353.

Hart, E.W., *Tran ASME J. Eng. Mat and Tech.*, Vol. 106, October (1984), 322.

Hayakawa, K. and Murakani, S., *Int. J. Damage Mech.*, Vol. 6, (1997), 333.

Hecker, S.S., *J. Eng. Mater. Technol. (Trans. ASME, H)*, Vol. 97, (1975a), 66.

Hecker, S.S., *Sheet Metal Industries,* Vol., 52, November (1975b), 671.

Hill, R., *J. Mech. Phys. Solids,* Vol. 1, (1952), 19.

Hosford, William F. and Caddell, Robert M., *Metal Forming (mechanics and metallurgy)*, 2nd edition, Prentice Hall, (1993).

Hutchinson, J.W. and Neale, K. W., *GMR Symposium "Mechanics of Sheet Metal Forming"*, Plenum Press, New York, (1978a), 127.

Hutchinson, J.W. and Neale, K. W., *GMR Symposium "Mechanics of Sheet Metal Forming"*, Plenum Press, New York, (1978b), 269.

Hutchinson, J.W., Neale, K. W. and Needleman, A., *GMR Symposium "Mechanics of Sheet Metal Forming"*, Plenum Press, New York, (1978), 111.

Hutchinson, W.B. and Arthey, R., *Src. Metal.*, Vol. 10, (1976), 673.

Joshi, Ramesh Baburao, *Study of inhomogeneous deformation of stretch-forming sheet metal using digital image processing technique*, PhD thesis, Washinton State University, (1992).

Kachanov, L. M., *Foundations of Fracture Mechanics*, Nauka, Moscow (1974).

Kachanov, L. M., *Introduction to Continuum Damage Mechanics*, Martious Nijhoff Publishers, (1986).

Kachanov, L. M., *Izv. Akad. Nauk.* SSSR Otd.Tech. Nauk., Vol. 8, (1958), 26.

Keeler, S.P. and Backofen, W.A., *Trans. Am. Soc. Metals*, Vol. 56, (1963), 25.

Keeler, S.P., *Machinery*, Vol. 74, (1968), 94.

Keeler, S.P., *Sheet Metal Industries*, Vol. 42, (1965), 683.

Kikuma, T and Nakazima, K., *Iron Steel Inst.*, Japan, Vol. 11, (1971), 827.

Kobayashi, T., Ishigaki, H. and Abe, T., *Proc. 7th IDDRG Congress*, Amsterdam, Vol. 8, (1972), 1.

Koistinen, Donald P. and Wang, Neng-ming, *Mechanics of sheet metal forming (material behavior and deformation analysis)*, Plenum Press, (1978).

Krajcinovia, D. and Lemaitre, J., *Continuum Damage Mechanics*, Springer-Verlag, (1987).

Krajcinovic, D., and Fenseka, G.U., *Journal of Applied Mechanics,* Vol. 48, (1981), 809.

Krajcinovic, D., *Applied Mech. Reviews*, Vol. 37, No.1, January, (1984), 1.

Krajcinovic, D., *J. Applied Mech.*, Vol. 50, June (1983), 355.

Lacy, T.E., McDowell, D.L., Willice, P.A. and Talreja, R., *Int. J. Damage Mech.*, Vol. 6, January (1997), 62.

Ladeveze, P., *Proceedings of the forth international conference of composite materials, ICCM-IV*, (1982), 649.

Lauknois, J.V. and Gosh, A.K., *Metal. Trans.*, Vol. 9A, (1978), 1849.

Le Roy, G., Embury, J.D., Edward, G. and Ashby, M.F., *Acta Metallurgica*, Vol. 29, (1981), 1509.

Lee, H., Wang, J. and Peng, K., *J. Huazhong Uni. of Sci. Tech.*, Vol. 13, No. 1, February, (1985), 1.

Lee, W.B., Tai, W.H. and Tang, C.Y., *J. of Materials Processing Tech.*, Vol. 63, (1997), 100.

Lee, W.B., Tai, W.H., and Tang, C.Y., *Proc. of the Seventh International Manufacturing Conference with China*, Harbin, China. ISBN 962-367-189-X (1995), 597.

Lekheniskii, S.G., *Theory of Elasticity of an Anisotropic Body*, Holdon day, (1983).

Lemaitre, J. and Chaboche, J.L., *Mechanics of Solid Materials*, Cambridge University Press, (1990), Chapter 2 and 7.

Lemaitre, J., *A Course on Damage Mechanics*, Springer-Verlag, (1992).

Lemaitre, J., *ICM4,* (1983), 1059.

Lemaitre, J., *Nuclear Engineering and Design,* Vol. 80, (1984), 233.

Lemaitre, J., *Trans. ASME J. Engng. Mater. Techn.*, Vol. 107, (1985), 83.

Li, D.L. and Chow, C.L., *Int. J. Damage Mech.*, Vol. 2, October, (1993), 385.

Li, H., Peng, K., Lu, Y. B. and Yu, L. G., *J. Huazhong Unv. of Sci. & Tech.*, Vol. 11, No. 5, October, (1983), 63.

Lloyd, D.J. and Sang, H., *Metal. Trans.*, Vol. 10A (1979), 1767.

Lu, Zhong-Hao, *Instability analysis in sheet metal forming processes*, PhD thesis, Rensselaer Polytechnic Institute, Troy, New York, December (1987).

Lubarda, V.A., Krajcinovic, D. and Mastilovic, S., *Engng. Fracture Mech.*, Vol. 49, No. 5, (1994), 681.

Luo, Albert C.J., Mou, Yanghu and Han Ray, P.S., *Int. J. Fracture*,Vol.70,(1995),19.

Lynden, Edwards and Endean, Mark, *Manufacturing with Materials*, The Open University, Butterworths, 1st ed., (1990), 202.

Majlessi, Seyed Abdolvahab, *Modeling and experimental verification of sheet metal forming processes*, PhD thesis, Rensselaer Polytechnic Institute, Troy, New York, December (1987).

Marciniak, Z. and Kuczynski, K., *Int. J. Mech. Sci.*, Vol. 9, (1967), 609.

Marciniak, Z., Kuczynski, K. and Pokora, T., *Int. J. Mech. Sci.*, Vol. 15, (1973), 789.

McClintock, F. A., *J. Appl. Mech.*, Vol. 35, June, (1968), 363.

Mellor, P.B., *The Engineer*, Vol. 209, (1960), 517.

Mou, Yanghu and Han, Ray P.S., *Int. J. Damage Mech.*, Vol. 5, July (1996), 241.

Murakami, S., *J. Applied Mech.*, Vol. 55, June (1988), 280.

Murakami, S., Liu, Y. and Sugita, Y., *Int. J. Damage Mech.*, Vol. 1, April (1992), 172.

Najar, J., *Int. J. Damage Mech.*, Vol. 3, July (1994), 260.

Needleman, A. and Rice, J.R., *Mechanics of Sheet Metal Forming*, D.P. Koistinen and N.M. Wang, eds., Plenum Press, New York, (1978), 237.

Needleman, A. and Triantafyllidis, N., *J. Eng. Mater. Technol. (Trans. ASME, H)*, Vol. 100, (1978), 164.

Oh, Hung-kuk, *J. of Mater. Proc. Techn.*, Vol. 53, (1995), 582.

Onate, E., Kleiber, M. and Saracibar, C. A. D., *Int. J. Num. Meth. Eng.*, Vol. 25, No. 1, (1988), 227.

Painter, M.J. and Pearce, R., *J. Phys. D, Appl. Phys.*, Vol. 7, (1974), 992.

Parmar, A and Mellor, P.B., *Int. J. Mech. Sci.*, Vol. 22, (1980), 133.

Pilling, J. and Ridley, N., *Acta Metallurgica*, Vol. 34, No.4, (1986), 669.

Ranta-Eskola, A., *Proc. 11th IDDRG Congress*, Metz, (1980), 453.

Rao, K.P., Sing, W.M. and Mohan, Emani V.R., *Proc. 4th Int. Conf. (AMPT98), Advances in Materials Processing and Technologies*, Vol. 2, (1998), 612.

Rice, J. R. and Tracey, D. M., *J. Mech. Phys. Solids*, Vol. 17, (1969), 201.

Saanouni, K., Forster, Ch. and Ben Hartira, F., *Int. J. Damage Mech.*, Vol. 3, April (1994), 140.

Schmitt, J.H. and Jalinier J.M., *Acta Metallurgica*, Vol. 30, (1982), 1789.

Sheet Metal and Stamping Symposium, sponsored by Society of Automotive Engineers (SAE International) and North American Deep Drawing Research Group (NADDRG), Published by Society of Automotive Engineers, Inc. (1993).

Shen, W. and Wu, C.S., *Engng. Fracture Mech.*, Vol. 42, (1992), 159.

Shen, W., *Damage Mechanics* (in Chinese), Published by HUST Press, (1995).

Shen, W., *Journal of Mechanics and Practice* (in Chinese), Vol. 14, No. 2, (1992), 20.

Shen, W., Peng, L.H. and Yue, Y.G., *Engng. Fracture Mech.*, Vol. 33, No.2, (1989), 273.

Shen, W., Peng, L.H., Yang, F. and Shen, Z., *Engng. Fracture Mech.*, Vol. 28, No. 4, (1987), 403.

Shi, Mingfeng, *On formability of sheet metal and constitutive modeling in finite deformation plasticity*, PhD thesis, Michigan Technological University, (1989).

Stören, S. and Rice, J.R., *J. Mech. Phys. Solids*, Vol. 23, (1975), 421.

Stubbs, N. and Krajcinovic, D., *Proceedings of two sessions sponsored by the Engineering Mechanics Division of the American Society of Civil Engineers in conjunction with the ASCE Convention*, Detroit, Michigan, October 22, (1985).

Swift, H.W., *J. Mech. Phys. Solids*, Vol. 1, (1952), 1.

Tadros, A.K. and Mellor, P.B., *Int. J. Mech. Sci.*, Vol. 17, (1975), 203.

Tai, W. H. and Yang, B.X., *Engng. Fracture Mech.*, Vol. 25, No. 3, (1986), 377.

Tai, W.H. and Yang, B.X., *Engng. Fracture Mech.*, Vol. 27, No.4, (1987a), 371.

Tai, W.H. and Yang, B.X., *J. Mech. Working Tech.*, Vol. 15, (1987b), 39.

Tai, W.H. and Yang, B.X., *J. Mech. Working Tech.*, Vol. 15, (1987c), 319.

Tai, W.H., *Engng. Fracture Mech.*, Vol. 37, (1990), 853.

Tai, W.H., *Int. J. Solids Structures*, Vol. 24, No.10, (1988), 1045.

Talreja, R., *Journal of Strain Analysis*, Vol. 24, (1989), 215.

Talreja, R., *Proceedings of Royal Society*, London, Vol. 399A, (1985), 195.

Tang, C.Y. and Lee, W.B., *Engng. Fracture Mech.*, Vol. 52, No.4, (1995a), 717.

Tang, C.Y. and Lee, W.B., *Scripta Metallurgica et Materialia*, Vol. 32, No. 12, (1995b), 1993.

Tang, C.Y. and Plumtree, A., *Engng. Fracture Mech.*, Vol. 49, No.4, (1994), 499.

Tang, C.Y., Chow, C.L., Shen, W. and Tai, W.H., *J. of Materials Processing Technology*, Vol. 91, No. 1-3, (1999), 270.

Tang, C.Y., Jie, M., Shen, W. and Yung, K.C., *Scripta Materialia*, Vol. 38, (1998a), 231.

Tang, C.Y., *Modeling of craze damage in polymeric materials: A case study in polystyrene and high impact polystyrene*, Thesis of Ph.D., The Hong Kong Polytechnic University, (1995).

Tang, C.Y., *Scripta Metallurgica et Materialia*, Vol. 29, (1993), 183.

Tang, C.Y., Shen W., Lee, T.C and Fung, L.C., *Proc. 8th Int. Manufacturing Conference (IMCC'98)*, Singapore, May 11-13, (1998b), 55.

Tang, C.Y., Shen, W., Fung, L.C. and Lee, T.C., *Int. J. of Mechanical Sciences,* Vol. 42, No. 1, (1999), 87.

Tang, C.Y., Tai, W.H., Fung, L.C. and Lee, T.C., *Key Engineering Materials*, Vol. 145-149, (1998c), 453.

Wang, J. and Chow, C.L., *Engng. Fracture Mech.*, Vol. 33, No.2, (1989), 309.

Wang, Tie-jun, *Engng. Fracture Mech.*, Vol. 48, No. 2, (1994), 217.

Wang, Tie-jun, *Engng. Fracture Mech.*, Vol. 51, No. 2, (1995), 275.

Williams, Kevin Vaughan, *The numerical prediction of strain distribution in sheet metal forming operations*, Master thesis, Carleton University, Ottawa, Ontario, December (1993).

Xiaoxue, Diao, *Engng. Fracture Mech.*, Vol. 52, No.1, (1995), 33.

Yazdani, S., *Int. J. Damage Mech.*, Vol. 2, April (1993), 162.

Zaverl, Frank Jr., *Effect of deformation history on the mechanical behavior and formability of sheet metal*, PhD thesis, Rensselaer Polytechnic Institute, Troy, New York, December (1982).

Zheng, M., Hu, C., Luo, Z.J. and Zheng, X., *Engng. Fracture Mech.*, Vol. 53, No. 4, (1996), 653.

Zheng, M., Lou, Z.J. and Zheng, X., *Engng. Fracture Mech.*, Vol. 41, (1992), 103.

Zhu, Y.Y. and Cescotto, Z., *Int. J. Solids Structures*, Vol. 32, No. 11, (1995), 1607.

Table 1 Summary of Damage Variables

Damage Variable	References	Application(s)	Advantage(s)	Limitation(s)
Scalar	Lemaitre 1985	ductile plastic damage, triaxiality strain effect, isotropic damage		
	Tai and Yang 1986	isotropic, ductile, plastic, void damage	predict void growth &void coalescence	hypothesis of isotropy of damage, isotropy of plasticity, hypothesis of constant triaxiality ratio during loading, i.e. proportional loading of plasticity
	Tai and Yang 1987a	a damage failure criterion for orthotropic materials has been derived, an isotropic damage for anisotropic material, uniaxial tension test, steel, Al2036T4 & 70:30 brass	predict fracture limit curves of sheet metals	assume void growth governing microstructural processes
	Tai and Yang 1987b	ductile fracture using characterizing parameters (K & J)	using parameters K & J to any specimen and plastic yielding, able to predict the initiation and propagation of crack	further investigation is needed to ductile fracture
	Tai 1988	for orthotropic materials $D = 1 - \frac{\overline{E}}{E}$ using isotropic plastic damage model in sheet metal forming	combined with M-K model, showing the effect of internal damage to the analysis of sheet metal forming limit	

Table 1 Summary of Damage Variables

Damage Variable	References	Application(s)	Advantage(s)	Limitation(s)
Scalar	Groche and Doege 1989	sheet metal forming, applied to hydraulic bulge tests and stretching processes	using micromechanical model, a yield surface equation obtained	difficult to quantitative description of the damage parameter
	Chaboche 1992	tensile & compressive loadings	describe unilateral damage	cannot reproduce anisotropy induced by damage
	Murakami, Liu and Sugita 1992	creep damage introducing A-parameter (fraction of cavitated grain boundaries), steel	provide physical background for CDM and foundation for creep damage theory	
	Zheng M., Lou and Zheng X. 1992	for porous material & analysis of metal forming processes, able to predict ductile damage & workability of materials		positive & negative stress triaxiality
	Li and Chow 1993	fatigue damage for isotropic material in offshore structure, low & high cycle fatigue and dynamic response	use the concept of duty strain range and history-dependent	

Table 1 Summary of Damage Variables

Damage Variable	References	Application(s)	Advantage(s)	Limitation(s)
Scalar	Saanouni, Forster and Ben Hartira 1994	general purpose, isotropic	RVE free from any kind of stress, able to define energy release rate, able to release store energy, formulate constitutive equation	
	Najar 1994	brittle damage with cyclic fatigue	use linear stress response to the effective strain and then resulted in kinematics formulation to numerical evaluations	
Vector	Kachanov 1974		to characterize the damage state on the area element of a normal n and under normal stresses σ_n	entire distribution of the vector variables in all directions of the damage state is needed
Damage matrix	Abdul-Latit and Saanouni 1994	uniaxial tension-compression cyclic loadings (fatigue) in FCC polycrystalline metals, uniaxial monotonic and cyclic tension-compression loadings, isotropic material	based on slip theory to define micro-damage, determine macroscopic anelastic behaviour	neglect the quasi-unilateral effect as well as the localization of the fatigue micro-cracks on the surface of the loaded material

Table 1 Summary of Damage Variables

Damage Variable	References	Application(s)	Advantage(s)	Limitation(s)
Scalar matrix, 2nd order non-symmetric	Tang and Plumtree 1994, Tang and Lee 1995a	polystyrene (PS), high impact polystyrene (HIPS), isotropic damage, scalar $D = 1 - \frac{E_1'}{E_1}$ anisotropic damage $D_1 = 1 - \left(\frac{E_1'}{E_1}\right)^{\frac{1}{2}}$ $D_2 = 1 - \frac{\nu_{12}}{\nu_{12}'}(1 - D_1)$ and $[E'] = \{[I] - [D]\}[E]$ for anisotropic damage, investigate the effect of elastic moduli and Poisson's ratio	provide information about stiffness changes in x-direction plane stress analysis, predict damage in x_2-direction and strengthening effect in transverse direction able to reproduce mechanical behaviour of orthotropic material by using damage effect matrix	one-dimensional over-estimate the transverse modulus
	Tang and Lee 1995b	Al2024T3 orthotropic damage, damage effect on shear modulus		
	Lee, Tai and Tang 1997	sheet metal forming in Al2024T3 under tensile test	predict forming limit curves by modifying the M-K model, without the assumption of an initial groove on the sheet metal surface	

Table 1 Summary of Damage Variables

Damage Variable	References	Application(s)	Advantage(s)	Limitation(s)
Tensor	Wang and Chow 1989	ductile fracture, Al2024T3 anisotropic model	accurate predict and measure the crack growth	
	Chow and Wei 1991a	fatigue damage in Al2024T3 under tensile specimens	combine elastic and plastic damage, predict number of cycles to failure under tensile loading	extend studies to cover tension-compression cycles
2^{nd} order tensor	Chow and Wang 1987b	tension test, effective stress tensor, for isotropic material	provide comprehensive theory of anisotropic CDM to solve practical engineering problems	damage threshold and stress damage relation of (σ-D) is the dame in compression as well as in tension
	Murakami 1988	anisotropic damage in creep	net area reduction from Cauchy tetrahedron, i.e. using effective stress caused by the distributed microcracks and cavities from damaged material	
	Shen, Peng and Yue 1989	glass-cloth/epoxy orthotropic and composite plate, anisotropic material with anisotropic damage (homogeneous), off-axis tension specimen with a central hole	using asymmetric 2^{nd} order tensor to construct the 4^{th} order tensor	

Table 1 Summary of Damage Variables

Damage Variable	References	Application(s)	Advantage(s)	Limitation(s)
2nd order tensor	Chow and Lu 1992a	Al2024T3, model developed with non-proportional loading	good agreement with experiment, capable to characterize the fracture initiation of notched plates with ductile material	
	Chow and Lu 1992b	mixed-mode ductile fracture for biaxial tension under non-proportional loading Al2024T4	anisotropic damage model based on energy equivalence hypothesis	stress history effect
	Chow, Yang and Asundi 1992	anisotropic material for large, thin and continuous composite laminates	a generalized damage model allow non-linear relationship to be established among state variables between stress and strain	needed to be extended to study flexure problems of composite laminates
	Tang 1993	anisotropy of material damage using matrix equation in uniaxial tension, high impact polystyrene (HIPS)		principal directions of material damage do not exist
	Luo, Mou and Han 1995	uniaxial tension, pure torsion and elastic-plastic behaviour of Al2024T3	using a new hypothesis of elastic energy equivalence to develop a large damage theory	

Table 1 Summary of Damage Variables

Damage Variable	References	Application(s)	Advantage(s)	Limitation(s)
2nd order tensor	Hall, Hayhurst and Brown 1996	creep damage in steel to predict creep crack growth in compact tension test	used with finite element based numerical procedure	more accurate result would be obtained if extremely fine mesh is used in the order of 6-7 grain diameters
	Hayakawa and Murakani 1997	elastic-plastic damage, torsion test in iron material	use Gibbs thermodynamic potential	
4th order tensor	Betten 1986	creep, anisotropic material		
	Betten 1992	creep, anisotropic material		4th order tensor assume to be symmetric
	Yazadni 1993	brittle, mortar and concrete anisotropic	capable to model non-linearity's in the lateral directions, formulated in terms of material parameter sensitive, remove snap-back in deformation	

Table 1 Summary of Damage Variables

Damage Variable	References	Application(s)	Advantage(s)	Limitation(s)
4^{th} order tensor	Chaboche 1993	creep, anisotropic material, concrete	using symmetry of the elasticity, eliminate the discontinuous stress-strain response	simple case of elastic behaviour and rate independent damaging processes in brittle materials
	Chaboche, Lesne and Maire 1995	brittle damage like concrete and ceramic composites, tension and compression tests isotropic material	describe elastic behaviour	verify the model by multiaxial experiments with non-proportional loading, did not like viscosity and hysteresis effects
	Mou and Han 1996	ductile damage material, carbon steels	capable to predict damage evolution with good accuracy	assume isotropic damage and constant stress triaxiality ratio during loading
	Lacy, Mcdowell, Willice and Talreja 1997	brittle damage	using a high order to predict the macroscopic response of solids containing highly interactive defects	use spatially-averaged damage descriptors in evaluation of the effective moduli

Table 2 The Principal Values of Continuity for Al2024T3 Sheet

Pre-strain, $\bar{\varepsilon}$ (%)	ψ_I	ψ_{II}	b
0.00	1.000	1.000	1.000
1.07	.982	.982	.999
2.40	.959	.957	.998
4.85	.948	.920	.971
9.45	.939	.906	.965
12.63	.946	.911	.964
16.09	.931	.898	.964
16.81	.903	.878	.972
18.77	.906	.877	.967
21.37	.914	.868	.950
22.41	.909	.852	.937

Table 3 The Experimental Values of the Effective Elastic Properties

Pre-strain ε_1 (%)	$\widetilde{E}_1$ (GPa)	$\widetilde{E}_2$ (GPa)	$\widetilde{G}_{12}$ (GPa)	$\widetilde{\nu}_{12}$
0.00	74.76	69.20	28.48	0.34
1.02	72.62	67.28	26.89	0.34
3.00	69.00	64.13	25.89	0.33
4.62	63.35	62.15	26.02	0.34
9.00	62.04	61.70	25.70	0.33
12.03	61.08	60.90	25.52	0.35
15.32	60.04	59.76	25.99	0.35
16.00	58.89	57.69	25.69	0.34
17.87	58.22	57.62	25.16	0.34
20.00	56.47	57.92	24.65	0.34
21.34	55.04	57.85	24.50	0.33

Table 4 The Values of the Damage Parameters

Pre-strain, ε_1 (%)	D_1	D_2	D_3	D_4
0.00	0.000	0.000	0.000	0.000
1.02	0.029	0.028	0.056	0.000
3.00	0.077	0.073	0.091	0.029
4.62	0.153	0.102	0.087	0.000
9.00	0.170	0.108	0.098	0.029
12.03	0.183	0.120	0.104	-0.029
15.32	0.197	0.136	0.088	-0.029
16.00	0.212	0.166	0.098	0.000
17.87	0.221	0.167	0.117	0.000
20.00	0.245	0.163	0.135	0.000
21.34	0.264	0.164	0.140	0.029

Table 5 The Expected and the Measured Values of $\tilde{\nu}_{12}$

Pre-strain, ε_1 (%)	**Measured $\tilde{\nu}_{12}$**	**Predicted $\tilde{\nu}_{12}$**	**Percentage Difference (%)**
0.000	0.340	0.340	0.00
1.020	0.340	0.345	1.47
2.280	0.330	0.338	2.42
4.620	0.340	0.336	-1.18
9.000	0.330	0.336	1.82
12.030	0.350	0.333	-4.86
15.320	0.350	0.340	-2.86
16.000	0.340	0.347	2.06
17.870	0.340	0.343	0.88
20.350	0.340	0.334	-1.76
21.340	0.330	0.332	0.61

Table 6 Mechanical Behaviours of Materials Used

Material	E (GPa)	ν	$\hat{\varepsilon}_1$	$\hat{\varepsilon}_2$	M
HS-3 steel	216	0.29	1.40	-0.39	7.69
A-K steel	216	0.29	1.65	-0.73	4.55

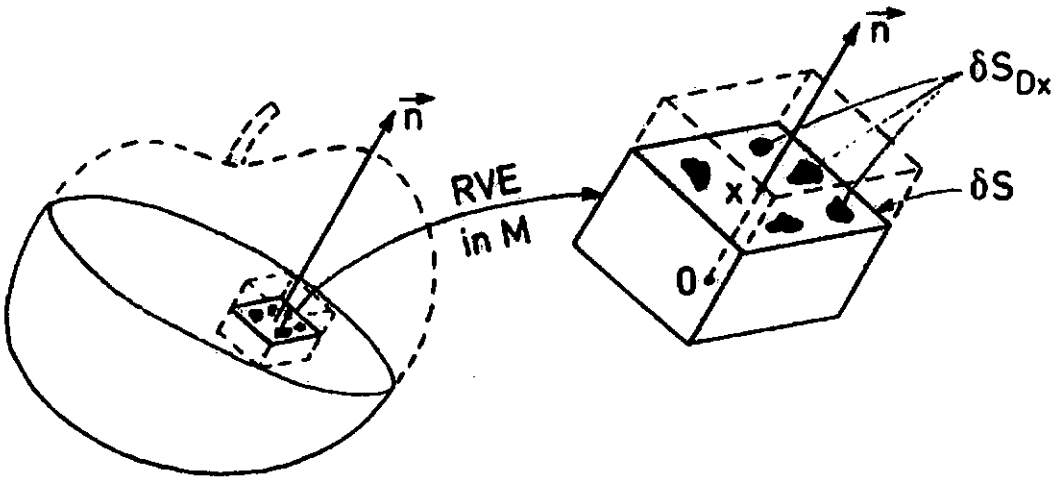

Figure 2-1 Micro-meso Definition of Damaged Element

Lemaitre, J., *A Course on Damage Mechanics*, Springer-Verlag, (1992).

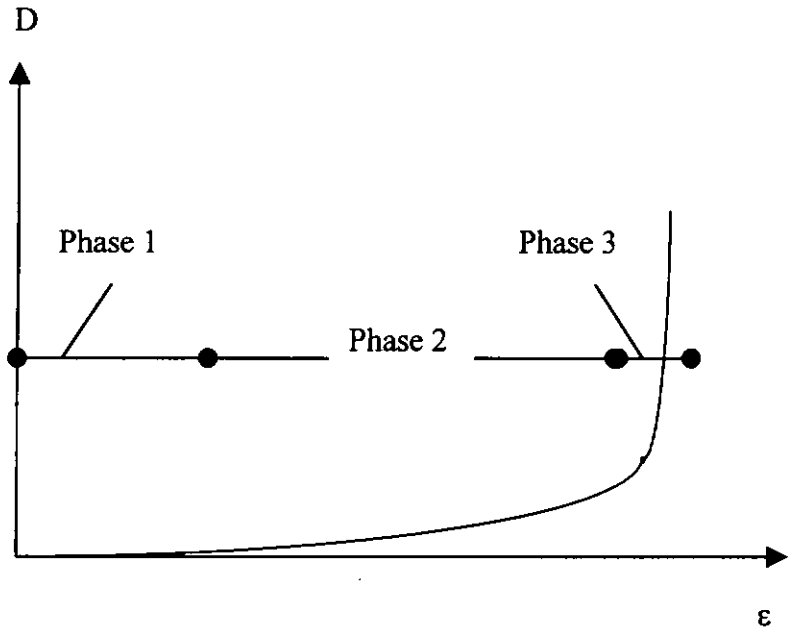

Figure 2-2 Diagram to Show the Progression of Damage Evolution (Mou and Han 1996)

where Phase 1 = damage generation
Phase 2 = damage growth
Phase 3 = damage instability

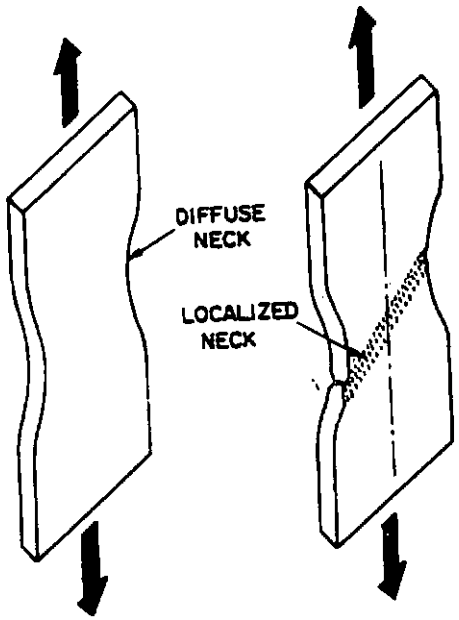

Figure 2-3 Illustration of Diffused and Localized Necking in Uniaxial Tension (Joshi 1992)

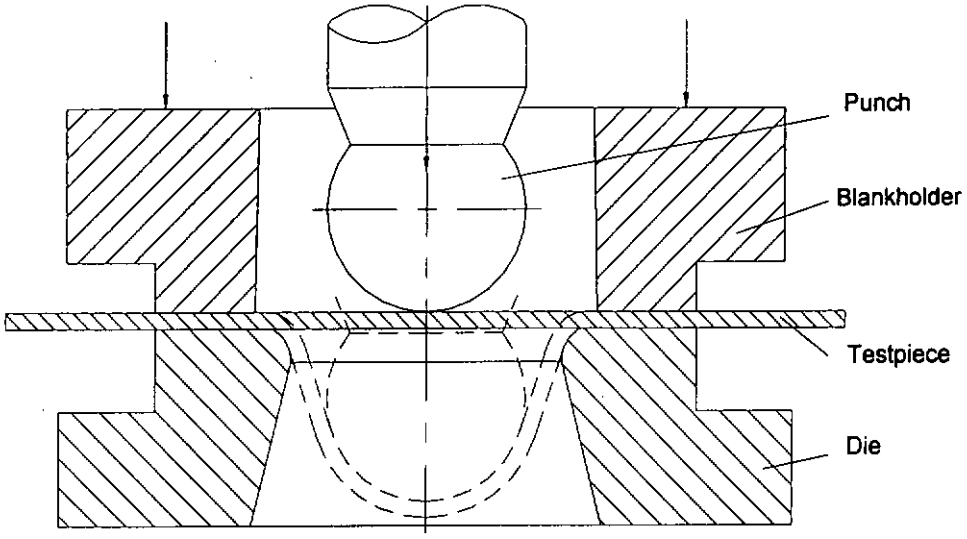

Figure 2-4 Typical Erichsen Test for Stretchability

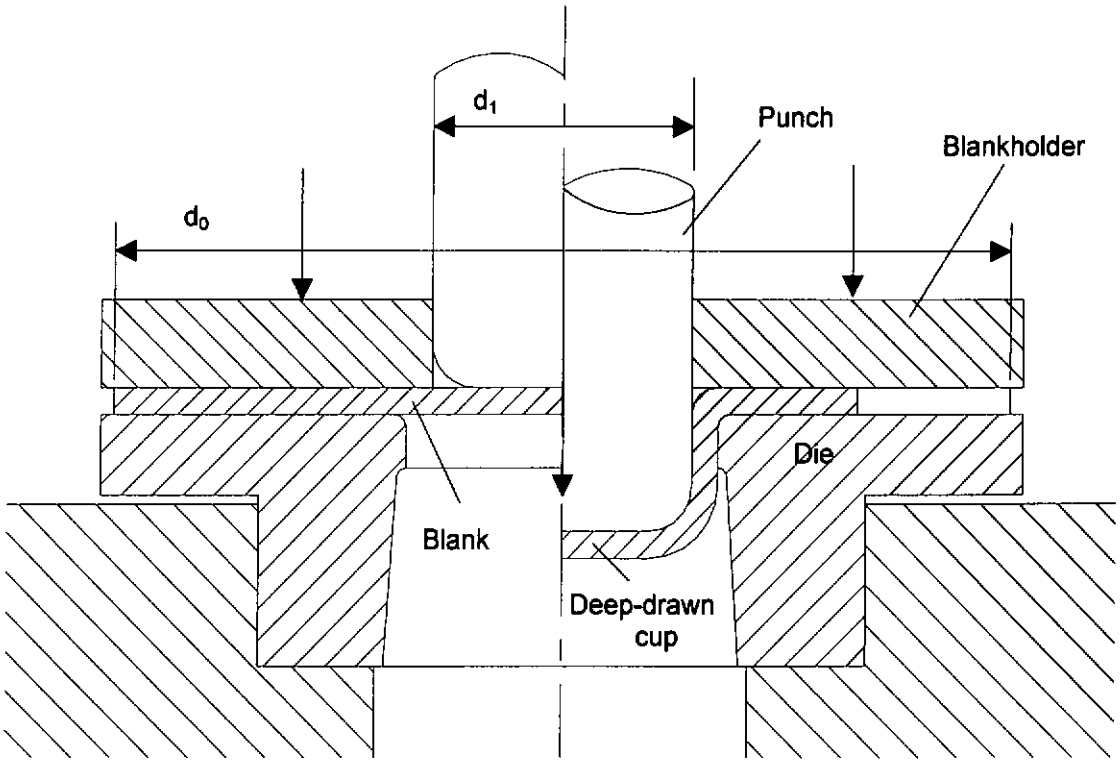

Drawing ratio $\beta = d_0/d_1$

Figure 2-5 Schematic Diagram of the Swift Test for Deep Drawing (Swift 1952)

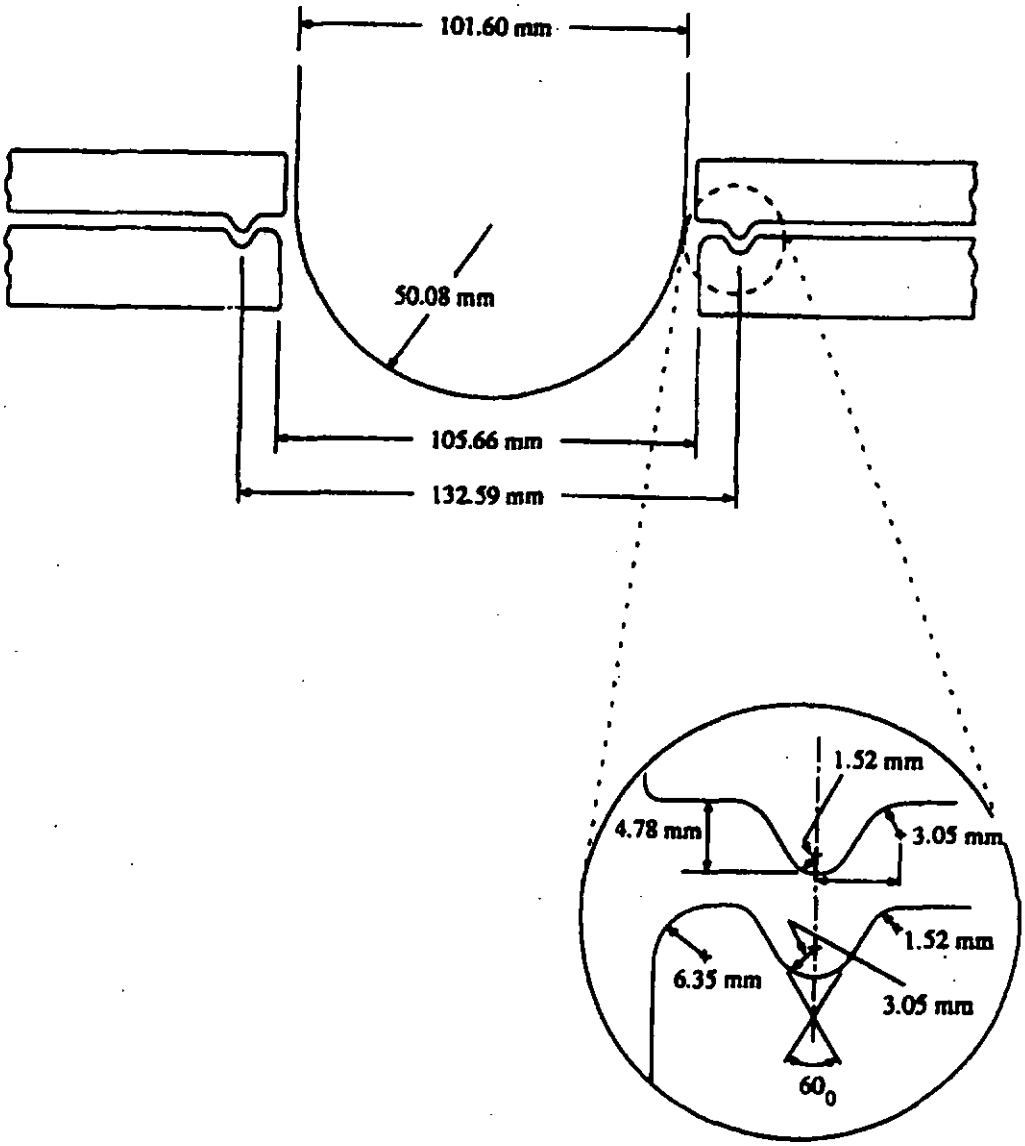

Figure 2-6 Schematic Diagram of the Punch and Drawbread arrangement of the Hecker and Ghosh Punch Test (Williams 1993)

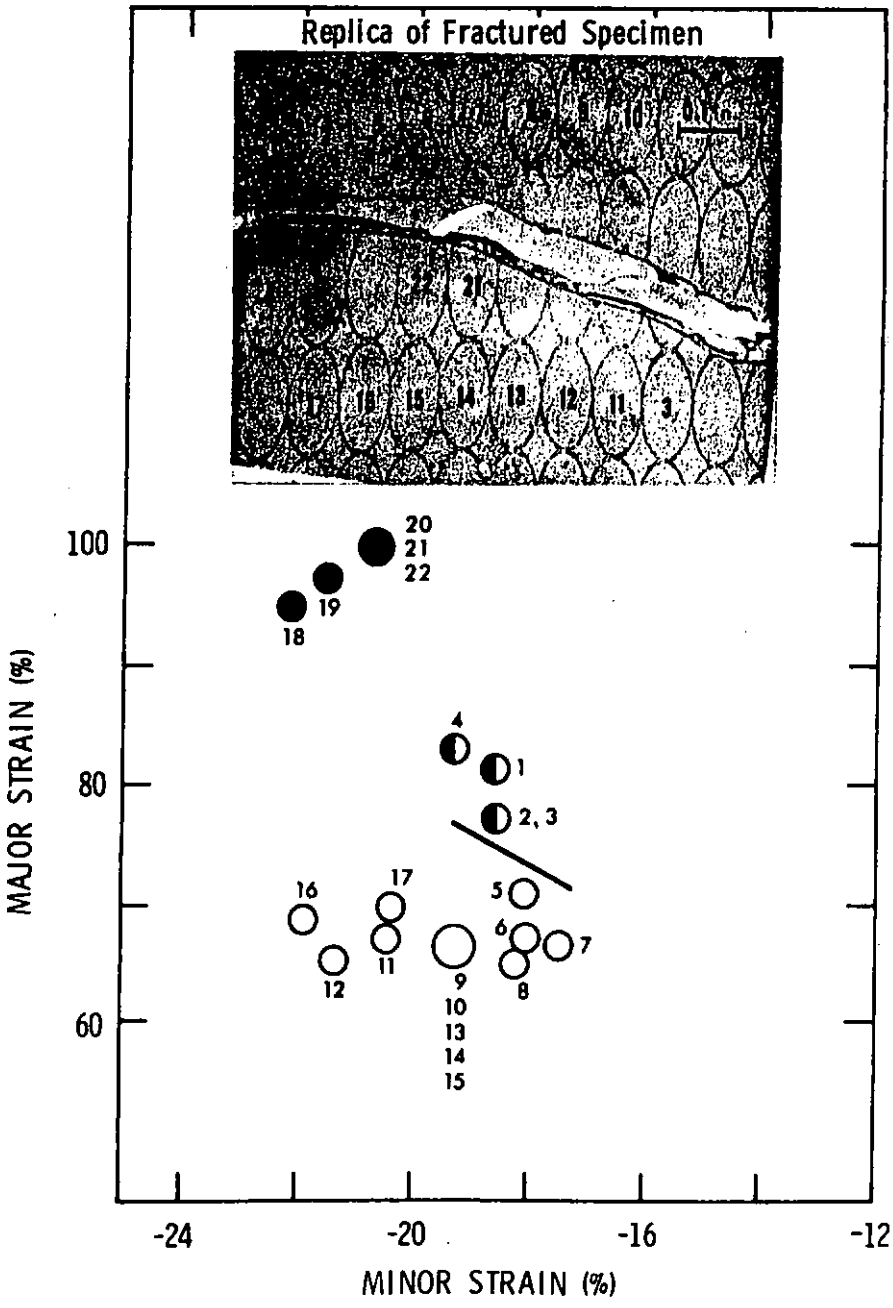

Figure 2-7 A Fractured Specimen and its Deformed Circles were Plotted on the FLD in terms of Major and Minor Strains (Hecker 1975b)

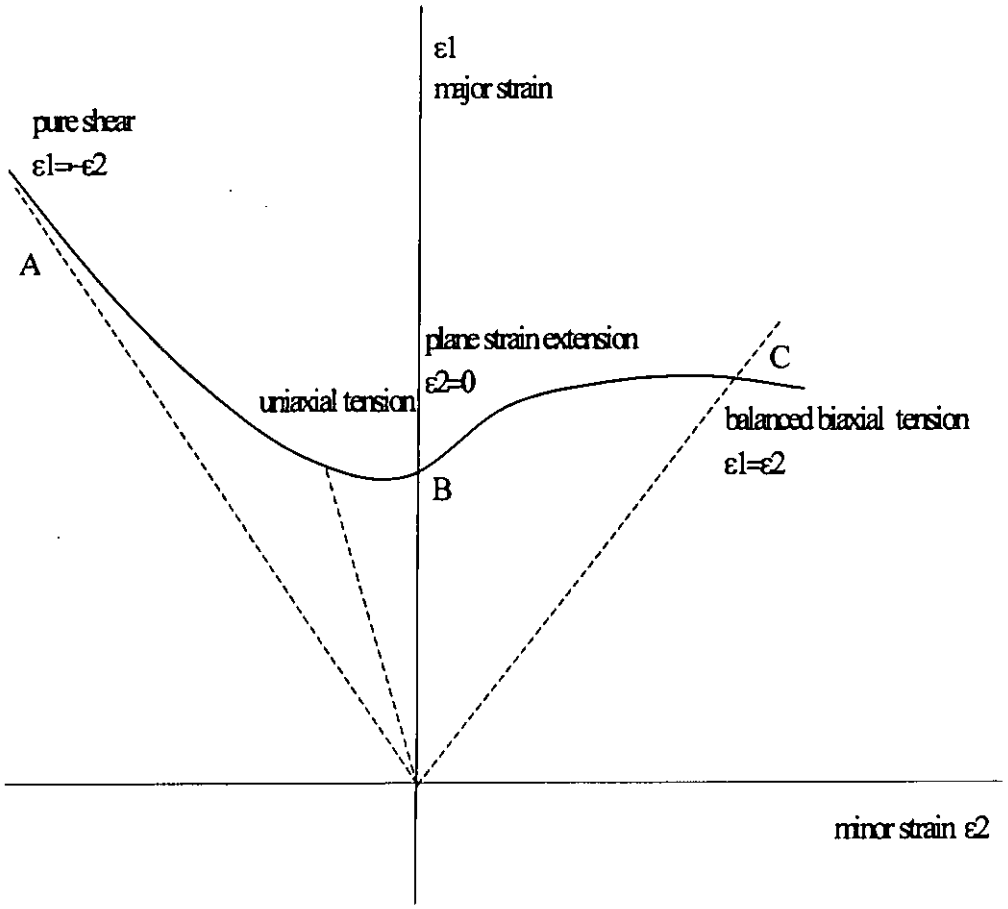

Figure 2-8 Schematic Drawing of a Forming Limit Diagram (FLD)

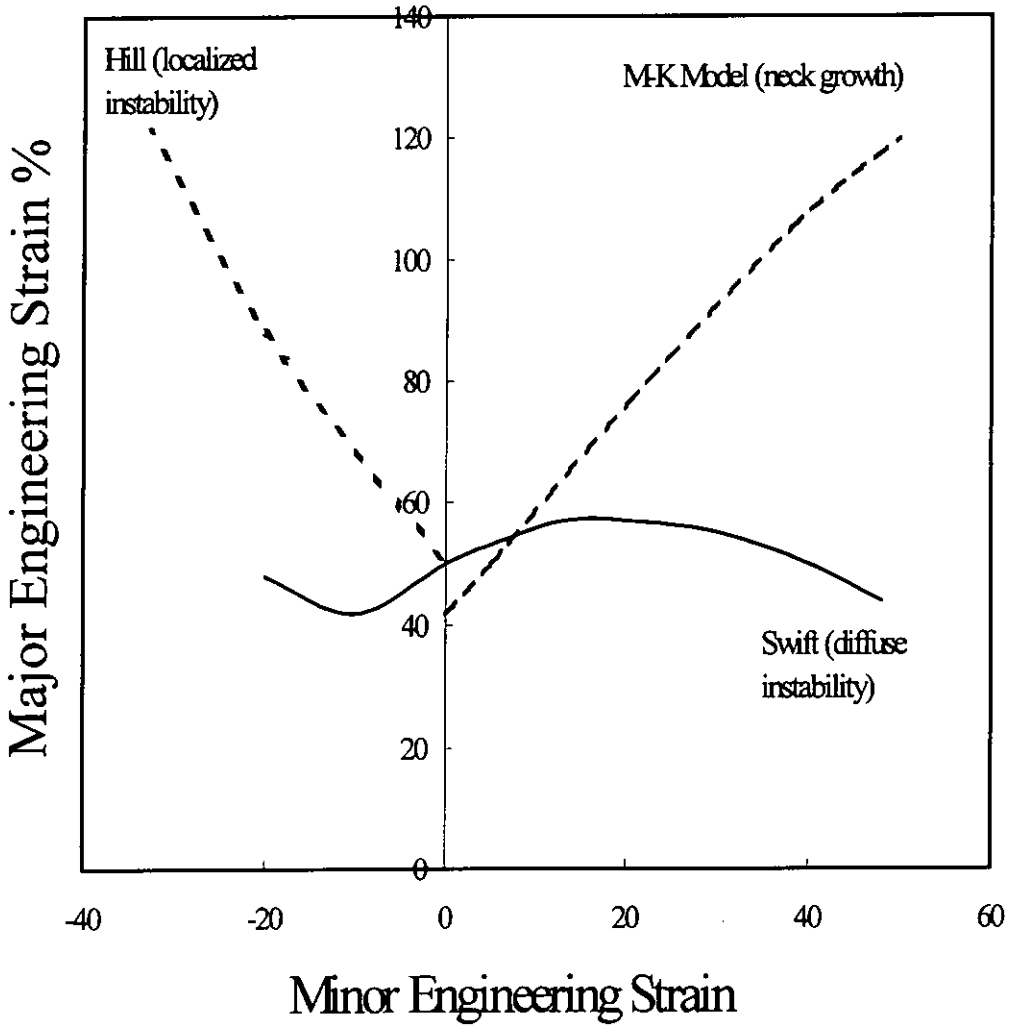

Figure 2-9 A Comparison Among the Prediction of the Hill and Swift Instability and M-K Neck Growth Models (Zaverl 1982)

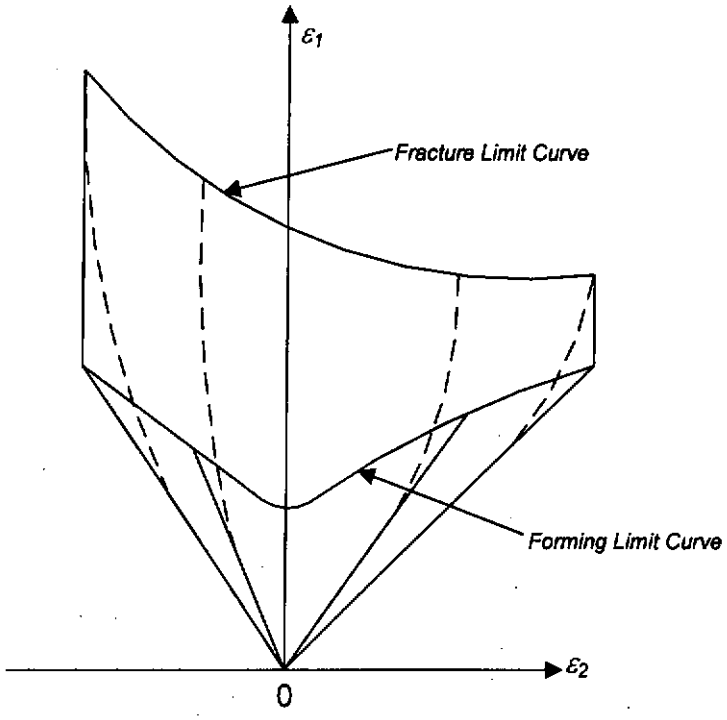

Figure 2-10 The Fracture Limit Curve and Strain Path in Sheet Metal Forming (Tai and Yang 1987c)

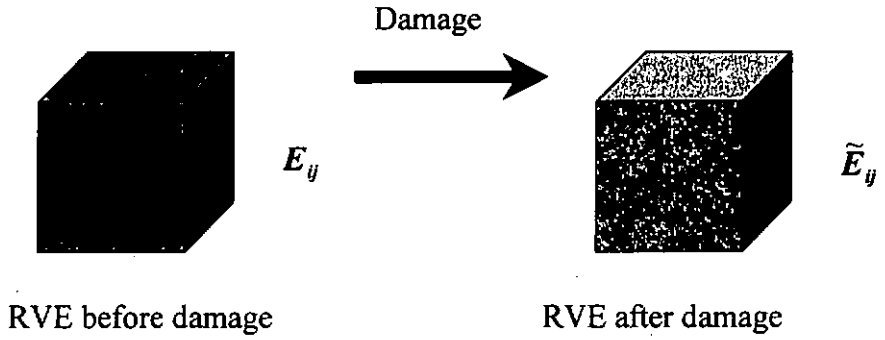

Figure 3-1 A Representative Volume Element

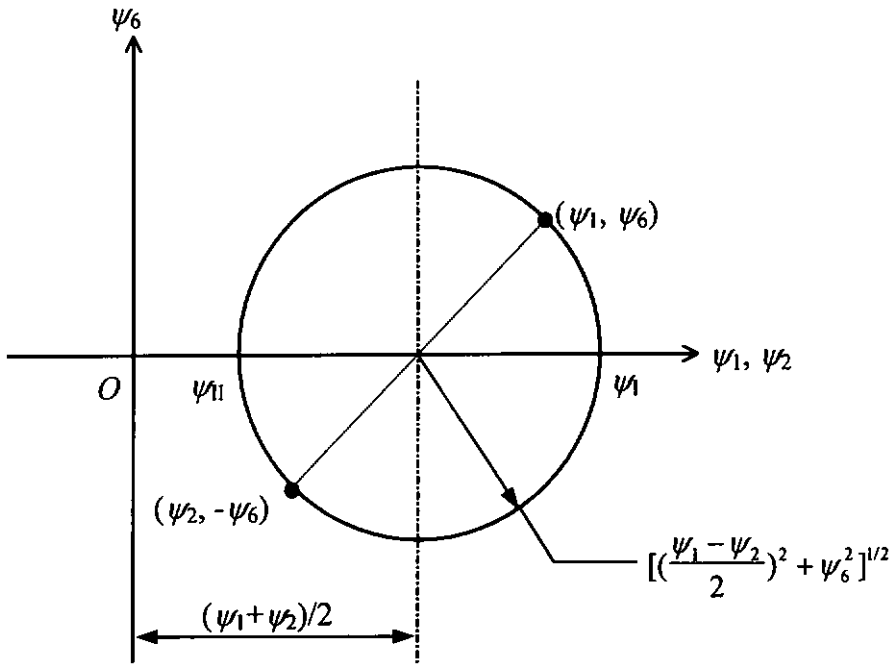

(*a*)

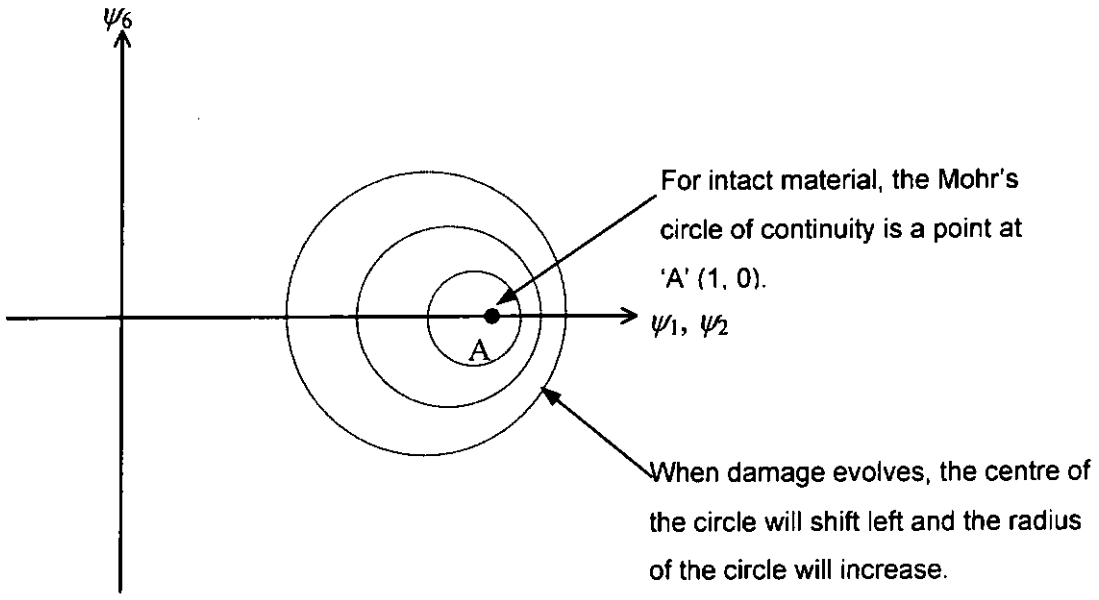

(*b*)

Figure 3-2 The Mohr's Circle of Continuity

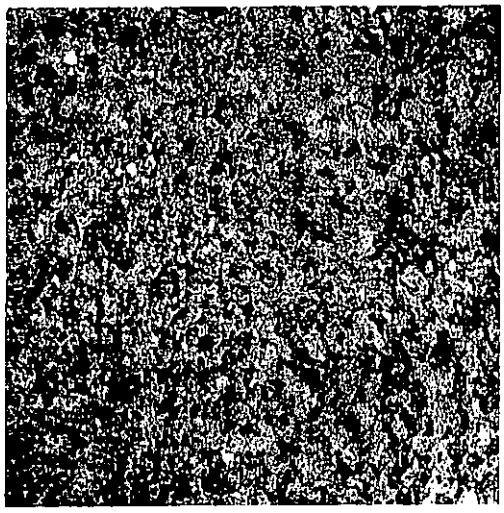

(a) Magnification 50×

Figure 4-1 Microstructure of undamaged Al2024T3 sheet.
The dark particles are the intermetallic compounds.

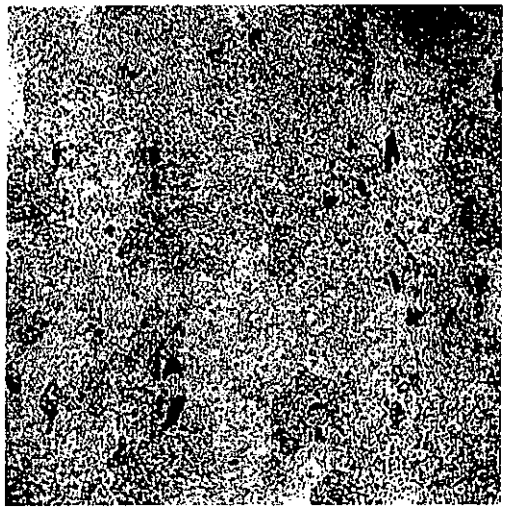

(b) Magnification 400×

Figure 4-1 Microstructure of undamaged Al2024T3 sheet.
The dark particles are the intermetallic compounds.

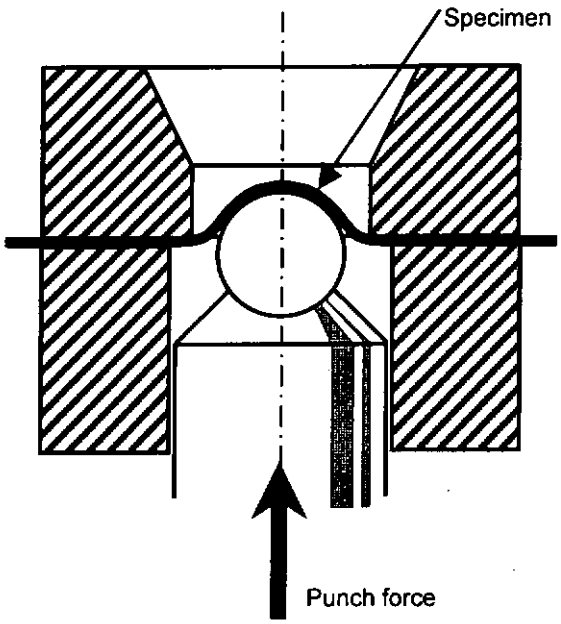

Figure 4-2 The Erichsen Cupping Test

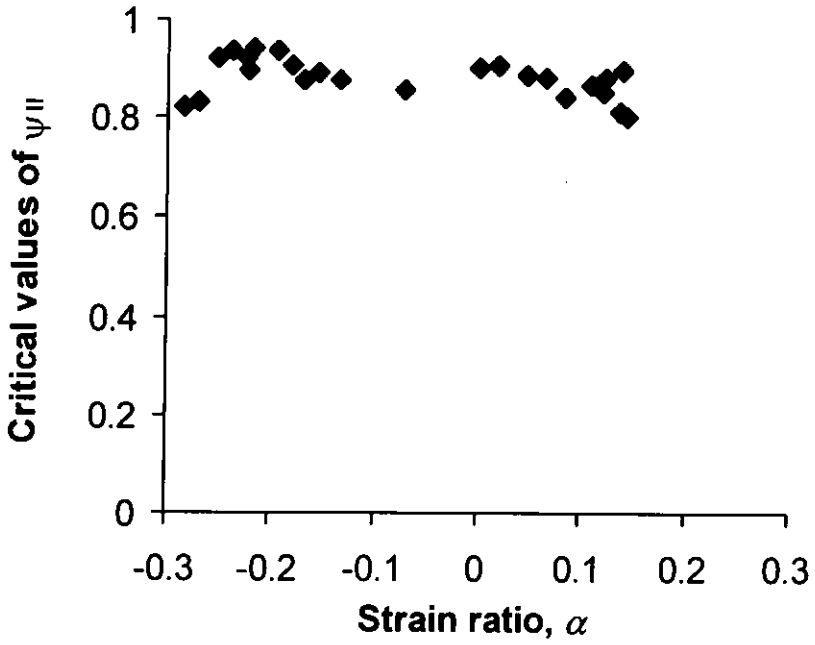

Figure 4-3 The Critical Value of ψ_{II}

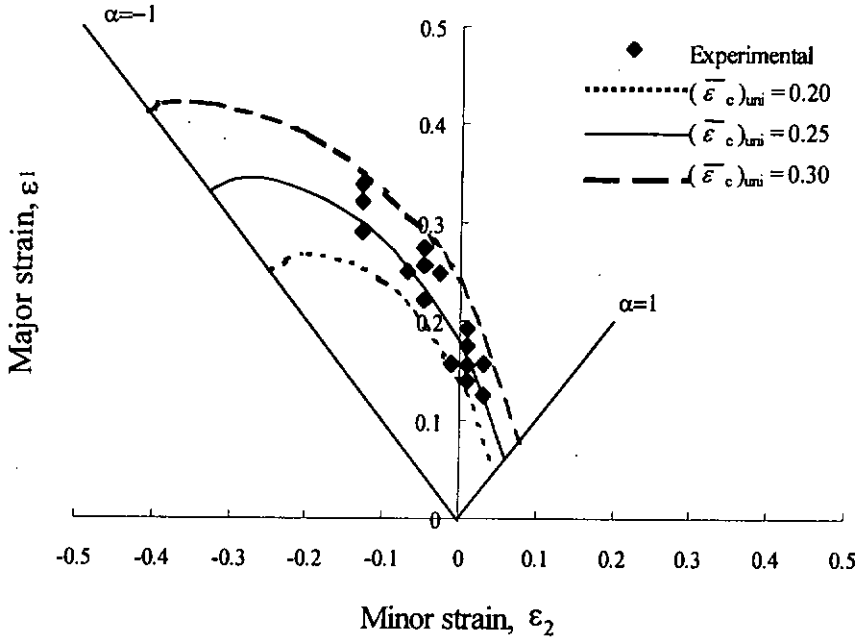

Figure 4-4 The Fracture Limit Curve of Al2024-T3

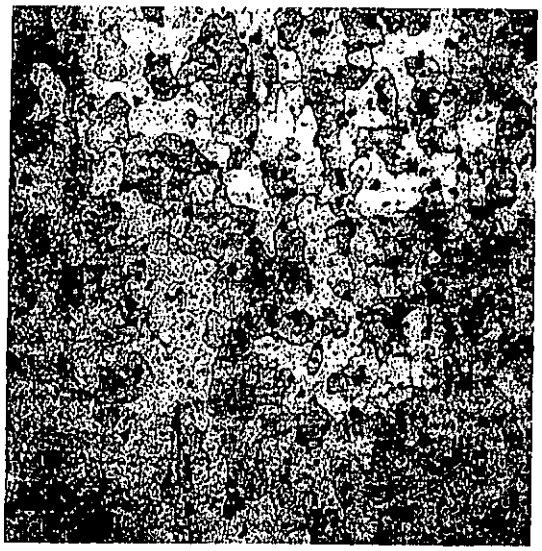

Figure 4-5 Aluminium Alloy 2024T3 sheet (200×).

Dark particles are intermetallic compounds, such as Cu_2MnAl_{20}, $CuMgAl_2$, and Cu_2FeAl_7

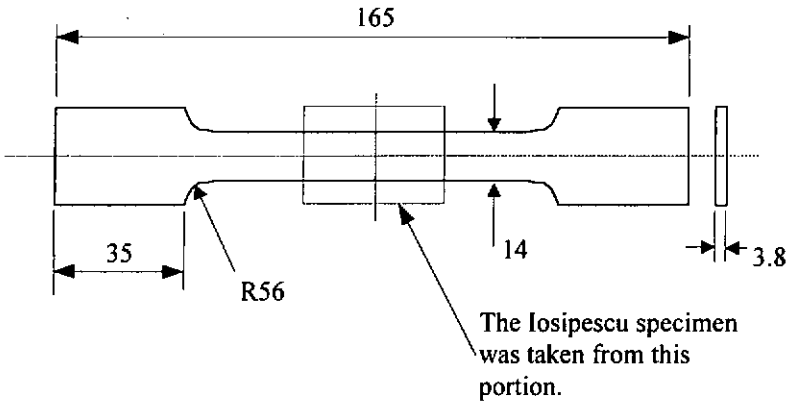

Figure 4-6 The Geometry of the Tensile Test Specimens (*all dimensions are in mm*)

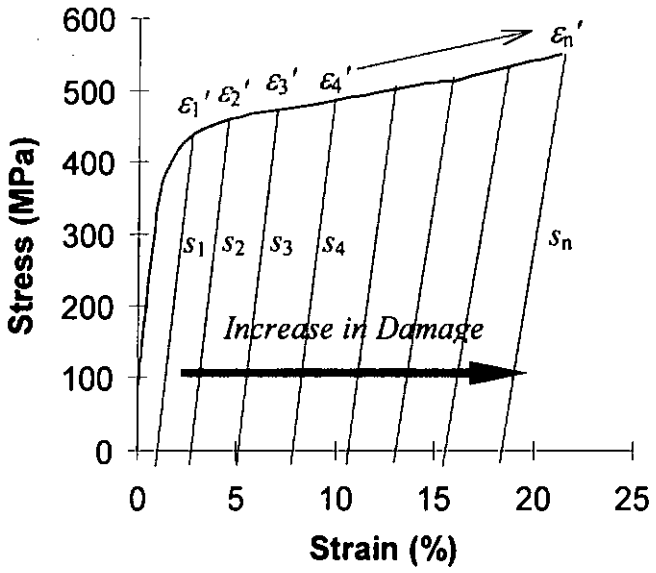

Figure 4-7 The Pre-straining of the Specimens (Al2024T3)

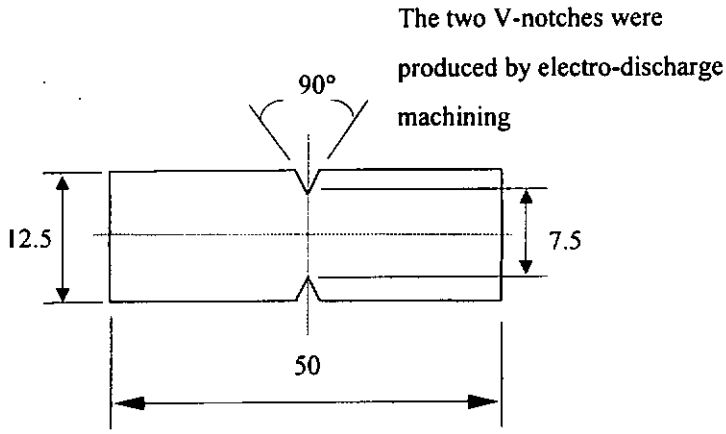

Figure 4-8 The Geometry of the Iosipescu Specimens (*all dimensions are in mm*)

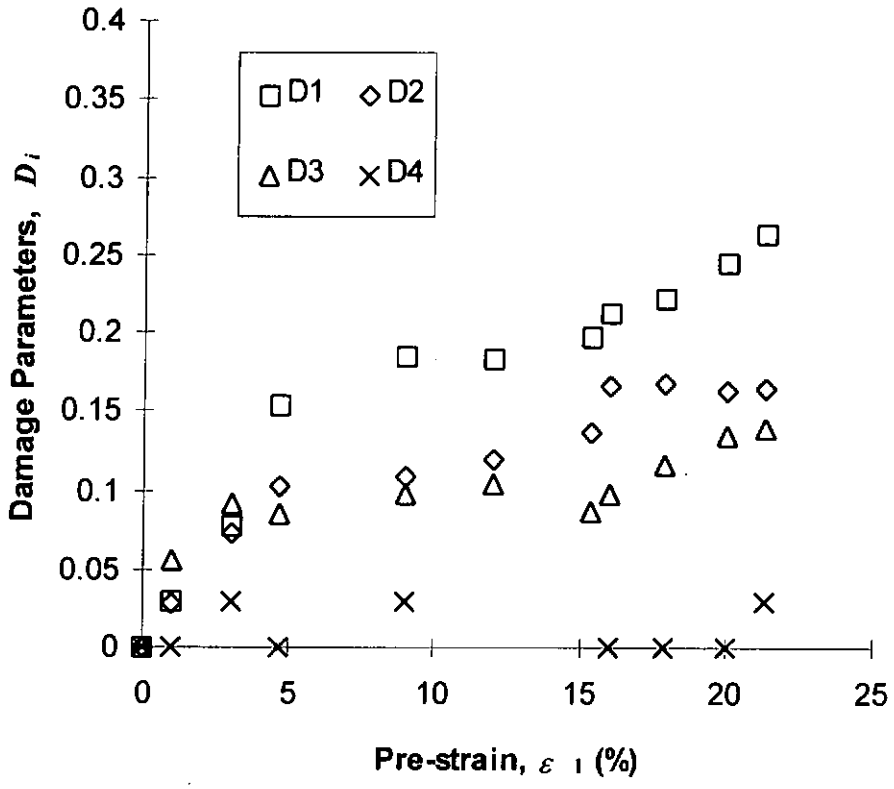

Figure 4-9 The Damage Parameters Versus the Pre-strain

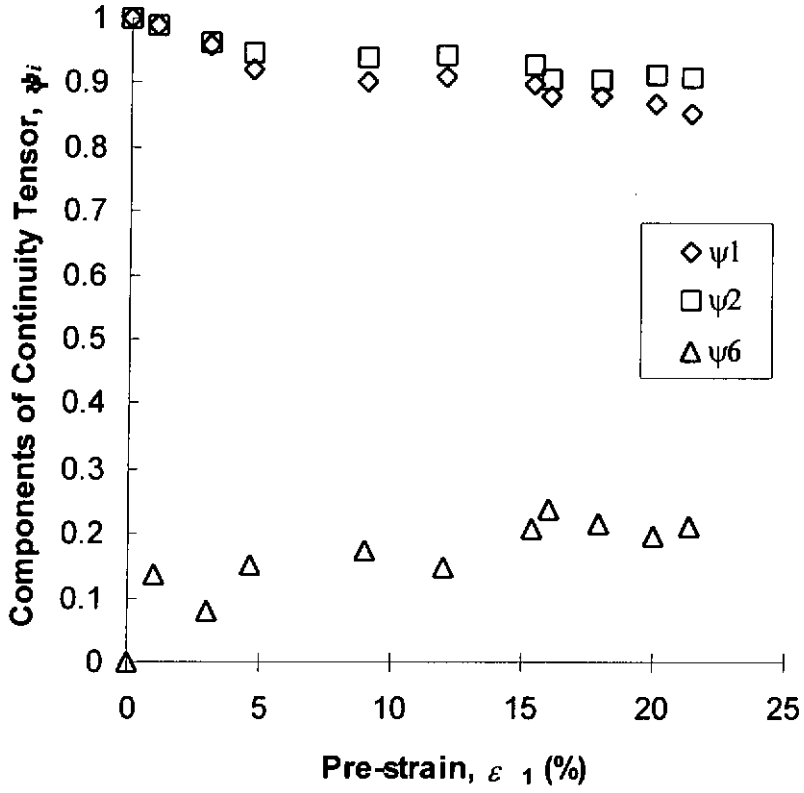

Figure 4-10 The Components of the Continuity Tensor Versus the Pre-strain

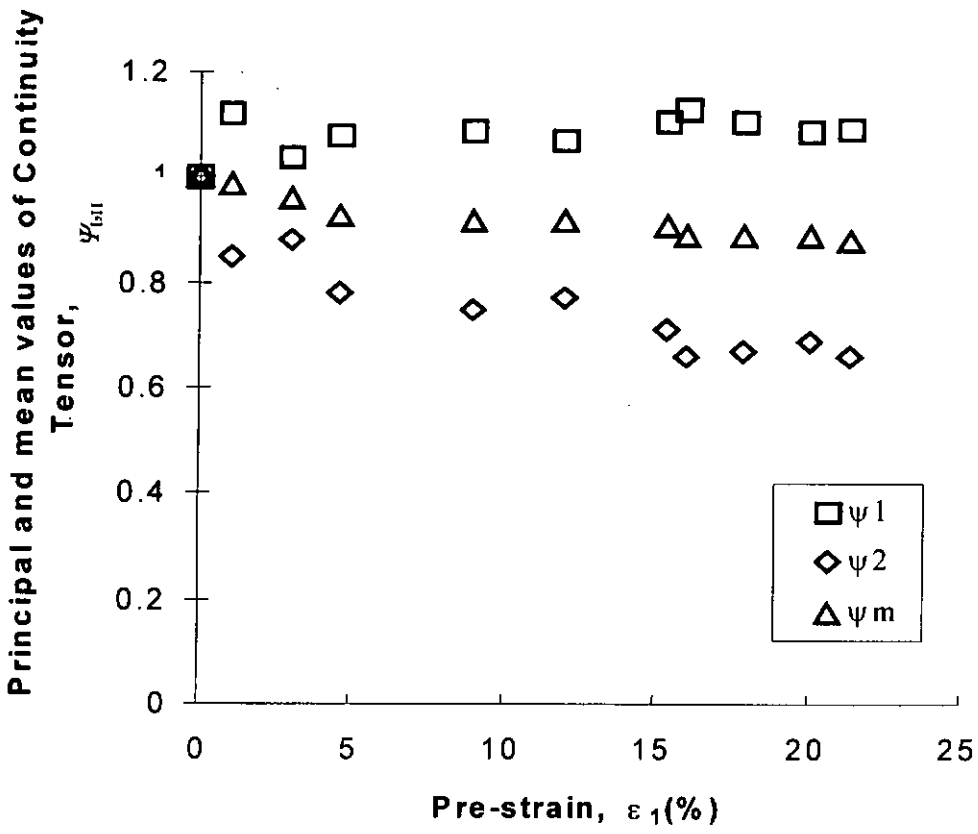

Figure 4-11 The Principal Values of Continuity Versus the Pre-strain

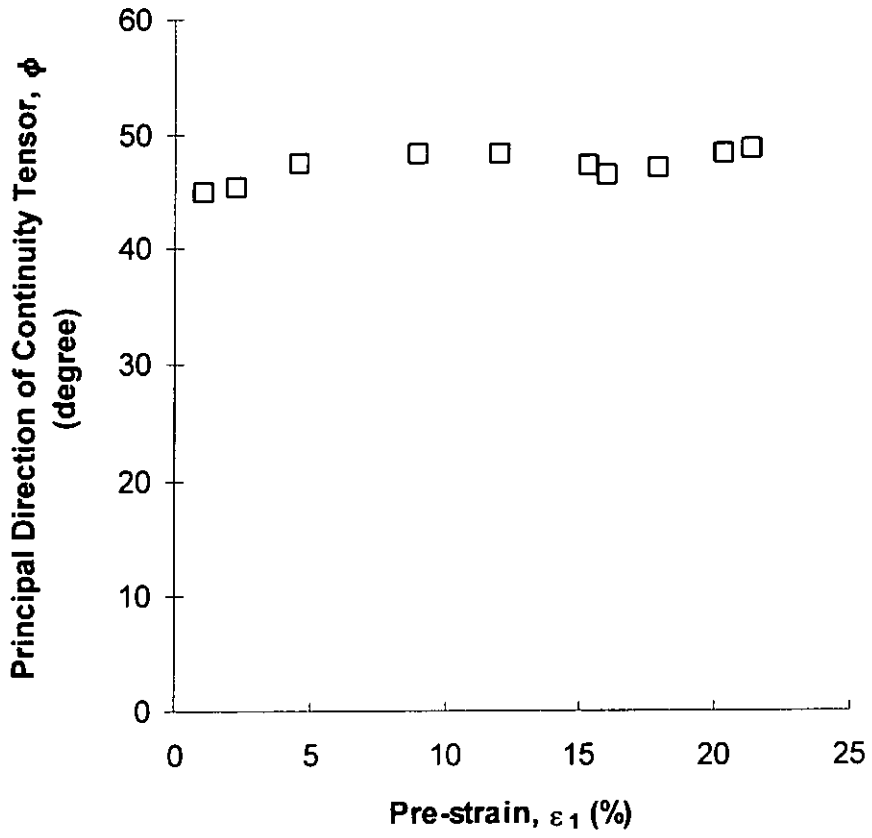

Figure 4-12 The Principal Direction of Damage Versus the Pre-strain

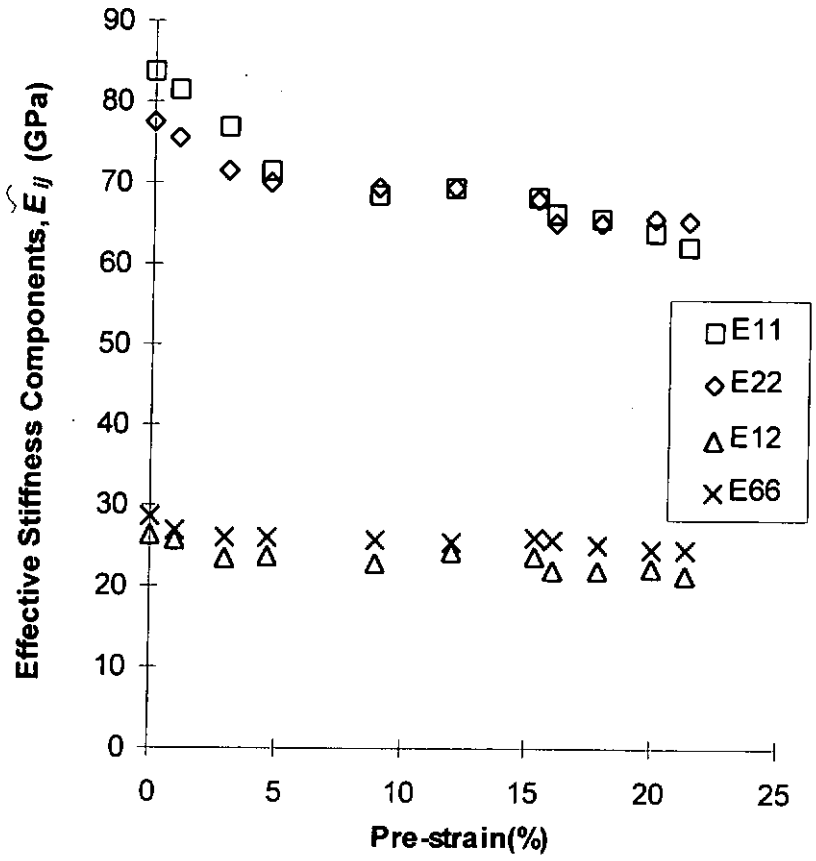

Figure 4-13 The Effective Elastic Stiffness Tensor Expressed in the Material Coordinate System

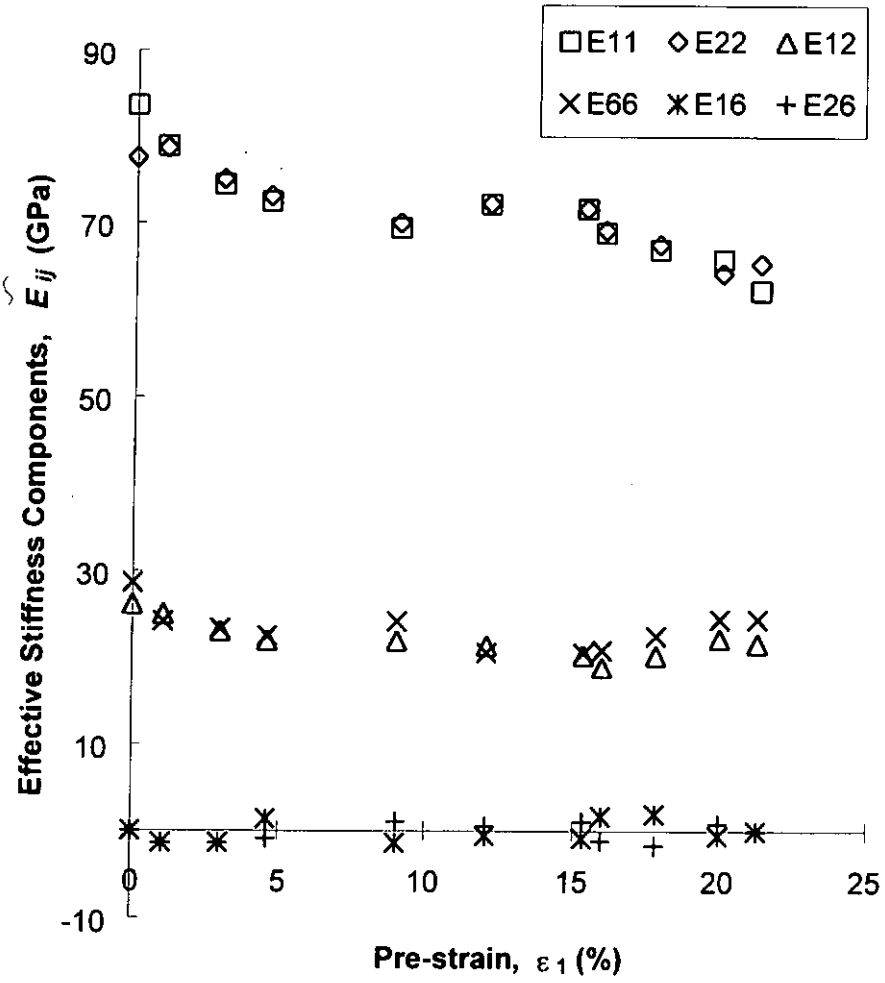

Figure 4-14 The Effective Elastic Stiffness Tensor Expressed in the Principal Damage Coordinate System

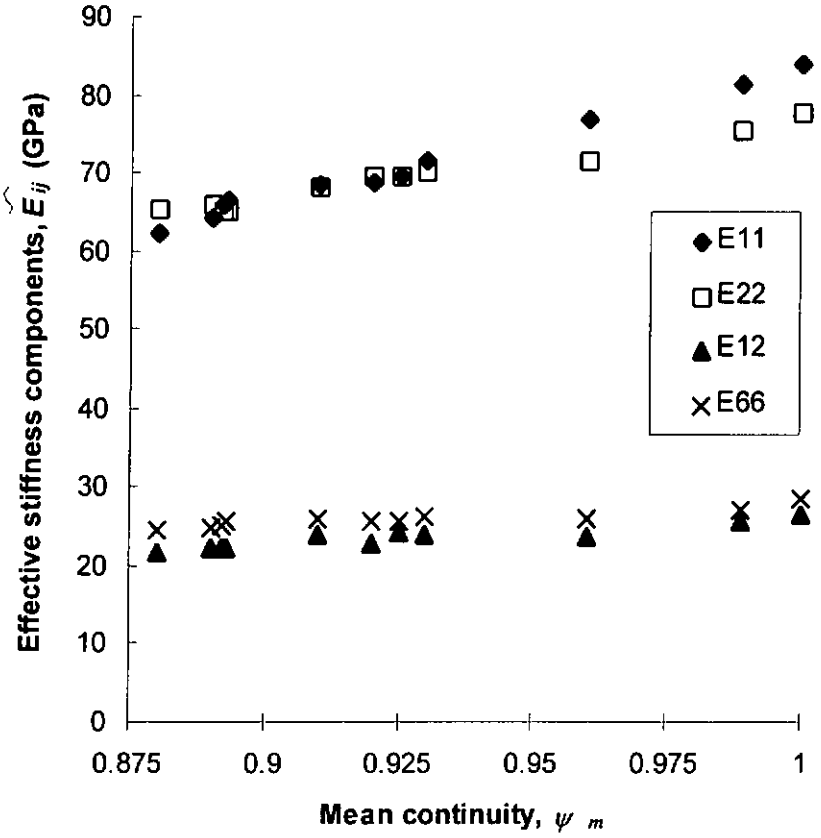

Figure 4-15 The Effective Stiffness Reduces with the Mean Value of the Continuity Tensor

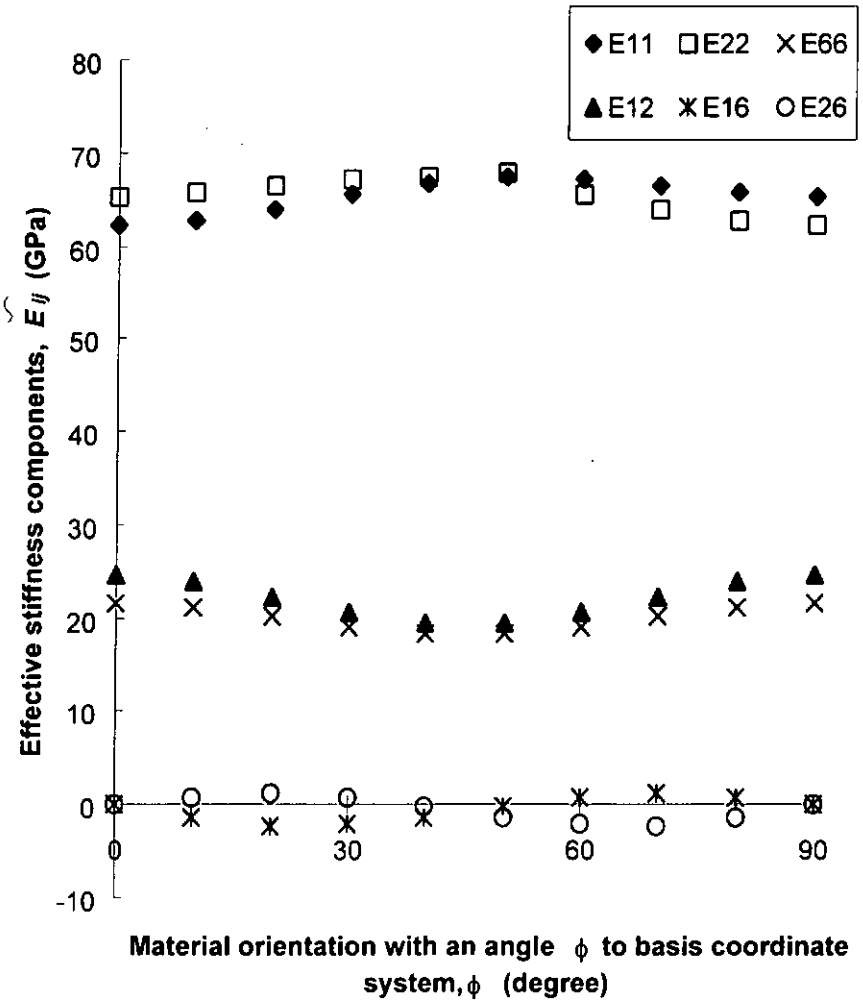

Figure 4-16 The Components of Effective Stiffness Tensor Under Different Material Orientations (at the pre-strain ε_1=21.34 %)

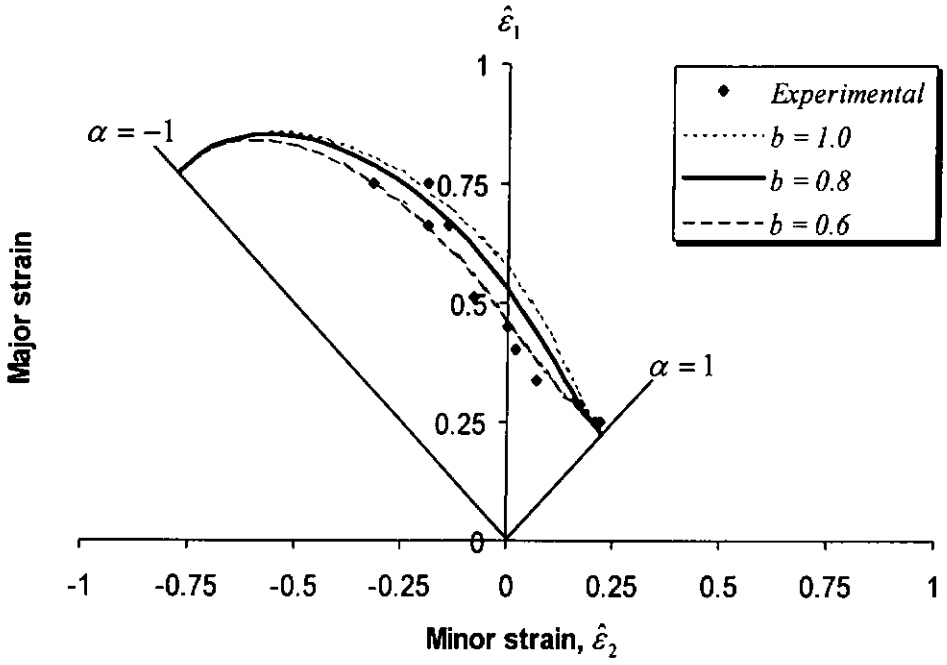

Figure 4-17 Fracture Limit Curves of Al2036T4 Sheet

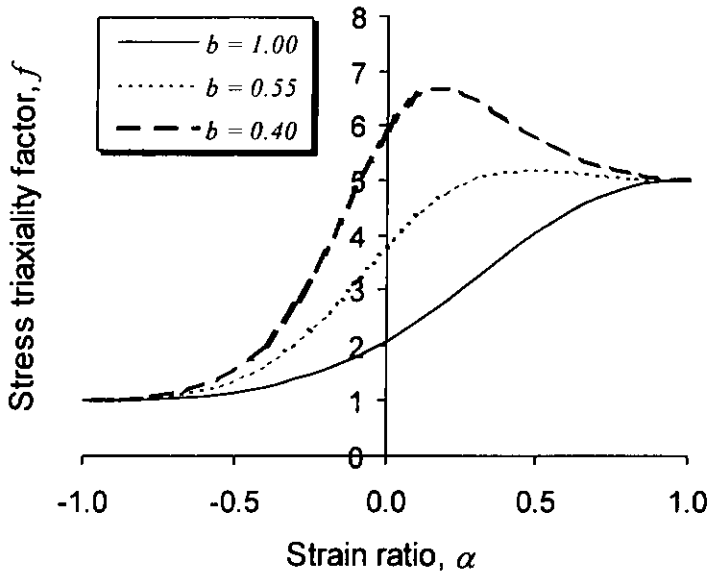

Figure 4-18 Effect of Damage Anisotropy on Stress Triaxiality for Al2036T4

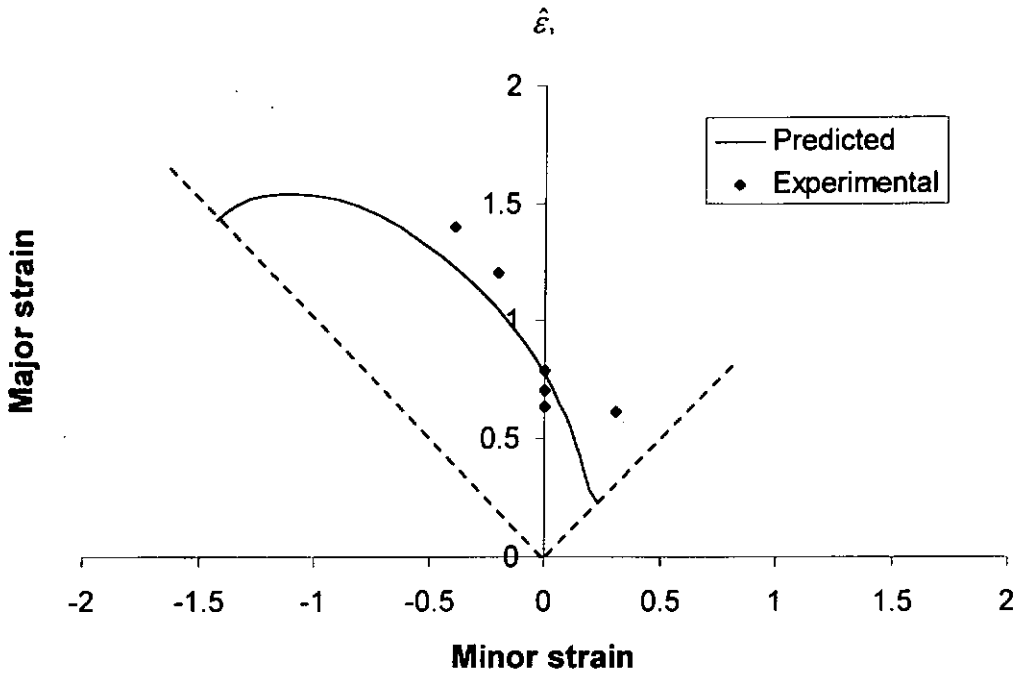

Figure 4-19 Fracture Strain of HS-3 Steel Sheet

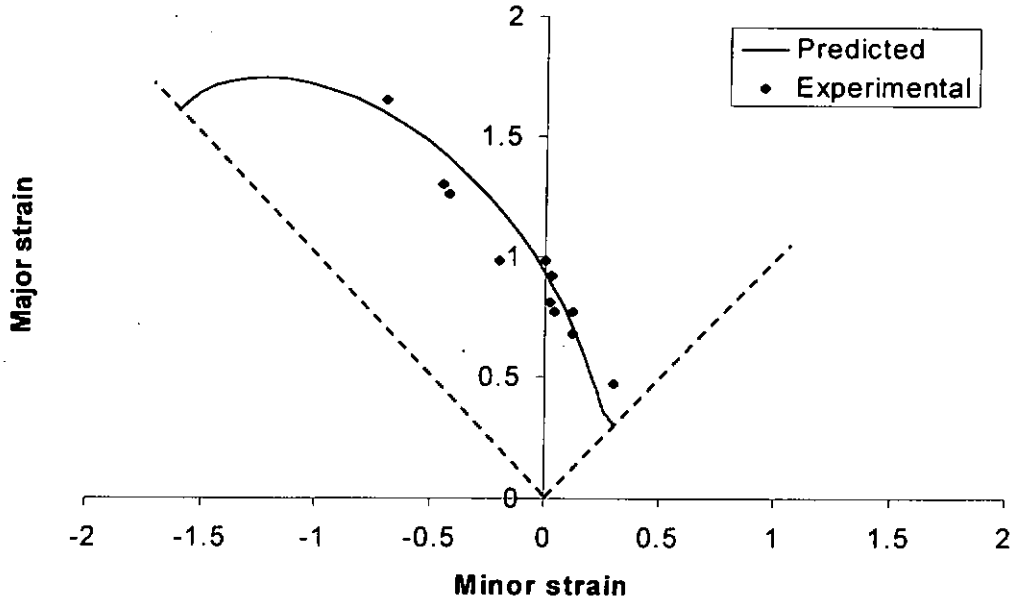

Figure 4-20 Fracture Strain of A-K Steel Sheet